

POLITECNICO DI TORINO

MECHANICAL AND AEROSPACE ENGINEERING DEPARTMENT
Master's Degree Course in Automotive Engineering

Master's Degree Thesis

Simulation of MacPherson strut side force reduction and influence in the dynamics of vehicle in Adams



Supervisors:

Prof. Giovanni MAIZZA

Research Advisor:

Dr. Umid JAMOLOV

Student:

Giovanni SAVIOTTO

ACADEMIC YEAR 2019-2020

Index:

1.	Introduction.....	5
	a. Suspension components.....	7
	b. Suspension types.....	8
2.	Analytical analysis of vehicle dynamics and forces acting on the suspension.....	19
	a. The full vehicle models.....	20
	b. Model of Macpherson Suspension.....	23
3.	Simulations on Adams and recollection of information.....	28
	a. Definition of the type of vehicle used and preparation of the models.....	28
	b. Static Analysis and Test Definition.....	32
	c. Results obtained.....	39
	d. Introduction of the Spherical Joint in the Top Mount	56
4.	Conclusion.....	75
5.	Picture index.....	76
6.	Bibliography.....	79
7.	Acknowledgements.....	81

Abstract

The purpose of this degree work is to analyse side force reduction on the upper mount of a MacPherson automotive front suspension, assembled on a vehicle. Adams software was used as it allows simulating a vehicle on realistic driving conditions and calculates the forces on a vehicle (points/joints). By changing the inclination of the spring axis with respect to the shock absorber axis, numerous analyses were made considering various driving conditions, all attributable to operations that a driver can access during normal use of the car. Parametric modelling software was used to change the inclination of the spring with respect to the shock absorber, which made it possible to obtain the hypothetical variants, considering the physical limits imposed by the geometry of the suspension itself. Starting from the original situation, the spring tilted in two different directions, one in the direction of the outside of the car and one inward. And for each direction different stages have been considered, in order to have a more accurate measurement of the influence of the inclination. A variation of trajectory was therefore considered following the directives ISO 3888-2: 2011 that define the Moose Test, a test during braking and the passage of the car on an artificial bump (DPR 495/1992, as modified by DPR 610/96, in Art. 179. (Art. 42 Cod. Str.) Comma 5). The values relating to the dynamic behaviour of the vehicle and the relative displacements of the upper top mount of the suspension were extrapolated, in addition to the value of the lateral force acting on it. The results obtained with modified inclination angle are compared with the original configuration which allowed establishing the correct inclination to obtain significant decrease in lateral force and then subsequently an optimization of the results obtained. Subsequently, the use of a spherical joint on the top mount strut was introduced to verify the influence of this joint on vehicle dynamics, displacements and lateral force in order to determine whether this modification will improve the parameters considered.

1. Introduction

An automobile is a complex structure made up of numerous components. Its main objective is to allow people or goods to move inside it on a road. To do this it uses wheels, in a number equal to or greater than three, which allow the movement. To do this, the wheels and the car must be connected, and the wheels must preferably be all in contact with the road. So, we have two alternatives: either we use a structure so flexible as to allow the wheels to always be in contact with the ground, or we use deformable systems that connect the vehicle with the wheels. These structures are called suspensions and are the topic that we will discuss in this thesis.

In addition to this function, structural deformations must be added to the deformation of the suspensions which affect the vehicle's handling and comfort characteristics.

To perform their task, the suspension must:

- Allow a distribution of the forces, exchanged by the wheels with the ground, in compliance with the design specifications in all load conditions.
- Determine the trim of the vehicle under the action of static and quasi-static forces.

It should not be overlooked that, by introducing a deformable connection on a vehicle, geometric variations of the position of the body according to the load and its position are introduced; these variations are described through the three coordinates of the centre of gravity and the three angles of the body's reference system (yaw, roll, angle of inclination). This information is included under the term static vehicle trim.

In addition to this function, which is performed substantially with an elastic system, there is another function, no less important: absorbing and attenuating the impacts received by the wheel from road irregularities and transmitted to the body.

It should be remembered that this task requires the application of an adequate damping system; this function is so important that the suspension is also applied to two or three-wheel vehicles that are not hyperstatic bodies.

Theoretically, the only tires would be enough to isolate the vehicle body from the forces coming from the road, but their elastic and damping properties are not sufficient to achieve adequate handling and comfort objectives, unless the speeds are very low and the road surface is sufficiently smooth. Suspensions are therefore essential to obtain adequate behaviour in terms of road holding (handling) and comfort, since they determine the distinctive characteristics of each vehicle.

The wheels must also be free to move in a direction almost perpendicular to the ground, in addition to the rotation and movement of the steering. This vertical movement must be managed through the suspension connections in order to ensure the correct position of the tire in relation to the ground. The ability of a tire to react to adequate forces is, in fact, determined by the angles between the equatorial plane of the wheel with the ground and with the speed of the hub.

We can therefore consider the suspension as a filter between road and bodywork, with the task of limiting the forces generated by road irregularities and by the manoeuvres carried out by the driver, without however compromising the controllability of the vehicle in various driving situations.

The suspensions therefore play an essential role in road holding, which does not depend solely on the mass and geometric properties of the vehicle or on the tires alone.

There are several families of suspensions, and a first classification can be made considering their behaviour with the other components of the vehicle. We can therefore define three groups, independent suspensions, dependent suspensions and semi-dependent suspensions.

The independent suspensions, as the name suggests, are suspensions that are not influenced by the other wheels, do not have a direct mechanical connection with the hubs of the wheels of the same axle, the forces acting on these suspensions do not affect the other suspensions (it is not considered the contribution of the anti-roll bars, auxiliary frames and steering connections).

The dependent suspensions or rigid axles on the contrary influence the behaviour of the suspensions of the same axle in case of irregularities in the road surface, due to the rigid connection between the wheels.

The semi-dependent suspensions finally have the characteristics of both the solutions mentioned above. The wheel hubs of this type of suspension cannot be considered independent, they are in fact not connected with an articulated structure. Furthermore, the flexibility of the structure should not be overlooked. An example of a semi-dependent suspension is twist axles.

Another feature that distinguishes the various suspensions is their steering system. In fact, independent suspensions can also be steering suspensions while in the case of dependent and semi-dependent suspensions this is no longer used, except cases such as in industrial and off-road vehicles.

Considering the contribution of the elastic and damping systems present in the suspension, another classification is possible: passive and active suspensions.

Passive suspension means a structure in which the elastic reaction of the suspension system can be absorbed (totally or partially) by the damping system.

In the second group, on the other hand, the elastic reaction of the suspension can be influenced by external systems of the same (such as an engine or a storage system outside the engine), which can limit the movements of the car to achieve static balance. The driver will therefore perceive greater stability.

To continue with the discussion, it is important to define some properties of the vehicle and the suspension.

We define as suspended mass that part of the mass of the vehicle that is free to move in reference to the ground, due to the application of the suspension. That part of the mass that does not change position is called unsprung mass.

Some suspension components contribute partly to the suspended mass, partly to the unsprung mass. To evaluate the two contributions, the mass of these elements must be divided into two parts, ideally concentrated in the suspension joints, to preserve the moment of inertia and the position of the centre of gravity.

a. Suspension components.

Now we will describe the components that allow you to meet the requirements discussed above.

- Bearing components or linkages.
These components provide the connection between the car body and the wheels, guaranteeing the degrees of freedom of the wheels and their position relative to the ground. They determine the relative movement of the wheel with reference to the vehicle body; they also transfer part of the load supplied by the tire contact area to the vehicle.
- Primary elastic members
These include springs (spiral, bar and leaf springs), anti-roll bars and stop springs. These members elastically connect the wheel to the body and store the energy produced by an irregular road profile. They not only store this energy but determine the position of the body as a function of the size and position of the payload.
- Secondary elastic members

The elastic bushings on the connection joints fall into this category. These joints have a certain elastic conformity. In the past it was seen as a disadvantage avoiding the lubrication of the joints using elastomeric joints, but recently it was understood that this feature could be exploited to improve the design of the elasto-kinematic behaviour of the suspension and its comfort properties. The deformation of these joints plays an important role in determining vehicle dynamics.

- Damping members

These are basically shock absorbers, but we should remember that the primary and secondary elastic elements make their contribution in absorbing energy. The shock absorbers have the task of dissipating the elastic energy stored by the elastic elements and allowing the damping of the oscillations of the vehicle bodywork, avoiding stationary vibrations or resonance.

b. Suspension types

If we consider the case of independent suspensions, the connections must constrain five of the six degrees of freedom of the wheel (or better, of the wheel hub, because the wheel is therefore free to rotate around its axis). The degree of freedom released will therefore be the translation in a direction perpendicular to the ground. Unfortunately, none of the suspensions currently on the market used exactly meet this requirement. Therefore, solutions are used that allow to obtain the best performance in terms of performance. It is important to consider that, in general, the movement of the wheel is not planar and consequently the study of kinematic behaviour is not simple.

Since the suspensions must constrain five degrees of freedom, they can be made as a system consisting of five bars with spherical hinges at the ends (Fig. 1). This layout, often referred to as multilink suspensions, has the advantage of allowing great freedom of adjustment. changing the length of the bars by screwing or unscrewing the joints. But, given its complexity and consequently the high cost, it has

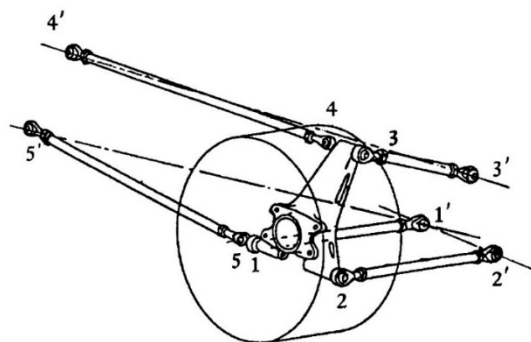


Figure 1 – Multilink Suspension

little application, if not in the field of luxury cars. From five-bar multilink suspension it is possible to obtain almost all configurations by grouping these bars in different ways.

Afterwards, we will list the major types of suspension by listing their main features and focusing on their advantages and disadvantages.

Multilink

By penalizing weight and costs, this solution achieves the best result in terms of comfort and handling.

In multilink suspensions (fig. 1) the hub is connected to the body with five connections, how many degrees of freedom are to be subtracted from the hub, leaving only the movement of the suspension stroke. The shock absorber has no structural functions.

Each connection between the hub and the car body is set on an auxiliary frame to increase comfort, handling and to facilitate assembly.

Advantages:

- Stabilization of changes in the toe angle as a function of cornering and braking forces
- Recovery of the camber
- Increase in wheelbase in compression
- Suitable for avoiding the torque steering effect on rear wheel drive cars

Disadvantages:

- High mechanical complexity
- Long development time
- High production costs
- High volume and weight
- High sensitivity to changes in the elastic behaviour of the bushings

Double wishbone suspension

Starting from the definition of multilink suspension (fig. 2), it is possible to notice that in this type of suspension the points 1-2, and 3-4 are coincident. We therefore have two triangular arms which have the function performed in the multilink suspension by the connecting bars. It will be the upper arm and the lower arm.

The double wishbone suspensions are applied to luxury sedans and sports cars because they allow a design of the elasto-kinematic parameters that provides an optimal compromise between handling and comfort.

Since the upper arm is generally shorter than the lower one to allow a certain recovery of the camber, these are also called short and long arm suspensions, with the acronym of SLA suspensions.

The shock absorber has no structural functions. Hysteresis and the consequent comfort penalty are therefore limited. According to the position of the upper arm with respect to the wheel, the suspensions of this type are classified as high or low.

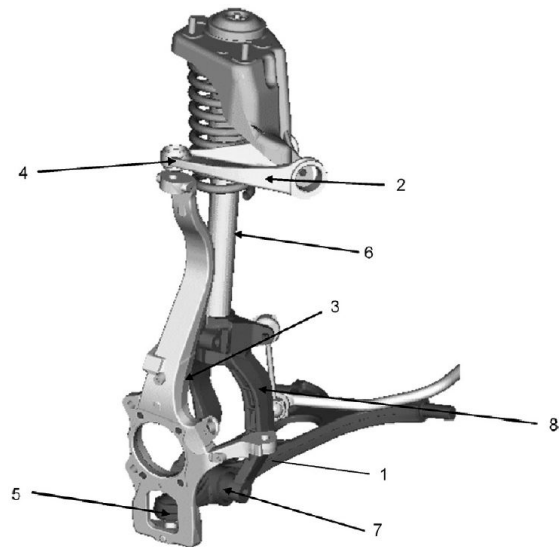


Figure 2 – Double Wishbone Suspension

The difference between these two solutions is imposed by the transverse mass of the engine and the stroke that must be obtained by the car.

The upper arm 1 and the lower 2 are connected to the body by means of elastic bushings. The same arms are connected to the strut 3 by means of ball joints 4 and 5 which allow rotation of the steering of the strut. The line connecting the two ball joints is the axis of the pin of the pin.

The shock absorber and the coil spring are joined, this group is connected to the lower arm through the elastic bushings 7 and is fork-shaped, to free most of the half-shaft.

The piston rod of the shock absorber is connected to the body by means of an elastic bearing; in this case the pin is not present, since the steering movement involves only the wheel post. A support includes the upper arm bushings and the shock bearing and is bolted to the body.

The lower arm is connected to an auxiliary frame. The torsion bar is connected to the shock absorber via a pendulum rod. As in previous suspensions, the subframe is also used for the installation of the steering column.

Advantages:

- Optimal design of the elasto-kinematic parameters in particular about the recovery of the camber,

- Shock absorbers have no structural function; comfort can be improved by reducing hysteresis,
- Possibility to lower the hood profile, for the low version.

Disadvantages:

- Production costs are higher, due to the increase in the number of parts,
- Additional parts for upper suspension attachment,
- The space occupied by the upper arm is considerable. The transverse motors require the high version: the reduced length of the upper arm of this version compromises the possibility of reaching the maximum elasto-kinematic performance,
- The increase in the number of joints and bearings can affect the corners of the wheels due to permanent deformations in the rubber of the bush, with negative consequences on tire wear.
- The high value of the braking loads can adversely affect longitudinal flexibility.

MacPherson

MacPherson suspensions are the most used for the front axles and apply to all small and medium-sized cars. Some manufacturers also adopt this solution on large cars and sometimes also on sports cars; sometimes it is also applied to the rear axles.

If the upper triangle is replaced by a prismatic guide, a MacPherson suspension is obtained (Fig. 3). Its simplicity and the fact that it leaves a lot of free space for the engine have made it a common solution for automotive front axles, particularly in small cars.

The main feature that distinguishes this type of suspension from the others is the fact that the upper arm of the suspension is not present, or at least is integrated in the spring-shock absorber assembly. In fact, in this case the shock absorber has a very important structural function because it is

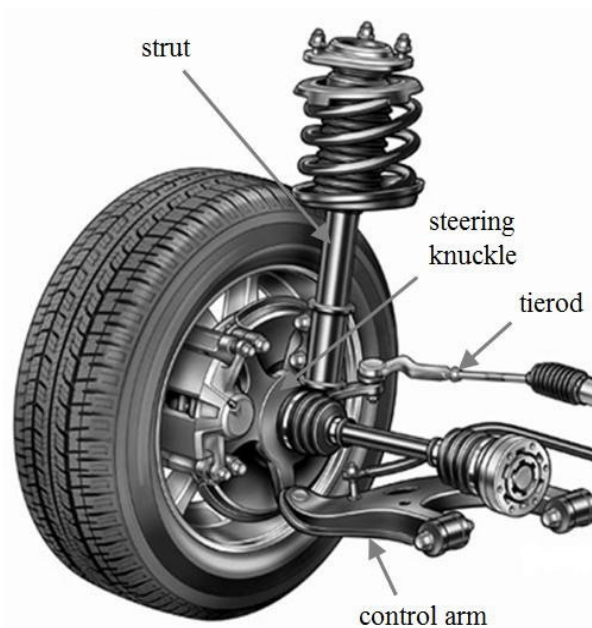


Figure 3 – MacPherson Suspension

connected directly to the frame. Then the stresses and loads that come from the road through the wheels are transferred to the frame via the shock absorber. Consequently, the correct suspension design, including the inclinations of the components, play a decisive role in the comfort and handling of the car.

The lower arm is connected to the body through an auxiliary frame, also called the subframe, in two different points through elastic bushings. The lower arm is also connected to the hub through a ball joint.

Two brackets are welded to the base of the shock body, which are rigidly fixed to the hub. The spring rests on two seats, a lower seat fixed to the shock absorber and an upper seat fixed to a thrust bearing; the upper ring of this bearing rests on an elastic support, fixed to the frame, in the wheel box.

MacPherson suspension uses the shock piston to guide the wheel along the travel of the suspension. This detail ensures that the external forces applied to the wheel at the point of contact with the ground determine, in terms of suspension geometry, a lateral force and a moment applied to the piston itself.

The reaction forces and the deflection of the piston rod have a great influence on the characteristics of the shock absorber.

The shock absorber should exert a force ideally proportional to the extension of the suspension and the compression speed; forces and bending, on the other hand, cause an almost constant friction that is independent of speed. This and other types of friction cause suspension hysteresis, which can be interpreted as the minimum force that we must apply to suspension to make it move.

Hysteresis is not desired because it causes the suspension to lock when the applied forces are less than a minimum value. This feature of the MacPherson suspension must be recognized as an inconvenience.

Advantages:

- Simple planning and reduced costs.
- Due to the relative separation of the body's joints, the forces exerted on the body are low compared, for example, to a double wishbone suspension.
- Higher suspension travel than other suspensions (for example the double wishbone suspension with high arm).
- Transversal size contained, due to the absence of the upper arm; useful when using a transverse motor.

- Ability to design with superior longitudinal flexibility, without significantly affecting the wheel angle.
- Freedom in designing elasto-kinematic properties; the recovery of the camber is limited only by practicable positions for the upper pin and the fixed joint of the lower arm.
- The relationship between suspension and shock travel is close to one. The shock absorbers therefore work well with limited loads, low oil heating and valve wear.

Disadvantages:

- Lower performance in the recovery of the camber.
- The characteristic geometry of the suspension determines a position for the interface of the upper pin with the body, generally called the dome, which is usually very far from the more rigid structures of the body, the lateral beams. This causes significant problems with the suppression of vibrations and road noise.
- Deformation of the damper piston rod can increase friction and hysteresis.
- Considerable height for the upper pin, so that the spring and the shock absorber are positioned above the wheel; this fact could penalize the aerodynamics of the vehicle and the body style in the case of a sports car.

Trailing arm suspension

This architecture is widely applied in small and medium-sized cars only on the rear axles.

Both wheels are fixed to a longitudinal arm free to rotate with respect to the body: the rotation axis of the two arms is generally the same and is parallel to the vehicle axis (fig. 4).

During the suspension stroke the wheelbase is involved but the tip angles remain unchanged. The camber of the wheel with reference to the ground is equal to the body roll; so, there is no recovery of the camber.

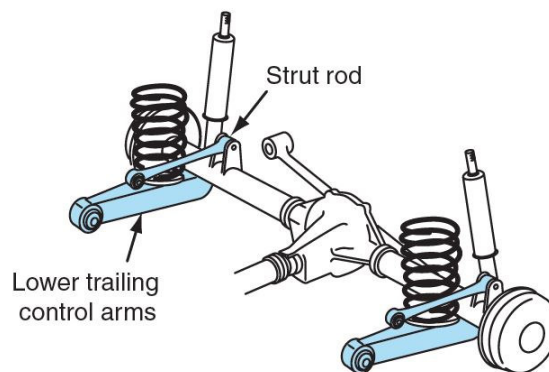


Figure 4 – Trailing Arm Suspension

The axis has two oscillating arms connected to an auxiliary frame through a transversal rotation axis; the subframe is connected to the body by four elastic bearings. This auxiliary frame consists

of two shells of stamped sheet steel, welded to a tubular beam. If the subframe is not applied, the arm bearings can be fixed directly on the body.

The part of the upper lower spring is connected in each shell. The upper part of the springs is connected to the frame via a bracket.

The suspension arm integrates the lower part and the spring support, the shock absorber base and the wheel bearing housing or pin.

The anti-roll bar is fixed to the arms directly in two different points on each arm; it is not fixed directly on the frame. For this reason, it is also called floating bar.

Advantages:

- The hysteresis is very low with the roller bearing versions.
- The intrusion into the suspension in the trunk is minimal.
- High simplicity and therefore low production costs.
- Easy assembly.
- Also suitable for drive axles.
- Reduced value for unsprung mass.

Disadvantages:

- Transverse deformations of the rear arms caused by cornering forces have an oversteering effect.
- No recovery of camber.
- Low longitudinal flexibility due to the rigidity of high load bearings.
- There are no independent parameters to tune to improve elasto-kinematic behaviour.
- High transmission of vibrations from the wheel due to the rigidity of the bearing, also due to the value of the loads acting.

This solution is mainly used in low-end market segments.

Semi-trailing arm suspension

Unlike trailing arm suspension, which have arms that rotate around the same transverse axis, in this case semi-trailing arm or triangles rotate around two different symmetrical axes (fig. 5).

The inclination angles of the arm allow to obtain a modest recovery of the camber and a certain variation of the toe angle with understeer effect, with a slight improvement of the elasto-kinematic behaviour.

The axle is formed by two oscillating triangular arms articulated on an auxiliary frame, being fixed to the bodywork.

The auxiliary frame consists of a cylindrical tube with two moulded steel shells at the two ends; the arms are also made with two moulded half-shells welded together.

Unlike the trailing arm suspension, here it is possible to use elastic bushings for the connections of the arm to the body, thanks to the greater distance between the two points of articulation.

This type of suspension also allows, given its small size, to be able to install a spare wheel under the hood.

The axis of rotation of the arm can cross the centre of the joint at constant speed; this condition avoids the variation of the shaft length and allows the application of very simple joints.

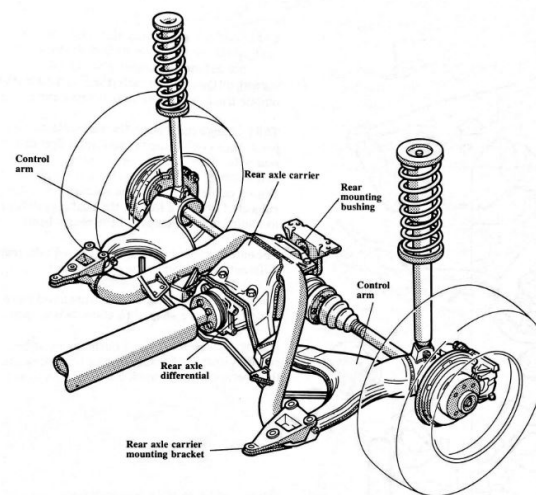


Figure 5 – Semi Trailing Arm Suspension

Advantages:

- Limited vertical size
- Limited unsprung mass
- Reasonable design possibilities in terms of elasto-kinematic properties
- Construction simplicity
- Suitable for rear wheel drive

Disadvantages:

- The transverse dimension penalizes the layout of the underbody components
- An excessive variation of the track due to the suspension travel can cause premature tire wear

This solution is currently used only on microcars or quadricycles.

Guided trailing arm suspension

The guided trailing arm suspensions (fig.6) were designed to improve the trailing arm suspensions; therefore, the degrees of freedom have increased compared to the previous one, leaving its strength, its impact in the trunk unchanged.

The name is not universally recognized, many manufacturers use different names, but with this name you can guess its derivation and its functioning considering the suspension from which it derives.

In guided drive arm suspensions, two or three additional arms are connected to the drive arm, in order to improve the elastic-kinematic performance of the suspension.

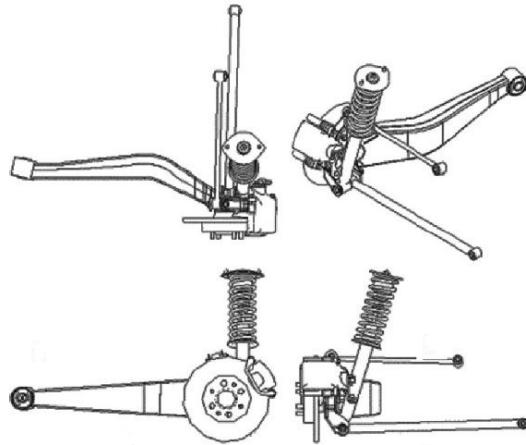


Figure 6 – Guided Trailing Arm Suspension

To restore the correct number of degrees of freedom of the mechanism, the connection between the driving arm and the body or the auxiliary frame is made by a sufficiently flexible rubber bushing.

The driving arm is guided by two additional transverse arms which identify a steering axis through the two elastic bushings. This axle is designed to create a certain variation of the understeer toe angle, under the action of the cornering force or the braking force. The elastic bushings can provide excellent longitudinal flexibility and therefore greater comfort and allow longitudinal movements without having unwanted steering rotation.

On the market there are also cases in which the transverse arms are not two, but three, with a further increase in the elasto-kinematic properties (in this case the two arms can provide the correct recovery of the camber while the third reacts to longitudinal loads to stabilize the vehicle in an understeer situation).

Advantages:

- Variation of the toe angle in curves and longitudinal forces with stabilizing effect
- Adequate camber recovery
- Good longitudinal flexibility
- Limited underfloor volume similar to simple suspension

Disadvantages:

- Limitation of the wheel box if the shock absorbers are applied to the rear arms
- Many adjustment points for correct assembly on the subframe
- Greater cost complexity than previous solutions

Because of these characteristics, guided trailing arm suspension are used on medium-sized cars, where it represents a good compromise between sophisticated multilink suspension and trailing arm suspension or MacPherson suspension; this architecture could be widely adopted in the future.

Twist beam axle suspensions

This type of suspension (fig. 7) is of the semi-independent type. It can be imagined as two rear arms fixed to the frame with an elastic bush; the intrinsic instability of the resulting structure is corrected by a crossbar. The spring shock absorber is fixed between the arms and the frame.

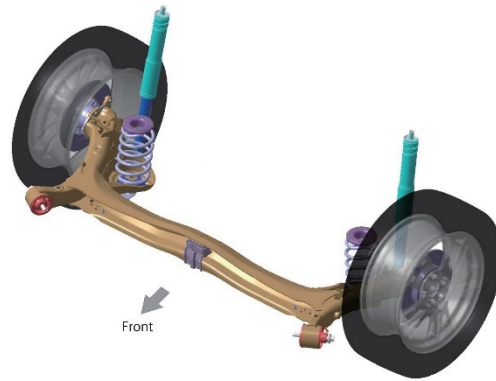


Figure 7 – Twist Beam Axle Suspension

The arm consists of two shells in pressed and welded steel. The hub will be flanged on the plate welded on the arm. The seat of the spring is modelled on one of the moulded shells, building the arm; the attachment of the lower shock absorber will be screwed onto a tube, also welded on the shell.

The crosshead has a U-shaped cross section and is welded to the arms at its end. The anti-roll bar is also welded to the arms.

The crosshead has a U-shaped cross section and is welded to the arms at its end. The anti-roll bar is also welded to the arms.

In the event of a symmetrical suspension stroke, the arms rotate around the axis obtained by joining the two centres of the elastic bushings of the arms; there are no variations in the tip angles and camber due to the suspension travel, in addition to the structural deformation caused by external forces.

Following an asymmetrical stroke, the crosspiece is twisted by the difference in torque applied to the arms and, only because of this deformation, the arms can have different angles around the non-coincident axes.

We will therefore have a minor variation in the camber angle in the event of a symmetrical stroke. Furthermore, to obtain variations on the toe angle and on the camber angle it will be necessary to modify the cross section.

A parameter that affects the comfort and handling of the vehicle is the position of the spring and the shock absorber. The optimal position for the shock absorber is perpendicular to the arm and as far as possible from the point of articulation with the frame. This however involves a problem with the spring, because this must reduce the load compartment by ending up inside the wheel arch, especially in the case of a spring coaxial with the shock absorber.

A further system to limit the lateral deformation of the arms due to the cornering forces is the use of a Panhard bar; this system is suitable for heavy cars, such as high-end minivans, when other solutions can negatively affect comfort.

Advantages:

- Simplicity of planning
- Easy assembly
- Small vertical size
- Almost total recovery of the camber by asymmetric strokes
- Ability to control the angle of the tip by rolling the body
- Smaller unsprung mass as with a rigid axle
- Reasonable longitudinal elasticity

Disadvantages:

- Wide width of the wheel box due to the variation of the camber change expected
- Low rigidity of the roll
- Highly stressed parts (torsion beam and its welding)
- Not suitable for drive axles
- Toe angles too sensitive to load
- Significantly different behaviour in empty or full load conditions

These suspensions are widely used on small and medium-sized cars.

2. Analytical analysis of vehicle dynamics and forces acting on the suspension

A MacPherson strut suspension is usually used for front suspension of vehicles. A MacPherson strut suspension lacks an upper arm, so a damper and a spring play the role of upper arm. Hence, a MacPherson strut suspension, having a simple structure, may save space and can be manufactured as a light system. A MacPherson strut suspension can save manufacturing cost and thus it is usually applied to production cars.

However, due to the structural characteristics, a side load is generated at the damper of MacPherson strut suspension when wheel moves up and down and it results in friction at the damper, reducing the riding comfort. During the vehicle driving, the abrupt accelerations can occur by an obstruction. And when the side load is generated at the damper, the damper cannot react sufficiently to the abrupt accelerations. Therefore, acceleration is transmitted directly to the vehicle and this reduces the riding comfort. Many studies have been conducted to decrease the side load generated at the damper to improve the riding comfort.

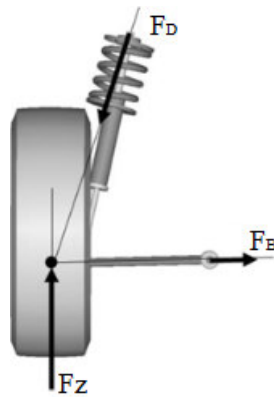


Figure 8 – Forces acting on the MacPherson strut suspension

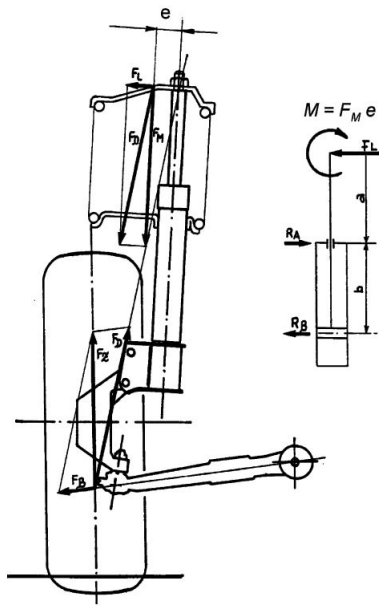


Figure 9 – Generation of the side load

$$R_A = \frac{1}{b} [F_L(a + b) - M]$$

$$R_B = \frac{1}{b} [F_L a - M]$$

$$R_T = |R_A| + |R_B|$$

Fig. 8 illustrates the forces acting on a MacPherson strut suspension.

F_z is the force acting on the wheel, F_B is the reaction force of the link, and F_D is the reaction force of the top of damper. Considering the reaction force of the spring, F_D , the forces can be illustrated as in Fig. 9 by using force vectors. This shows that the reaction force of the spring, F_D , is not consistent with the reaction force of the top of damper, therefore the side load F_L is generated which acts perpendicularly on the axis of the shock absorber. As shown in Fig. 9, the side load F_L causes the reaction forces R_A and R_B , at two points of the damper where the rod and the piston are in contact with the cylinder, respectively. The side load is inevitably generated due to the structure of the MacPherson strut suspension and decreases the riding comfort by causing friction at the damper.

Thus, in order to find the value of the lateral force acting on the damper, it is necessary to initially analyse the dynamic behaviour of the vehicle and then the MacPherson suspension.

a. The full vehicle models

The performance of the vehicle is presented through a full vehicle model with eight degrees of freedom which is presented in Fig. 10. The vertical, rolling and pitching motions indicate the performance of vehicle. The yaw motion of vehicle is not considered since its influence on road holding and comfort of vehicle is negligible. The suspension and vehicle seat are expressed by a parallel mounting of a linear damper and spring. Equivalent spring stiffness is substituted with

the tire; damping of tire is neglected. The equations of motion for the vehicle model, which is indicated in Fig. 10, are attained by utilizing the Newton–Euler theory. In the full vehicle model, each of four unsprung mass and driver seat has one degree of freedom and chassis has 3 degrees of freedom which are declared as bounce, pitch and roll. The vehicle model consists of the following parameters: m_p , m_s , m_{us_1} , m_{us_2} , m_{us_3} and m_{us_4} which are the masses for the passenger, vehicle sprung mass and first, second, third and fourth unsprung masses, respectively; damping coefficients are presented by c_p , c_{us_1} , c_{us_2} , c_{us_3} , c_{us_4} . The spring stiffness coefficients are expressed by k_p , k_{s_1} , k_{s_2} , k_{s_3} , k_{s_4} which are the stiffness of the passenger seat and suspension springs; k_{t_1} , k_{t_2} , k_{t_3} and k_{t_4} present stiffness of the tire. In this case, equations of motion would be calculated through Eqs. 1 to 18

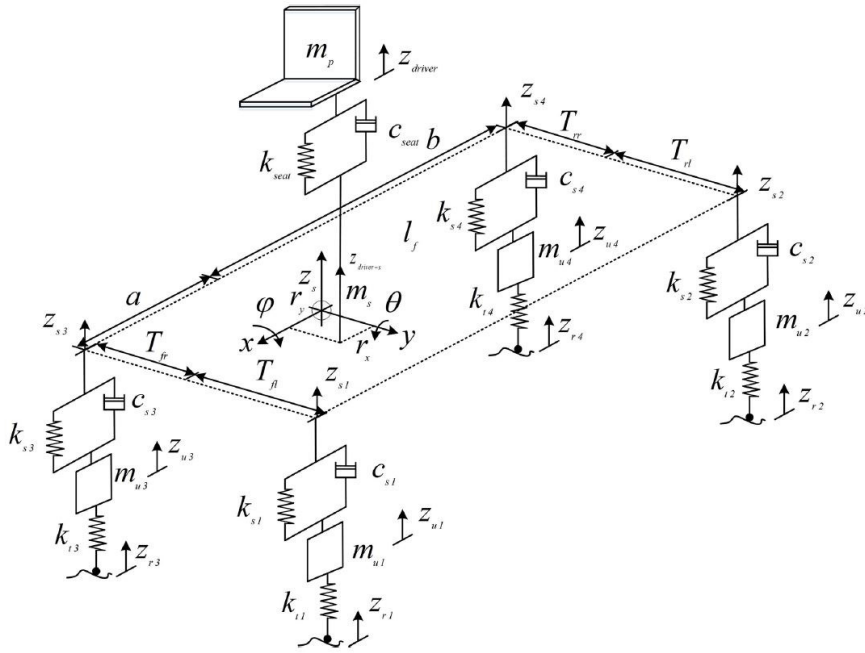


Figure 10 – Vehicle vibration model with 8 degrees of freedom

$$z_{driver-s} = z_s - r_x \theta + r_y \varphi \quad (1)$$

$$z_{s_1} = z_s - a\theta + T_{fl}\varphi \quad (2)$$

$$z_{s_3} = z_s - a\theta + T_{fr}\varphi \quad (3)$$

$$z_{s_2} = z_s + b\theta + T_{rl}\varphi \quad (4)$$

$$z_{s_4} = z_s + b\theta + T_{rr}\varphi \quad (5)$$

$$F_{ss} = k_p(z_{driver} - z_{driver-s}) + c_p(\dot{z}_{driver} - \dot{z}_{driver-s}) \quad (6)$$

$$F_{s_1} = k_1(z_{s_1} - z_{u_1}) + c_1(\dot{z}_{s_1} - \dot{z}_{u_1}) \quad (7)$$

$$F_{s_2} = k_2(z_{s_2} - z_{u_2}) + c_2(\dot{z}_{s_2} - \dot{z}_{u_2}) \quad (8)$$

$$F_{s_3} = k_3(z_{s_3} - z_{u_3}) + c_3(\dot{z}_{s_3} - \dot{z}_{u_3}) \quad (9)$$

$$F_{s_4} = k_4(z_{s_4} - z_{u_4}) + c_4(\dot{z}_{s_4} - \dot{z}_{u_4}) \quad (10)$$

$$m_c \ddot{z}_{driver} = -F_p \quad (11)$$

$$m_c \ddot{z}_s = -F_{s_1} - F_{s_2} - F_{s_3} - F_{s_4} + F_p \quad (12)$$

$$I_{sy} \ddot{\theta} = aF_{s_1} + aF_{s_3} - bF_{s_2} - bF_{s_4} - r_x F_p \quad (13)$$

$$I_{sy} \ddot{\varphi} = -T_{fl}F_{s_1} - T_{fr}F_{s_3} - T_{rl}F_{s_2} + T_{rr}F_{s_4} + r_y F_p \quad (14)$$

$$m_1 \ddot{z}_1 = F_{s_1} - k_{t_1}(z_{u_1} - z_{r_1}) \quad (15)$$

$$m_2 \ddot{z}_2 = F_{s_2} - k_{t_2}(z_{u_2} - z_{r_2}) \quad (16)$$

$$m_3 \ddot{z}_3 = F_{s_3} - k_{t_3}(z_{u_3} - z_{r_3}) \quad (17)$$

$$m_4 \ddot{z}_4 = F_{s_4} - k_{t_4}(z_{u_4} - z_{r_4}) \quad (18)$$

It is assumed that rear wheels of the vehicle follow the front one with a same trajectory and delay of $T = (a + b)/v$. Which a and b indicate the distance of front and rear wheel from the center of mass gravity and v the velocity. Most of the times, the pitching rotation is more troublesome than vertical movement. For enhancing the road holding capability and decreasing the pitch rotations, the front suspension has a lower stiffness value than the rear suspension according to the center of gravity. The following expression indicates this matter:

$$\begin{aligned} b \cdot k_{us_2}^2 &\geq a \cdot k_{us_1}^2 \\ b \cdot k_{us_4}^2 &\geq a \cdot k_{us_3}^2 \end{aligned} \quad (19)$$

$k_{us_3}^2$ and $k_{us_4}^2$ are equivalent static stiffness of rear suspensions in left and right side. $k_{us_1}^2$ and $k_{us_2}^2$ are equivalent static stiffness of front suspensions in left and right side, respectively.

$$\begin{aligned} k_{us_1}^2 &= \frac{k_{s_1} k_{t_1}}{k_{s_1} + k_{t_1}} & k_{us_2}^2 &= \frac{k_{s_2} k_{t_2}}{k_{s_2} + k_{t_2}} \\ k_{us_3}^2 &= \frac{k_{s_3} k_{t_3}}{k_{s_3} + k_{t_3}} & k_{us_4}^2 &= \frac{k_{s_4} k_{t_4}}{k_{s_4} + k_{t_4}} \end{aligned} \quad (20)$$

b. Model of Macpherson Suspension

The schematic of a Macpherson strut suspension is shown in Fig.11. To model a Macpherson suspension system for control application, one should take into account both the kinematics and dynamics of the system subjected to the actuation force and road disturbances.

Kinematic

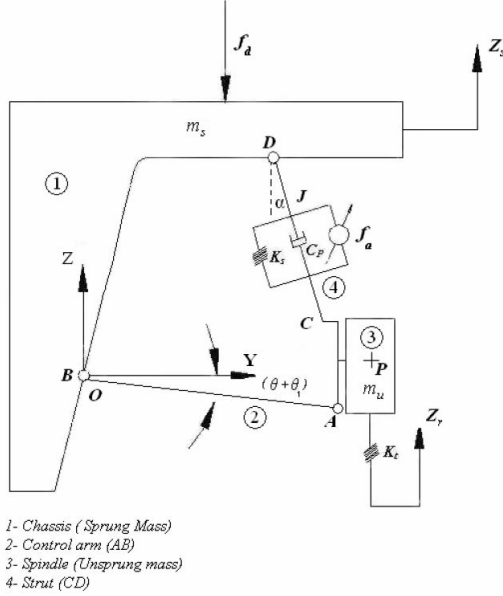


Figure 11 – Model of Macpherson suspension

Consider a Macpherson suspension system excited by road disturbance (z_r) as shown in Fig. 11. It comprises a quarter-car body, a spindle and a tire, a helical spring, control arm, load disturbance (f_d) and an actuation force (f_a). The structure has two degrees of freedom including vertical displacement of the sprung mass and rotational motion of the control arm when the mass of the strut is ignored and the bushing at point D is assumed to be a pin joint. In this research, we focus on building a two DOF model of a Macpherson suspension system.

The detailed assumptions in this modelling are made as follows: The sprung mass has only vertical displacement while movements in other directions are ignored. The unsprung mass (spindle and tire) is connected to the car body through the damper and spring as well as the control arm. The values of z_s , vertical displacement of the sprung mass, and θ , rotational displacement of the control arm, are measured from the static equilibrium position and are considered as generalized coordinates. It is assumed that, in the equilibrium condition, the camber angle is zero. Compared to the other links, the mass and stiffness of the strut are neglected. The spring and tire deflections and the damping force are assumed to be in the linear regions of their operation ranges. In Fig. 11, link AB represents the control arm, which is modelled as a rod, while line CD shows the strut of the mechanism. The revolute joint, located between the control arm and the chassis, is modelled as a rotational joint at point B. In addition, let assume that the origin of the coordinate system, O, is on point B and (y_A, z_A) , (y_B, z_B) , (y_J, z_J) , (y_P, z_P) , (y_C, z_C) and (y_D, z_D) denote the coordinates of the points A, B, J, P, C and D, respectively. Under road disturbances, the position of the key points on the sprung mass change as the following:

$$y_B = 0; z_B = z_s; y_D = y_{D_1}; z_D = z_{D_1} + z_s \quad (21)$$

In addition, the displacements of the main points on the spindle are introduced as:

$$\begin{bmatrix} y_C & y_J & y_P \\ z_C & z_J & z_P \\ 1 & 1 & 1 \end{bmatrix} = \begin{bmatrix} a_{11} & a_{12} & y_A - (a_{11}y_{A_1} + a_{12}z_{A_1}) \\ a_{21} & a_{22} & z_A - (a_{21}y_{A_1} + a_{22}z_{A_1}) \\ 0 & 0 & 1 \end{bmatrix} \times \begin{bmatrix} y_{C_1} & y_{J_1} & y_{P_1} \\ z_{C_1} & z_{J_1} & z_{P_1} \\ 1 & 1 & 1 \end{bmatrix} \quad (22)$$

where (y_{A_1}, z_{A_1}) , (y_{J_1}, z_{J_1}) , (y_{P_1}, z_{P_1}) , (y_{C_1}, z_{C_1}) are the coordinates of the points A, J, P and C at equilibrium position. Further,

$$\begin{aligned} a_{11} &= a_{22} = \cos \varphi \\ a_{12} &= -a_{21} = \sin \varphi \end{aligned} \quad (23)$$

where φ is the rotation angle of the wheel. System of equations (22), is made of six equations containing nine unknown parameters which are (y_A, z_A) , (y_J, z_J) , (y_P, z_P) , (y_C, z_C) and φ . To solve this system, it is necessary to employ constraint equations as follows:

$$\begin{aligned} z_C &= \alpha(y_C - y_D) + z_D \\ z_J &= \alpha(y_J - y_D) + z_D \\ y_A &= L_A \cos(\theta + \theta_1) + y_B \\ z_A &= L_A \sin(\theta + \theta_1) + z_B \end{aligned} \quad (24)$$

where α is the slope of the strut, L_A is the length of the control arm and θ_1 is the initial angle of the control arm resulting from the static deflection and structure design. Considering equations (22) and (24), results in ten equations including ten unknown parameters, namely, (y_A, z_A) , (y_J, z_J) , (y_P, z_P) , (y_C, z_C) , α and φ . Thus, the following equations of displacements can be established:

$$\begin{aligned} y_C &= (y_{C_1} - y_{A_1})a_{11} + (z_{A_1} - z_{C_1})a_{21} + y_A \\ z_C &= (y_{C_1} - y_{A_1})a_{21} + (z_{C_1} - z_{A_1})a_{11} + z_A \\ y_J &= (y_{J_1} - y_{A_1})a_{11} + (z_{A_1} - z_{J_1})a_{21} + y_A \\ z_J &= (y_{J_1} - y_{A_1})a_{21} + (z_{J_1} - z_{A_1})a_{11} + z_A \\ y_P &= (y_{P_1} - y_{A_1})a_{11} + (z_{A_1} - z_{P_1})a_{21} + y_A \\ z_P &= (y_{P_1} - y_{A_1})a_{21} + (z_{P_1} - z_{A_1})a_{11} + z_A \\ z_C &= \alpha(y_C - y_D) + z_D \\ z_J &= \alpha(y_J - y_D) + z_D \\ y_A &= L_A \cos(\theta + \theta_1) \\ z_A &= L_A \sin(\theta + \theta_1) + z_s \end{aligned} \quad (25)$$

When solving the above system of equations, one determines parameter φ as a function of generalized coordinates θ and z_s . Subsequently, the other unknown parameters including (y_A, z_A) , (y_J, z_J) , (y_P, z_P) , (y_C, z_C) and α can be specified. Hence, the displacements of all key points are determined as functions of independent variables θ and z_s . The next step is to find the velocities

of the key points. By taking the derivative of (25), one can obtain the velocity components of the main points. When solving the equations of velocities, the value of $\dot{\varphi}$ is determined as following:

$$\dot{\varphi} = \frac{(z_A - ay_A - z_D)(y_C - y_J)}{h} \quad (26)$$

Where

$$h = (y_C - y_A + az_C - az_A)(y_J - y_D) - (y_J - y_A - az_J - az_A)(y_C - y_D)$$

Equation of motion

Lagrange's method is used to obtain the equations of motion of the new model. The kinetic energy, T , is given by

$$T = \frac{1}{2}(m_s + m_{ca})(\dot{z}_s)^2 + \frac{1}{2}m_u(\dot{y}_p^2 + \dot{z}_p^2) + \frac{1}{2}I_u\dot{\varphi}^2 + \frac{1}{2}I_{ca}^B\dot{\theta}^2 \quad (27)$$

where m_s , m_u and m_{ca} , are the car body, wheel and control arm masses, respectively. I_u and I_{ca}^B represent, in turn, the inertia moments of the wheel and the control arm where the latter is around point B. The potential energy, V , is defined as

$$V = \frac{1}{2}K_s(\Delta L)^2 + \frac{1}{2}K_t(\Delta z)^2 \quad (28)$$

where K_s and K_t are the stiffness coefficients of the sprung and unsprung masses, respectively. Moreover, the deflection of the spring ΔL , and the deflection of the tire Δz are:

$$\Delta L = \sqrt{[(y_C - y_D)^2 + (z_C - z_D)^2]} - \sqrt{[(y_{C_1} - y_{D_1})^2 + (z_{C_1} - z_{D_1})^2]} \quad (29)$$

$$\Delta z = z_p - z_r = (y_{A_1} - y_{P_1})\varphi + (z_{P_1} - z_{A_1}) + L_A \sin(\theta + \theta_1) + z_s - z_r \quad (30)$$

The damping function, D , is given by

$$D = \frac{1}{2}C_p(\dot{\Delta L})^2 \quad (31)$$

where C_p is the damping coefficient and the relative velocity of damper $\dot{\Delta L}$ is:

$$\dot{\Delta L} = [\dot{y}_C(y_C - y_D) + (\dot{z}_C - \dot{z}_D)(z_C - z_D)] \times \frac{1}{\sqrt{[(y_C - y_D)^2 + (z_C - z_D)^2]}} \quad (32)$$

substituting the values of y_p and z_p , obtained from derivative of (25), and $\dot{\varphi}$, attained from (26), into (27) as well as using Lagrange's equations along with the generalized coordinates z_s and θ , one can obtain the accelerations of the generalized coordinates as the following:

$$\begin{aligned} & (m_s + m_u + m_{ca})\ddot{z}_s \\ & + m_u L_A \left[\cos(\theta + \theta_1) + [\cos(\theta + \theta_1) + \alpha \sin(\theta + \theta_1)] \frac{(y_C - y_J)(y_P - y_A)}{h} \right] \ddot{\theta} \\ & = f_1 \ddot{z}_s + f_2 \ddot{\theta} \quad (33) \end{aligned}$$

And

$$\begin{aligned} & m_u \left[L_A \cos(\theta + \theta_1) + (y_P - z_A) \frac{\partial \dot{\varphi}}{\partial \dot{\theta}} \right] \ddot{z}_s \\ & + \left[m_u L_A \left[[\cos(\theta + \theta_1) + \alpha \sin(\theta + \theta_1)] \frac{(y_C - y_J)(z_A - z_P)}{h} - \sin(\theta + \theta_1) \right] \right. \\ & \times \left[-L_A \sin(\theta + \theta_1) + (z_A - z_P) \frac{\partial \dot{\varphi}}{\partial \dot{\theta}} \right] \\ & + m_u L_A \left[L_A \cos(\theta + \theta_1) + (y_P - z_A) \frac{\partial \dot{\varphi}}{\partial \dot{\theta}} \right] \\ & \times \left[[\cos(\theta + \theta_1) + \alpha \sin(\theta + \theta_1)] \frac{(y_C - y_J)(y_P - y_A)}{h} + \cos(\theta + \theta_1) \right] \\ & \left. + I_u \dot{\varphi} \frac{\partial \dot{\varphi}}{\partial \dot{\theta}} \right] \ddot{\theta} = f_3 \ddot{z}_s + f_4 \ddot{\theta} \quad (34) \end{aligned}$$

Since the equations are highly nonlinear and too complicated, the higher order nonlinearities in Eqs. 33 and 34 are ignored to simplify the equations. Let us denote

$$\begin{aligned} H_1 &= -\frac{\partial T}{\partial z_s} & H_2 &= -\frac{\partial V}{\partial z_s} & H_3 &= -\frac{\partial D}{\partial z_s} \\ H_4 &= -\frac{\partial T}{\partial \theta} & H_5 &= -\frac{\partial V}{\partial \theta} & H_6 &= -\frac{\partial D}{\partial \theta} \end{aligned}$$

Hence, one has

$$f_1 \ddot{z}_s + f_2 \ddot{\theta} = \frac{\partial \vec{r}_C}{\partial z_s} \cdot f_a + f_d + H_3 - H_1 - H_2 = F_1$$

And

$$f_3 \ddot{z}_s + f_4 \ddot{\theta} = \frac{\partial \vec{r}_C}{\partial \theta} \cdot f_a + H_6 - H_4 - H_5 = F_2$$

The nonlinear equations of motion are obtained as below

$$\begin{aligned} f_1(z_s, \dot{z}_s, \theta, \dot{\theta})\dot{z}_s + f_2(z_s, \dot{z}_s, \theta, \dot{\theta})\ddot{\theta} &= F_1(z_s, \dot{z}_s, \theta, \dot{\theta}) \\ f_3(z_s, \dot{z}_s, \theta, \dot{\theta})\dot{z}_s + f_4(z_s, \dot{z}_s, \theta, \dot{\theta})\ddot{\theta} &= F_2(z_s, \dot{z}_s, \theta, \dot{\theta}) \end{aligned} \quad (35)$$

Solving the above system, the acceleration of the generalized coordinates are obtained as follows:

$$\begin{aligned} \ddot{z}_s &= \frac{f_4 F_1 - f_2 F_2}{f_4 f_1 - f_2 f_3} = g_1(z_s, \dot{z}_s, \theta, \dot{\theta}) \\ \ddot{\theta} &= \frac{f_1 F_2 - f_3 F_1}{f_4 f_1 - f_2 f_3} = g_2(z_s, \dot{z}_s, \theta, \dot{\theta}) \end{aligned} \quad (36)$$

At this point let us introduce the state variables as $[x_1, x_2, x_3, x_4]^T = [z_s, \dot{z}_s, \theta, \dot{\theta}]^T$, then (36) can be written in the state space format as follows.

$$\begin{aligned} \dot{x}_1 &= x_2 \\ \dot{x}_2 &= g_1(z_s, \dot{z}_s, \theta, \dot{\theta}, f_a, f_d, z_r) \\ \dot{x}_3 &= x_4 \\ \dot{x}_4 &= g_2(z_s, \dot{z}_s, \theta, \dot{\theta}, f_a, f_d, z_r) \end{aligned} \quad (37)$$

Since the equations are nonlinear and working with them is non-trivial task and employing a complex nonlinear controller is essential, all of equations are linearized at the equilibrium state where, $(x_{1_e}, x_{2_e}, x_{3_e}, x_{4_e}) = (0,0,0,0)$. The resulting equations are:

$$\begin{aligned} \dot{x} &= Ax(t) + B_1 f_a(t) + B_2 z_r(t) + B_3 f_d(t) \\ x(0) &= x_e \end{aligned} \quad (38)$$

$$A = \begin{bmatrix} 0 & 1 & 0 & 0 \\ \frac{\partial g_1}{\partial x_1} & \frac{\partial g_1}{\partial x_2} & \frac{\partial g_1}{\partial x_3} & \frac{\partial g_1}{\partial x_4} \\ 0 & 0 & 0 & 1 \\ \frac{\partial g_2}{\partial x_1} & \frac{\partial g_2}{\partial x_2} & \frac{\partial g_2}{\partial x_3} & \frac{\partial g_2}{\partial x_4} \end{bmatrix}_{x_e}$$

$$B_1 = \begin{bmatrix} 0 & \frac{\partial g_1}{\partial f_a} & 0 & \frac{\partial g_2}{\partial f_a} \end{bmatrix}_{f_a=0}$$

$$B_2 = \begin{bmatrix} 0 & \frac{\partial g_1}{\partial z_r} & 0 & \frac{\partial g_2}{\partial z_r} \end{bmatrix}_{z_r=0}$$

$$B_3 = \begin{bmatrix} 0 & \frac{\partial g_1}{\partial f_d} & 0 & \frac{\partial g_2}{\partial f_d} \end{bmatrix}_{f_d=0}$$

3. Simulations on Adams and recollection of information

a. Definition of the type of vehicle used and preparation of the models

In order to determine how to minimize the lateral forces on the suspension and analyse the components that determine a change in the stability of the vehicle, there are many ways to go. In our case, the solution designed was the introduction of an angle between the spring axis and the shock absorber axis to minimize the load on the top mount, and therefore on the shock itself.

To carry out these tests we used the MSC Adams software, in particular the application ADAMS/Car, which simulates the behaviour of a car in a number of conditions.

In the absence of a model of a real production car, the choice was to use one of the models that the program offers in its catalog. Among the various options, the model we have chosen corresponds to a Sedan-type car with front-wheel drive (fig. 12).

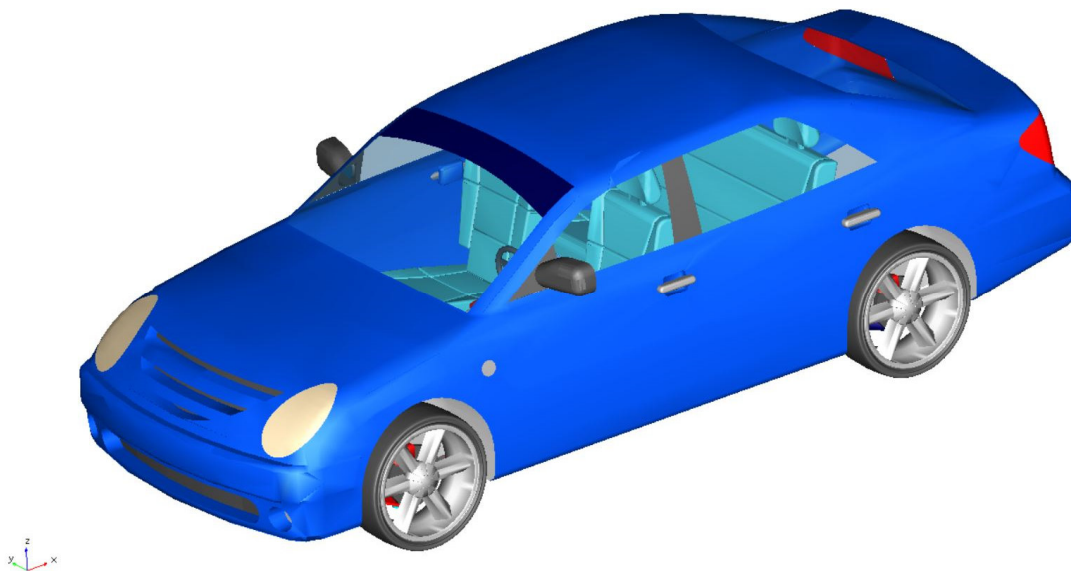


Figure 12 – Sedan AWD

The car in question has the following characteristics:

- Sprung mass = 1666.24 kg
- Mass = 1849.2183 Kg
- Wheelbase = 2720.43 mm
- Unsprung mass Front Suspension = 98.97 kg
- Unsprung mass Rear Suspension = 84.02 kg

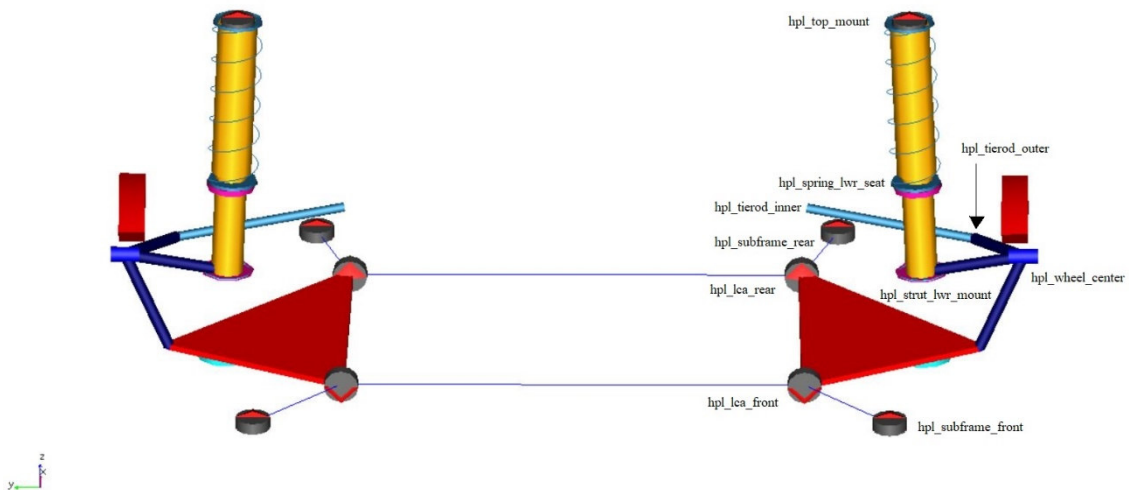


Figure 13 – MacPherson Suspension (Adams Version)

As for the values of the front MacPherson suspension (fig. 13), which is the reason for this discussion, we have:

- Toe Angle = -0.1646 deg
- Caster Angle = 7.64 deg
- Camber Angle = -0.4554 deg
- Kingpin Angle = 11.18 deg
- Scrub radius = 55.60 mm
- Caster trail = 38.43 mm

These values are to be considered as an average between the left side and the right side of the car.

In addition, the characteristics of the suspension are defined by:

- Spring stiffness = 20 kN/m
- Spring installed length = 110 mm
- Damper Coefficient = 1200 Ns/m

Once the type of car to be used was defined, the inclination of the spring axis with respect to the shock absorber axis was defined, using the top mount as the hinge for the inclination. In the configuration provided by Adams, henceforth called the default configuration, the axis of the spring and that of the shock absorber are coincident. So, it was necessary to change the angle.

The characteristic of the models used in Adams, and in particular the models related to the suspensions used, is that they are defined by particular points, called Hardpoints, which define

the layout and structure of the suspension itself. it is therefore obvious that the definition of the position of the spring in space is characterized by the values of these Hardpoints (in table 1 the values referred to the left suspension are shown).

	$X [mm]$	$Y [mm]$	$Z [mm]$
<i>hpl_lca_front</i>	60	-400	190
<i>hpl_lca_outer</i>	240	-700	175
<i>hpl_lc_rear</i>	460	-390	205
<i>hpl_spring_lwr_seat</i>	300	-590	465
<i>hpl_strut_lwr_mount</i>	300	-600	290
<i>hpl_subframe_front</i>	-140	-550	215
<i>hpl_subframe_rear</i>	66	-450	190
<i>hpl_tierod_inner</i>	467	-400	330
<i>hpl_tierod_outer</i>	410	-690	300
<i>hpl_top_mount</i>	317.5	-580	755
<i>hpl_wheel_center</i>	260	-776	340

Table 1 – Hardpoint MacPherson Suspension

Extracted the suspension hardpoints were imported on parametric 3D modelling software. Here, positioned in the space the points relating to the suspension, it was possible to act on the modification of the points.

The points taken into consideration for changing the spring coordinates are:

- *hpl_spring_lwr_seat*,
- *hpl_top_mount*.

By imposing physical limitations on the components in question, therefore the diameter of the coils of the spring and the external diameter of the shock absorber (provided by the characteristics of the components themselves on Adams), a variety of possible angular positions was assumed. The dimensions of the components themselves, with the progressive increase in inclination, caused the introduction, in the area relating to the top mount, of an eccentricity. Considering as negative the direction that goes towards the outside of the car and as positive towards the opposite direction, 40 possible variations have been defined, from -20° to $+20^\circ$, with intervals of 1° .

For each angle variation we obtained the spatial coordinates of the spring, which were transferred to the Adams suspension model. As many suspensions as, possible corner configurations were

created for the occasion, and therefore as many models of the car, in order to have all the possible configurations available.

Having defined the type of car to be used and obtained the possible configurations to be used, we considered what type of variables were to be taken into consideration to carry out the analysis and therefore obtain a suspension configuration that could solve the problem concerning the reduction of lateral forces and possibly an improvement in vehicle stability.

The variables studied are:

- Top Mount Lateral Force (Left and Right Wheel)
- Top Mount Lateral Displacement (Left and Right Wheel)
- Top Mount Longitudinal Displacement (Left and Right Wheel)
- Top Mount Vertical Displacement (Left and Right Wheel)
- Chassis Lateral Acceleration
- Chassis Longitudinal Acceleration
- Chassis Vertical Acceleration
- Camber Angle (Left and Right Wheel)
- Chassis Pitch Angle
- Chassis Roll Angle

b. Static Analysis and Test Definition

After defining the type of vehicle used and creating the variants to be examined, a verification of the characteristics of the car was carried out in static mode in the default configuration, therefore with the vehicle stationary. In this sense Adams allows us to carry out a simulation of the car in static conditions, considering the gearbox inserted in position N.

This test was then repeated for all the configurations created, to define, in a first approximation, the direction of the inclination of the spring that allows to obtain a variation of the lateral force and of the other parameters relating to stability.

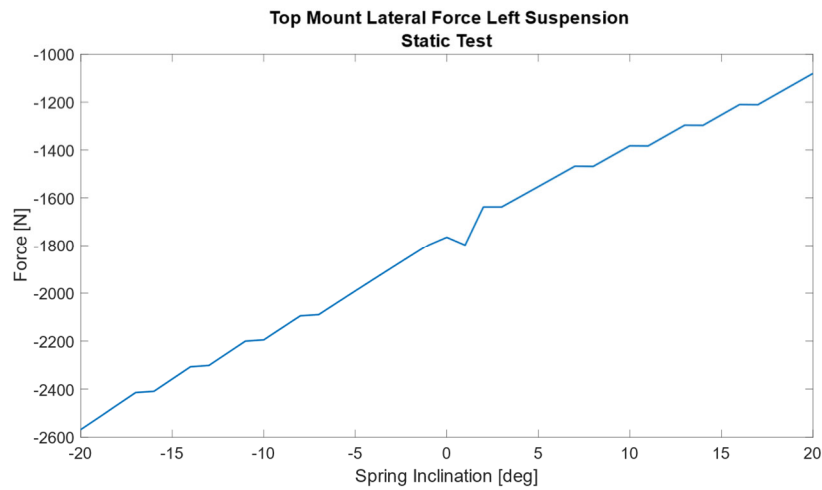


Figure 14 – Top Mount Lateral Force Left Suspension – Static Test

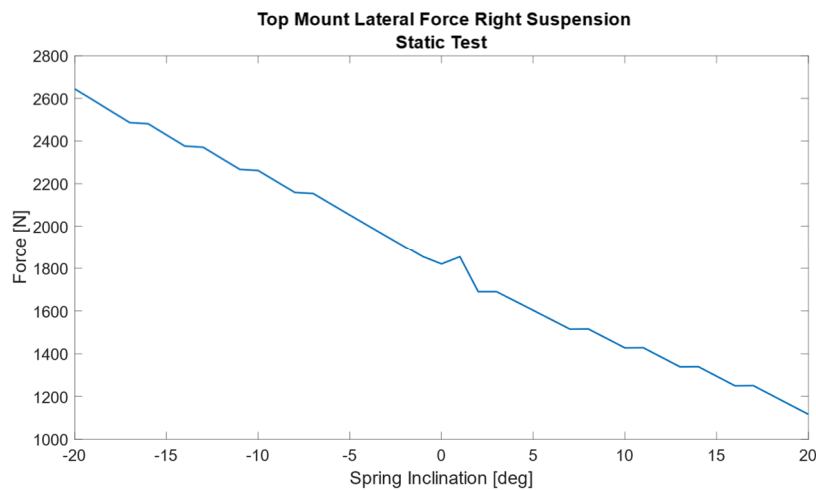


Figure 15 – Top Mount Lateral Force Right Suspension – Static Test

From figs. 14 and 15, it is easy to see that there is an almost linear decrease in the force applied when the inclination of the spring changes. Considering our initial goal, the reduction of the lateral

force acting on the top mount, we note that the inclination that the spring must have is the positive one.

Also, for the other variables we note that the trend is linear and follows that obtained for the lateral forces. However, we note that in the case of figs. 22, 23, 24 and 25, respectively the graphs showing the trend of the camber angle (left and right), of the pitch and of the roll angle, that the trend is no longer linear but follows a parabolic profile.

Another peculiarity in the graphs are the peaks that are noticed during the trend. These are due to the progressive introduction of eccentricity in the spring position.

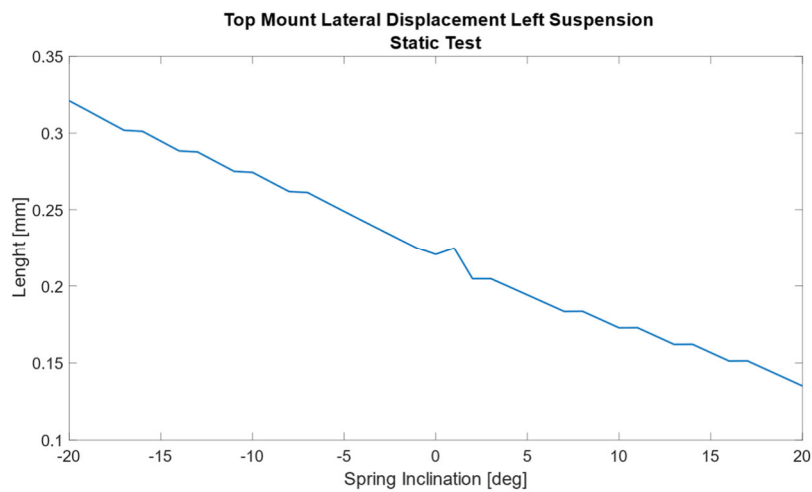


Figure 16 – Top Mount Lateral Displacement Left Suspension – Static Test

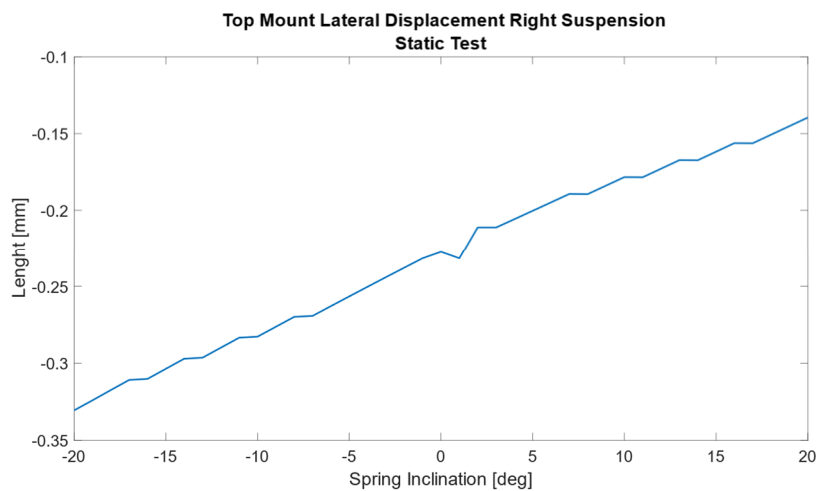


Figure 17 – Top Mount Lateral Displacement Right Suspension – Static Test

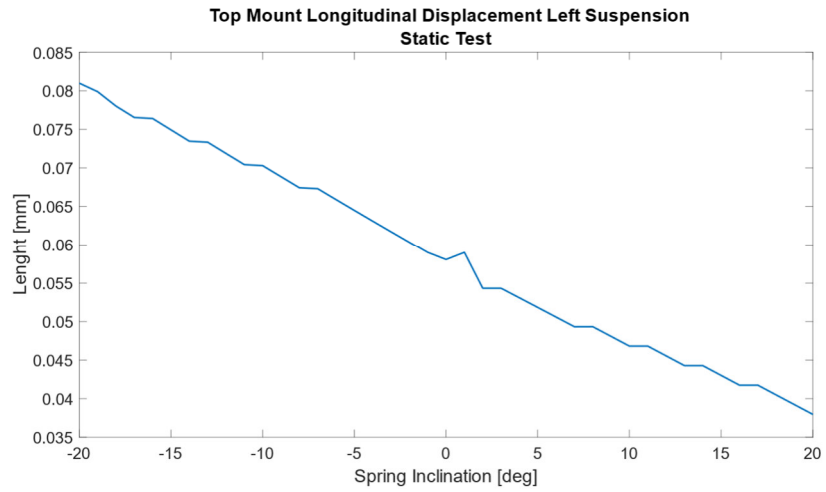


Figure 18 – Top Mount Longitudinal Displacement Left Suspension – Static Test

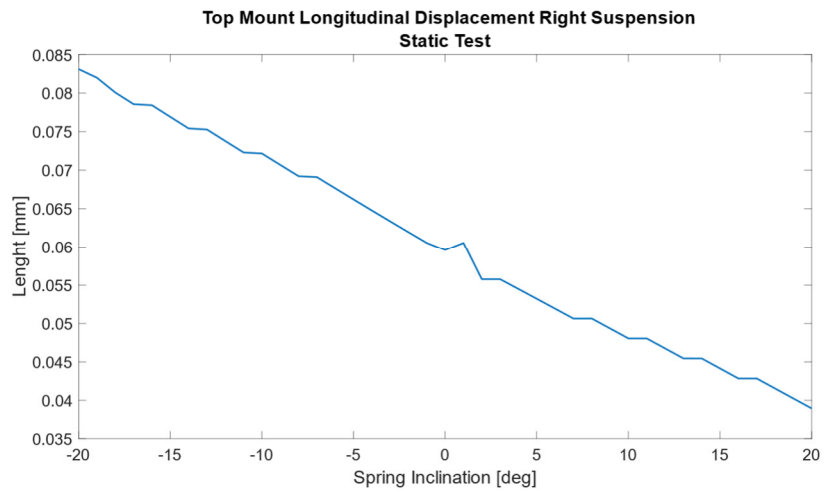


Figure 19 – Top Mount Longitudinal Displacement Right Suspension – Static Test

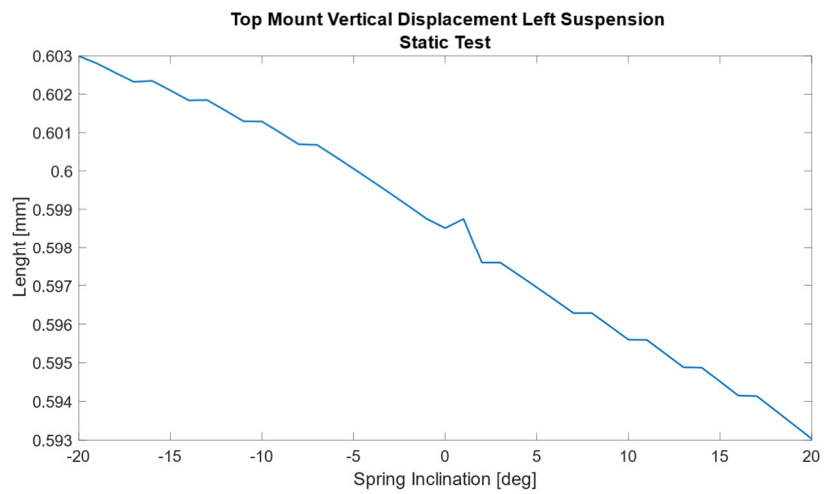


Figure 20 – Top Mount Vertical Displacement Left Suspension – Static Test

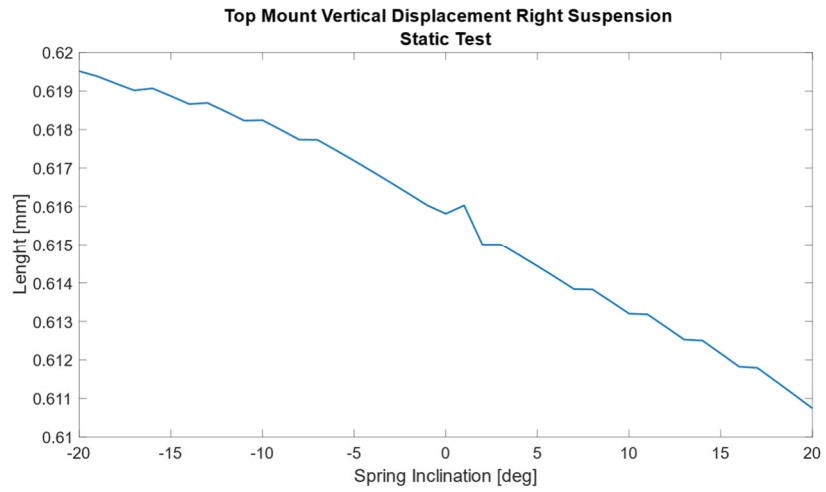


Figure 21 – Top Mount Vertical Displacement Right Suspension – Static Test

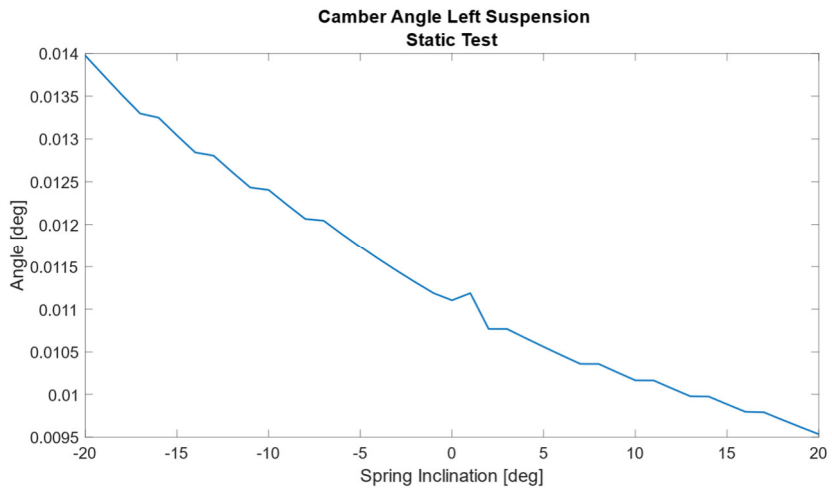


Figure 22 – Camber Angle Left Suspension – Static Test

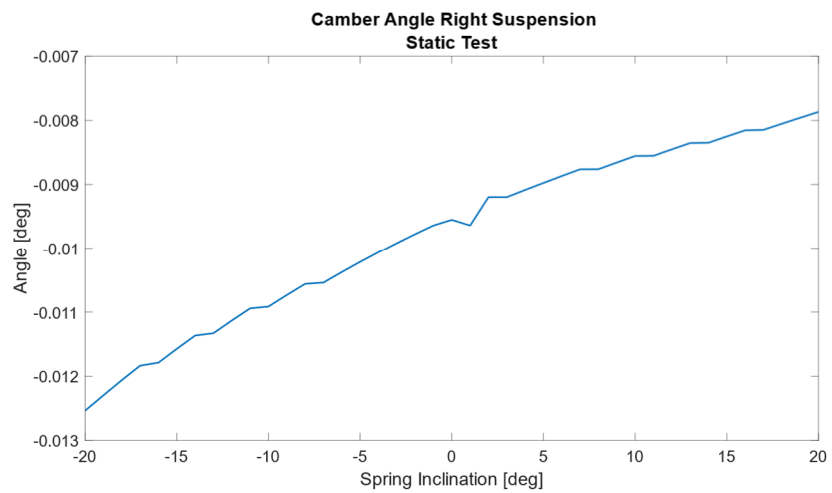


Figure 23 – Camber Angle Right Suspension – Static Test

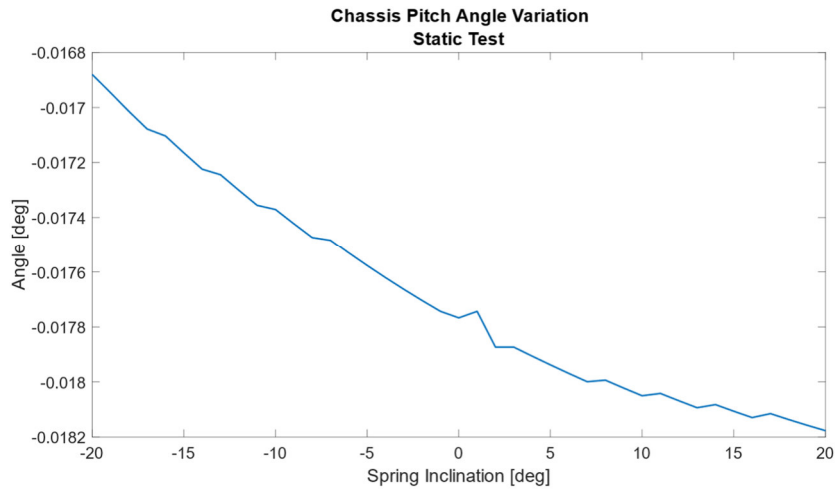


Figure 24 – Chassis Pitch Angle Variation – Static Test

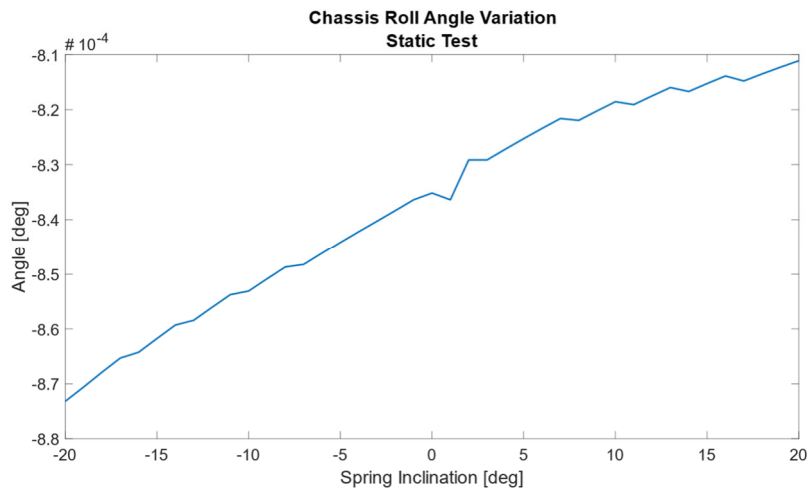


Figure 25 – Chassis Roll Angle Variation – Static Test

The way forward was therefore the study of simulations with this defined layout.

The next choice was the definition of the tests to be performed to replicate some of the situations that occur in driving under normal conditions. In our case a change of trajectory, a sudden braking and the passage of the car on a bump. The tests were carried out considering a smooth road surface.

ISO 3888-2: 2011, commonly known as Moose Test, was used for the change of trajectory.

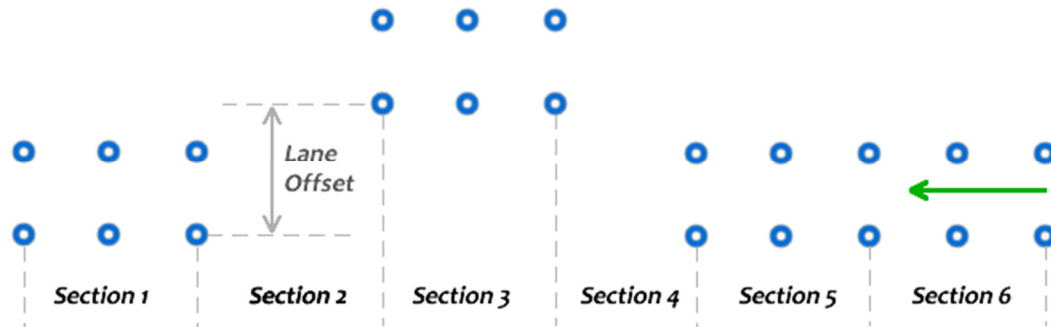


Figure 26 – Moose Test Procedure

As shown in the image (fig. 26), we have a change of trajectory, with a first steering to the right with a subsequent steering to the left to return to the initial lane. In the Moose Test the various sections are defined as follows:

- Section 1 = 6 [m]
- Section 2 = 13.5 [m]
- Section 3 = 11 [m]
- Section 4 = 13.5 [m]
- Section 5 = 6 [m]
- Section 6 = 50 [m]
- Lane offset = 4 [m]

The trajectory speed is 60 km/h.

For the braking test, braking was considered from a speed of 100 km/h until the car stopped completely, considering a deceleration of 3 m/s^2 . The test consists of the car launched at a predetermined speed and the application of the brake after 30 s from the start of the test (fig. 27).

For the test of the artificial bump we referred to the Italian regulation. DPR 495/1992, as modified by DPR 610/96, in Art. 179. (Art. 42 Cod. Str.) Comma 5, defines the maximum height and the shape that artificial bumps must have in Italy (fig. 28), and the maximum travel speed of the same, which turns out to be 30 km/h.

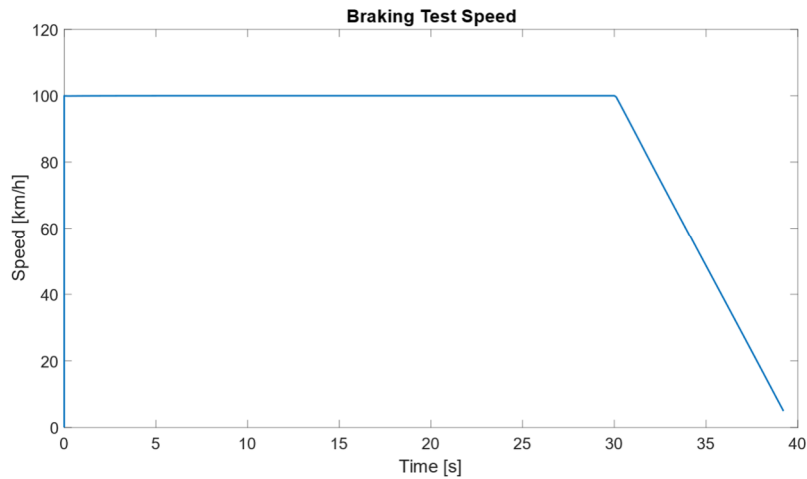


Figure 27 – Braking Test Speed

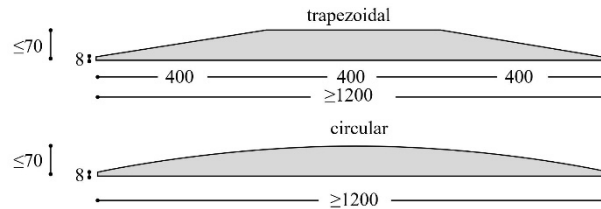


Figure 28 – Speed Bump Profile

Once you have defined the tests to which the vehicle must undergo and which type of solution to use about the spring, the graphs for the relative tests are shown below.

For ease of reading, only multiple angles of 5, therefore 5°, 10°, 15° and 20° have been considered. All values were compared with the tests carried out in the default configuration, to visually obtain a real comparison of the influence of the inclination of the axis of the spring on the various components examined.

c. Results obtained

The first tests are those carried out considering the Moose test. Fig. 29 and 30 show the trend of the lateral force acting on the top mount for the left and right suspension respectively. The increase in the inclination of the spring causes a considerable decrease in the applied force.

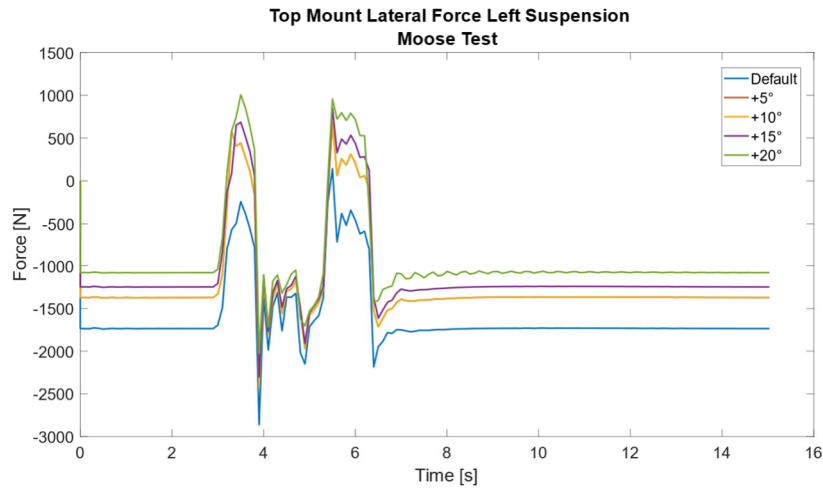


Figure 29 – Top Mount Lateral Force Left Suspension – Moose Test

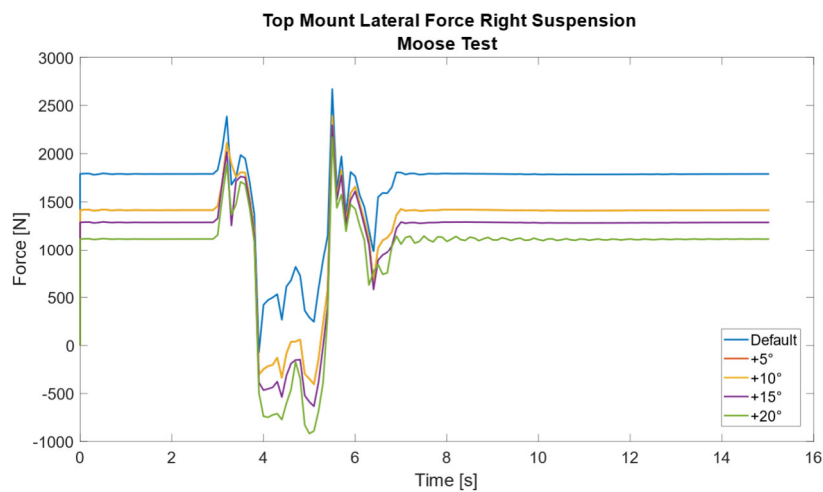


Figure 30 – Top Mount Lateral Force Right Suspension – Moose Test

The same applies to lateral displacement (figures 31 and 32), while for longitudinal displacement and especially vertical displacement (figures 33, 34, 35 and 36) we do not have a considerable variation.

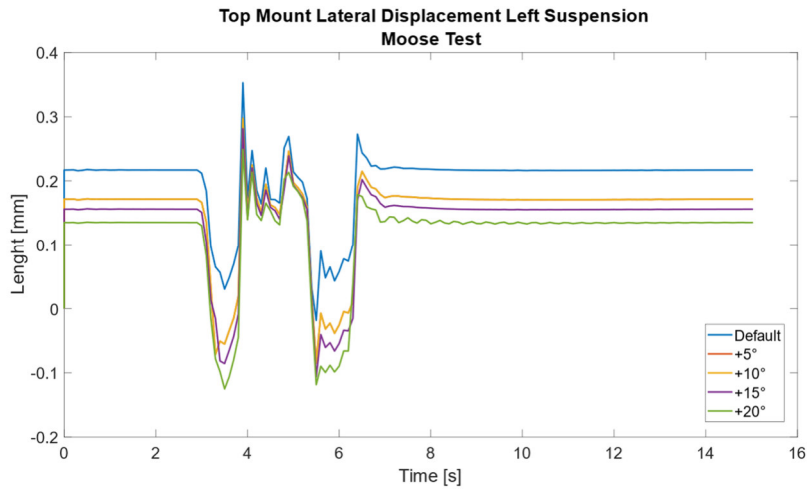


Figure 31 – Top Mount Lateral Displacement Left Suspension – Moose Test

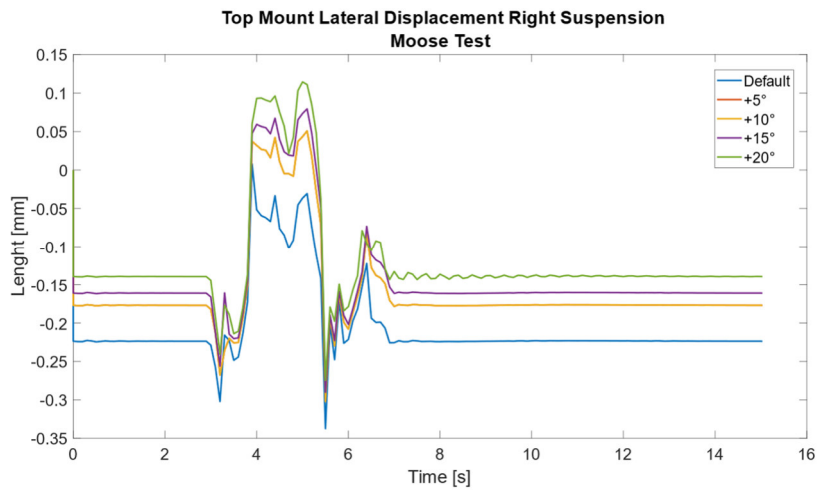


Figure 32 – Top Mount Lateral Displacement Right Suspension – Moose Test

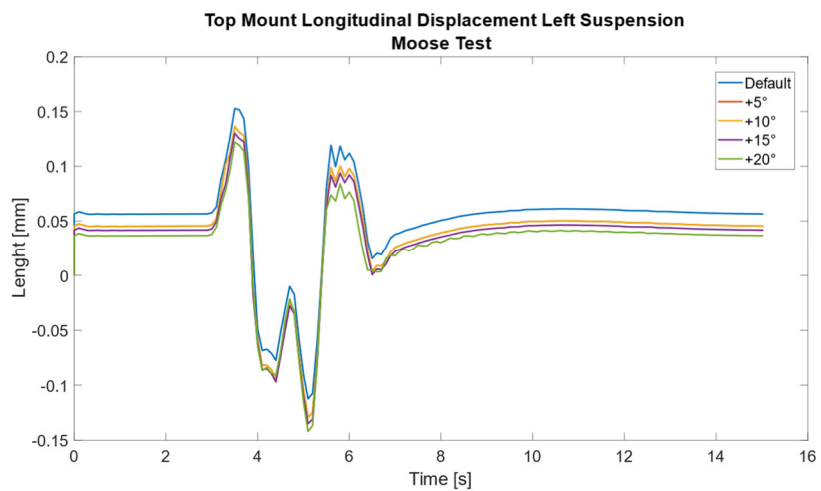


Figure 33 – Top Mount Longitudinal Displacement Left Suspension – Moose Test

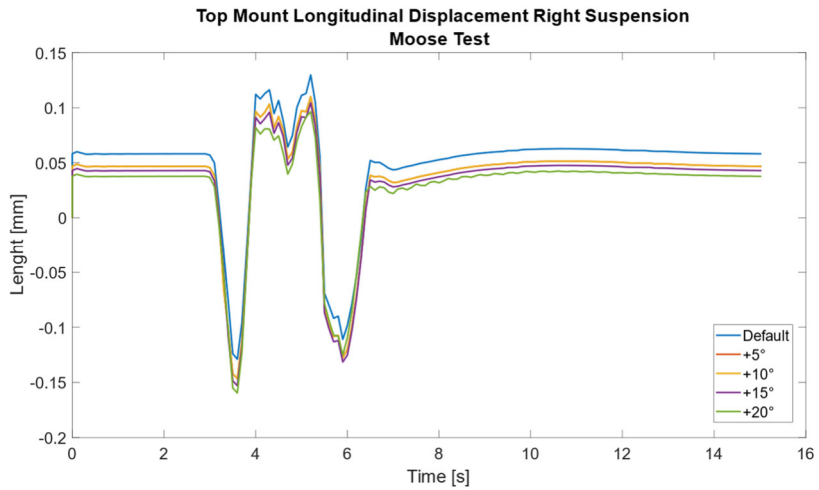


Figure 34 – Top Mount Longitudinal Displacement Right Suspension – Moose Test

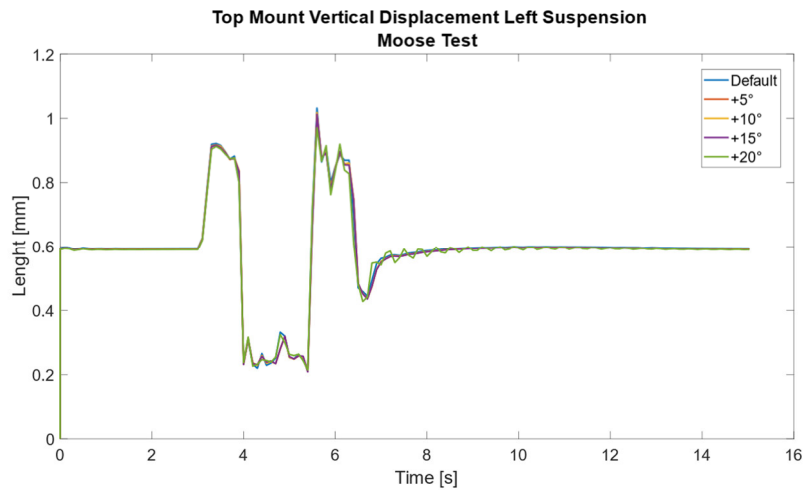


Figure 35 – Top Mount Vertical Displacement Left Suspension – Moose Test

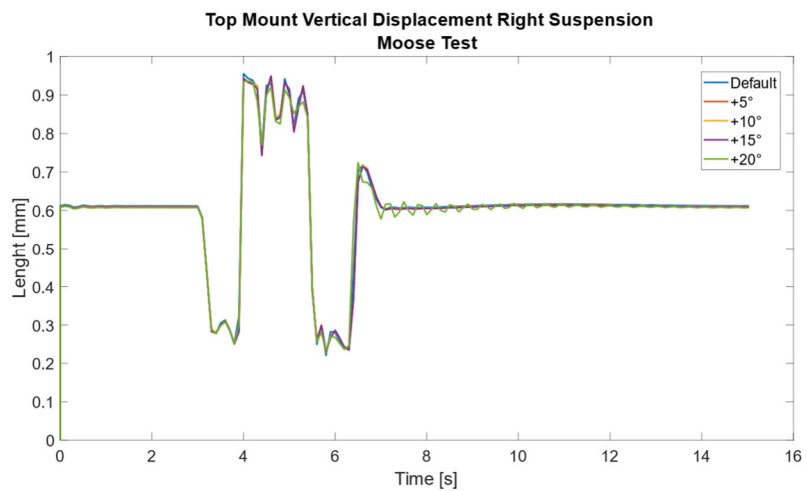


Figure 36 – Top Mount Vertical Displacement Right Suspension – Moose Test

As far as accelerations are concerned, we do not notice any improvement in this visualization. The change in the angle of the spring, during a lane change with the car, does not produce a significant variation on the dynamics of the vehicle.

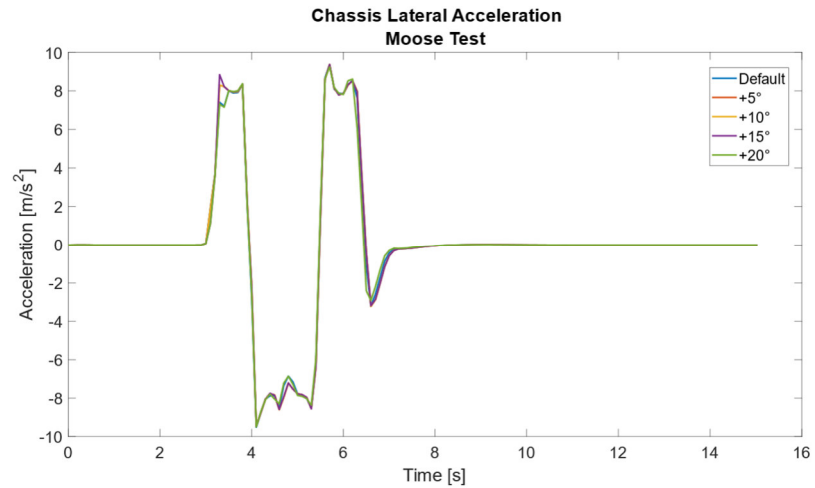


Figure 37 – Chassis Lateral Acceleration – Moose Test

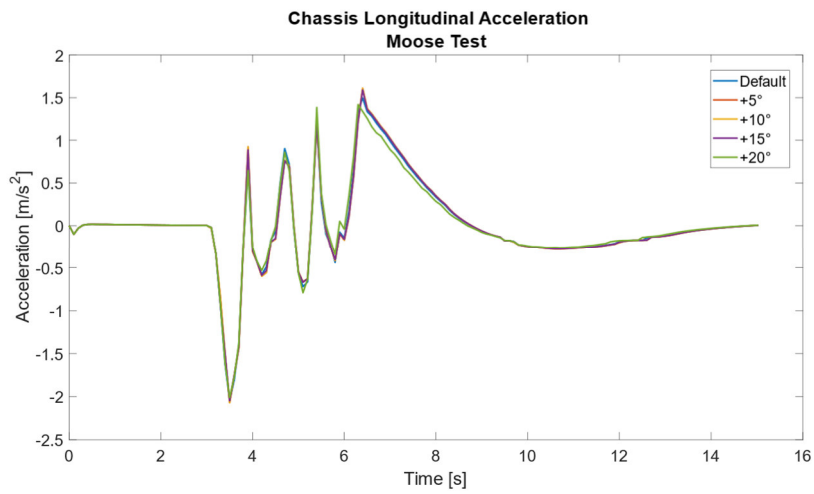


Figure 38 – Chassis Longitudinal Acceleration – Moose Test

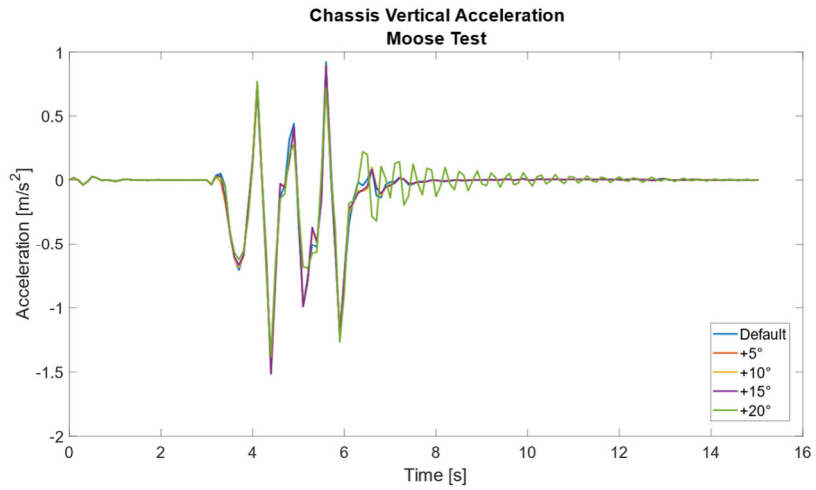


Figure 39 – Chassis Vertical Acceleration – Moose Test

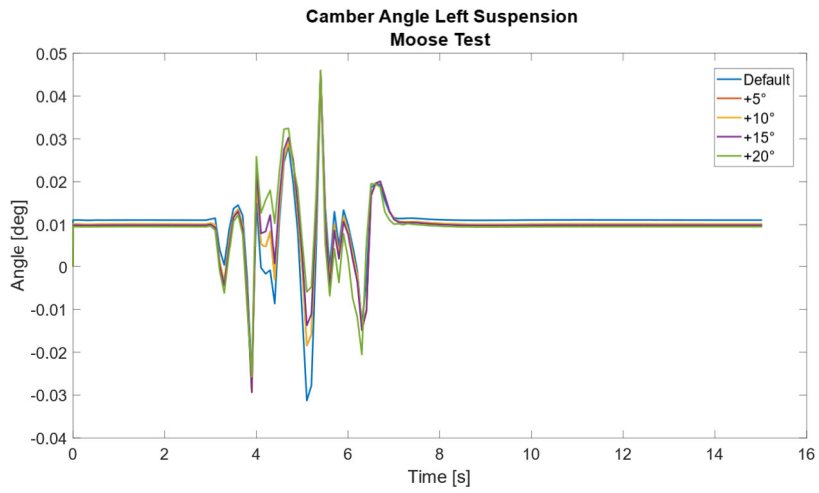


Figure 40 – Camber Angle Left Suspension – Moose Test

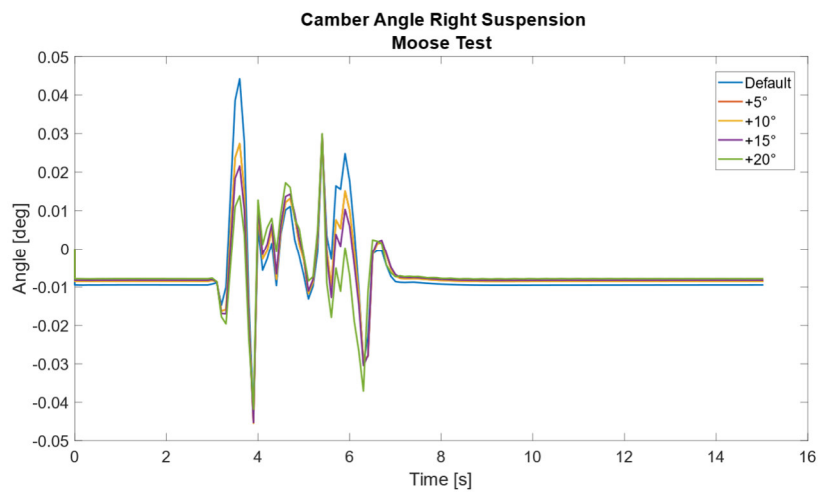


Figure 41 – Camber Angle Right Suspension – Moose Test

Analysing the variation of the camber we notice the differences between the default version and those with the modified angle, but the entities of the displacements are relatively low.

Finally considering the variations of the pitch angle and the roll angle relative to the chassis, we note that even here the quantities are to be considered important, the influence of the angle change in the study of these variables is not perceived.

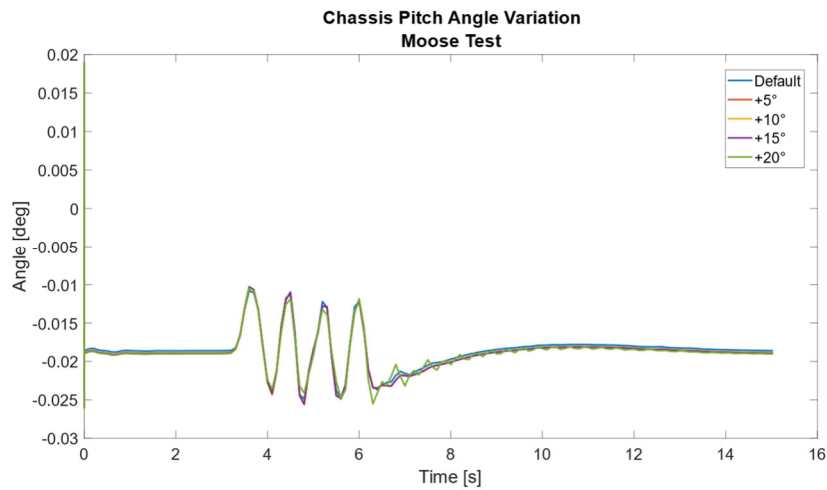


Figure 42 – Chassis Pitch Angle Variation – Moose Test

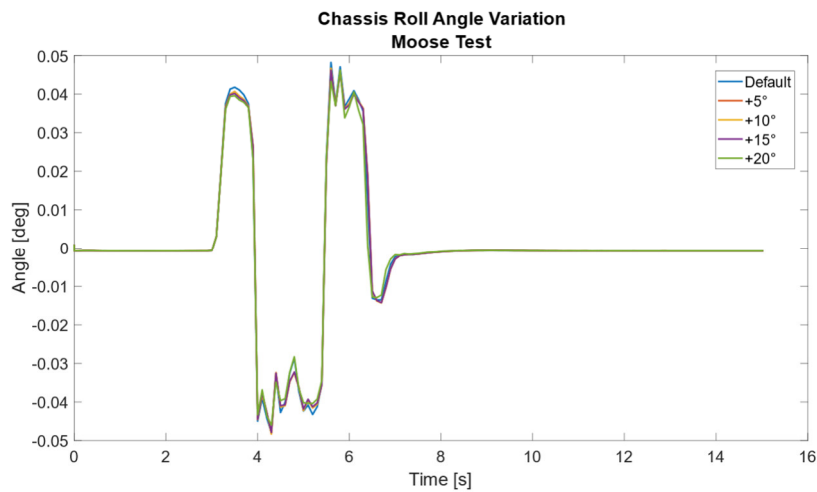


Figure 43 – Chassis Roll Angle Variation – Moose Test

The next analysis is on the brake test. Also, in this case, as we would have expected, the variable that benefits most from the change in the angle of the spring axis is the lateral force and lateral displacement. For the other variables we note that the behaviour is very similar to that obtained for the Moose Test.

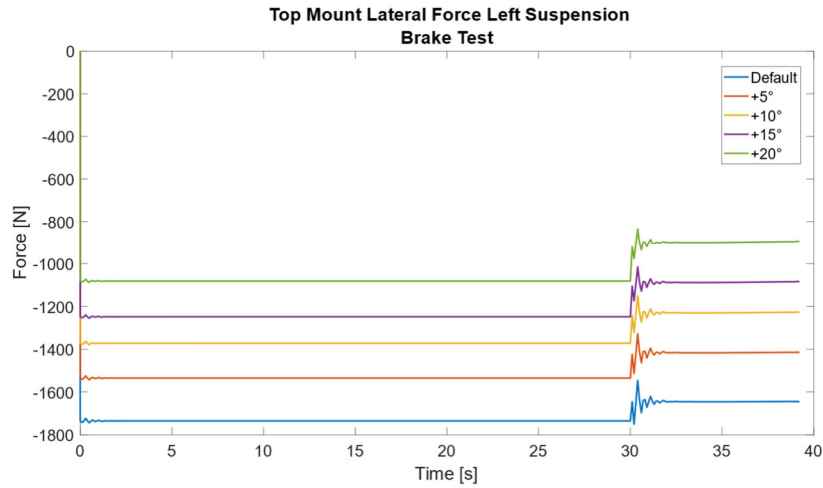


Figure 44 – Top Mount Lateral Force Left Suspension – Brake Test

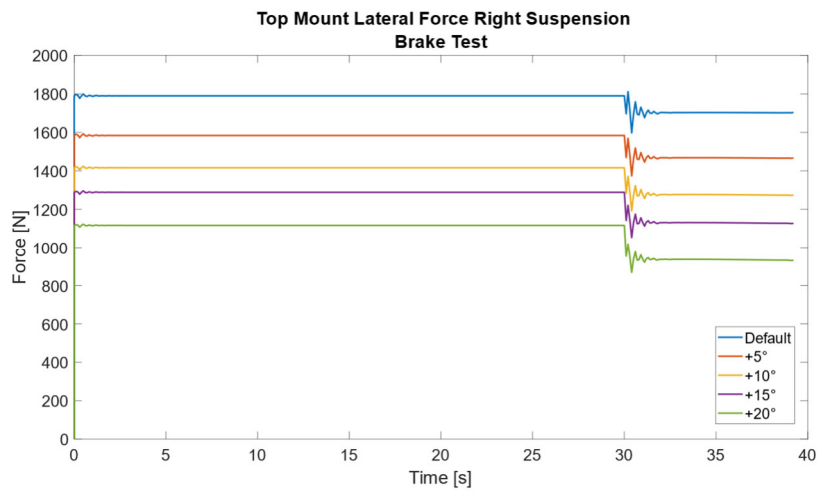


Figure 45 – Top Mount Lateral Force Right Suspension – Brake Test

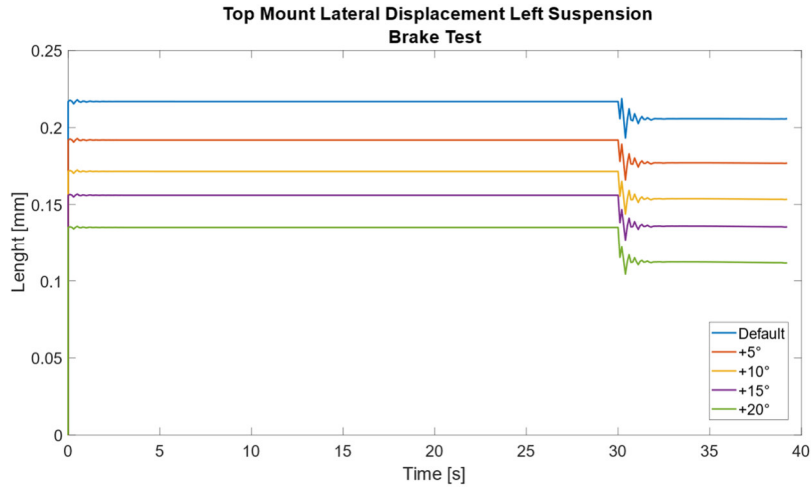


Figure 46 – Top Mount Lateral Displacement Left Suspension – Brake Test

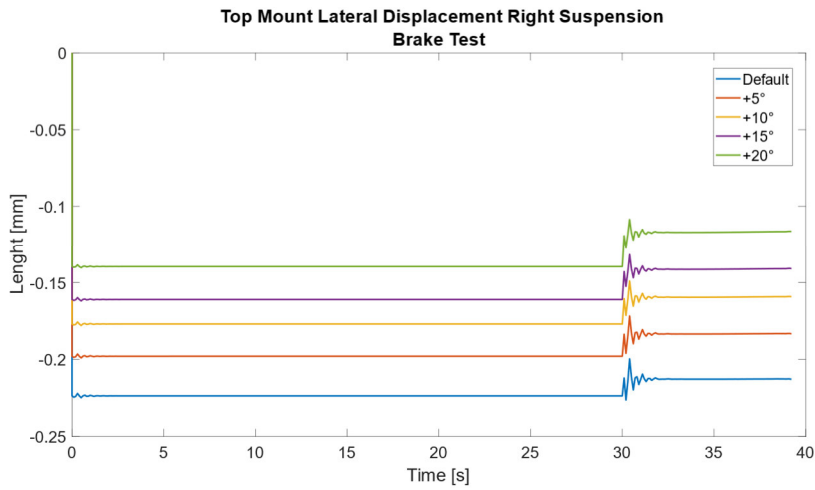


Figure 47 – Top Mount Lateral Displacement Right Suspension – Brake Test

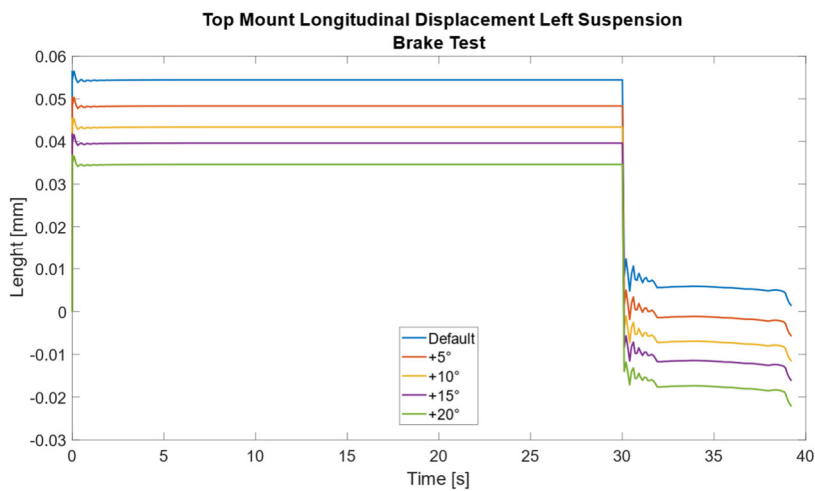


Figure 48 – Top Mount Longitudinal Displacement Left Suspension – Brake Test

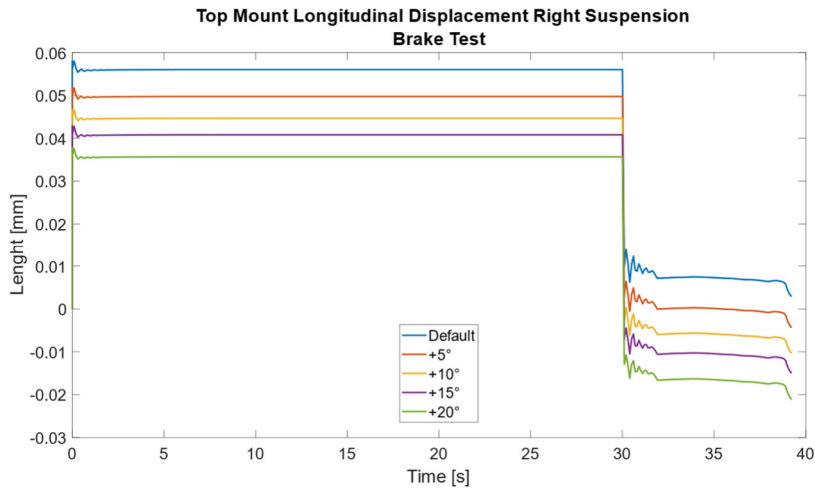


Figure 49 – Top Mount Longitudinal Displacement Right Suspension – Brake Test

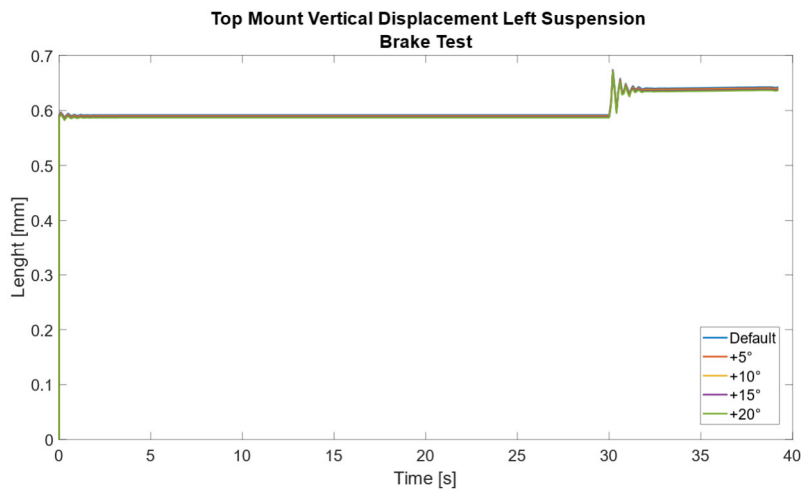


Figure 50 – Top Mount Vertical Displacement Left Suspension – Brake Test

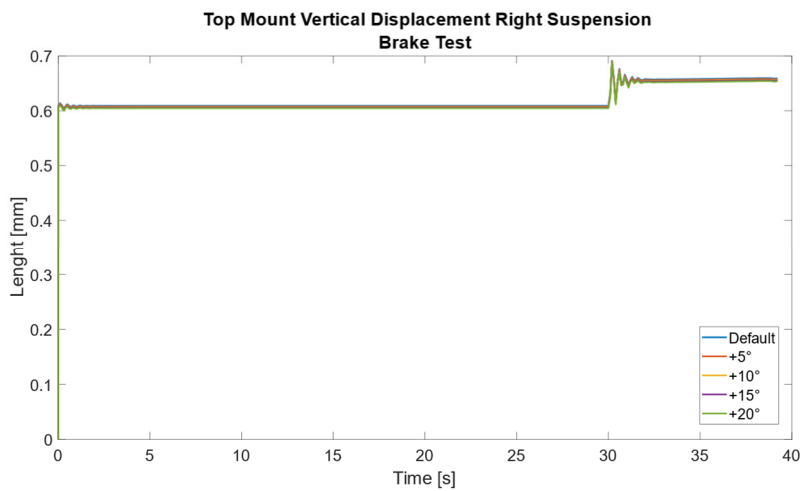


Figure 51 – Top Mount Vertical Displacement Right Suspension – Brake Test

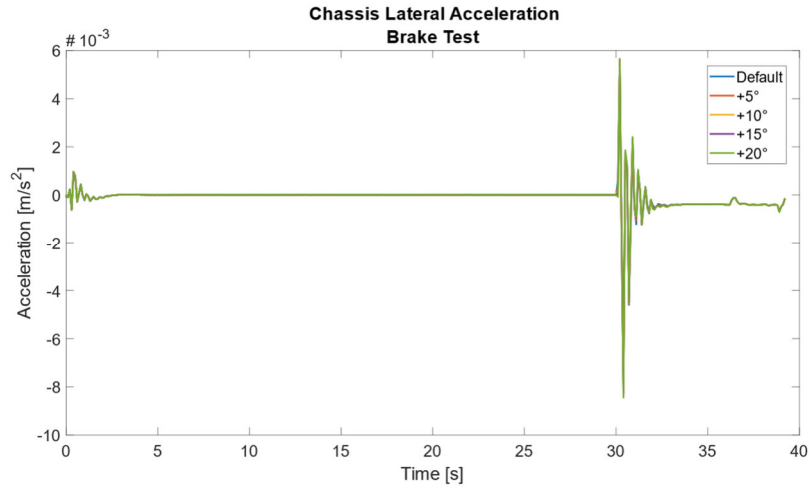


Figure 52 – Chassis Lateral Acceleration – Brake Test

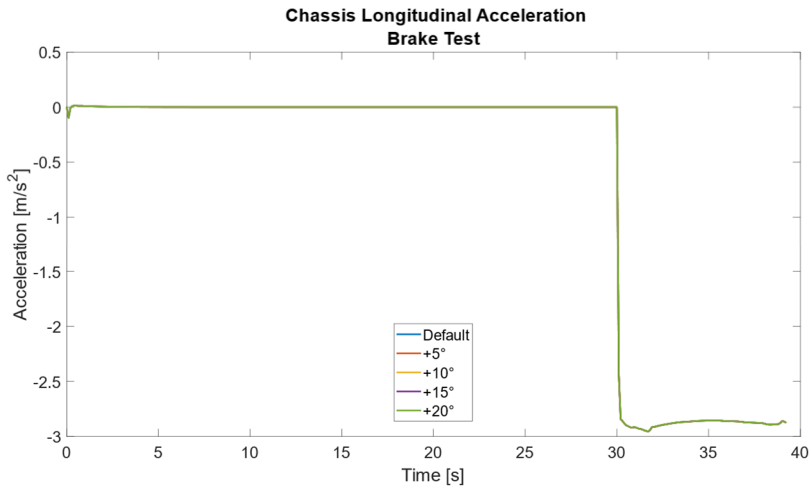


Figure 53 – Chassis Longitudinal Acceleration – Brake Test

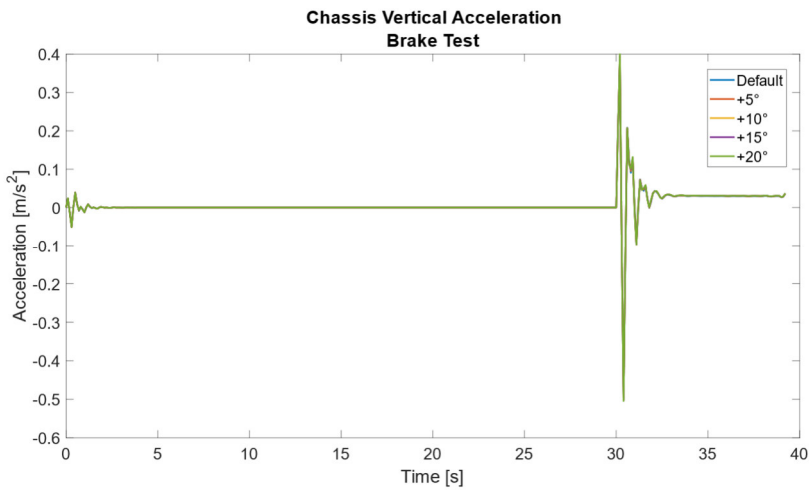


Figure 54 – Chassis Vertical Acceleration – Brake Test

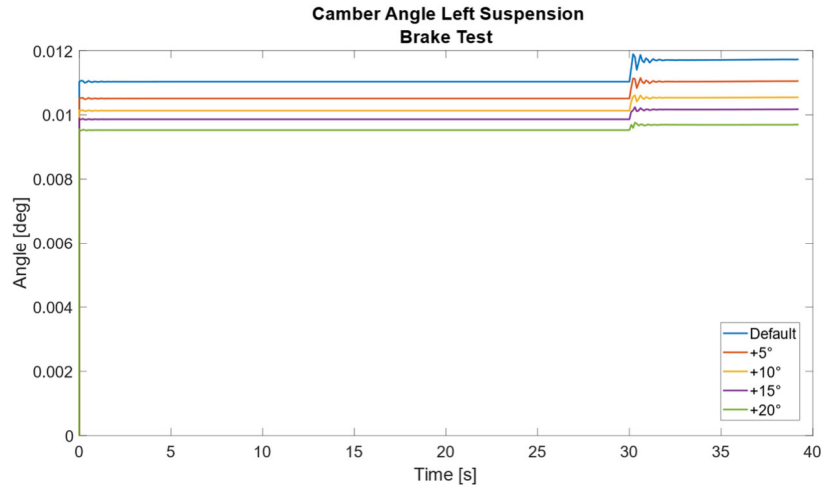


Figure 55 – Camber Angle Left Suspension – Brake Test

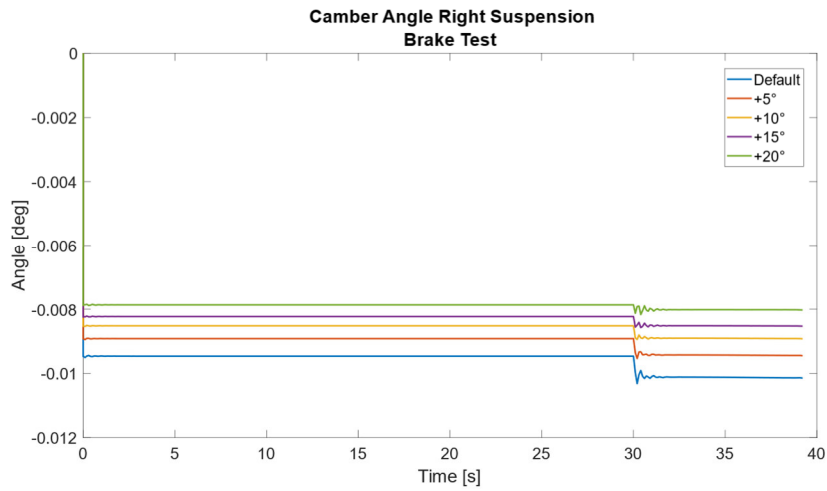


Figure 56 – Camber Angle Right Suspension – Brake Test

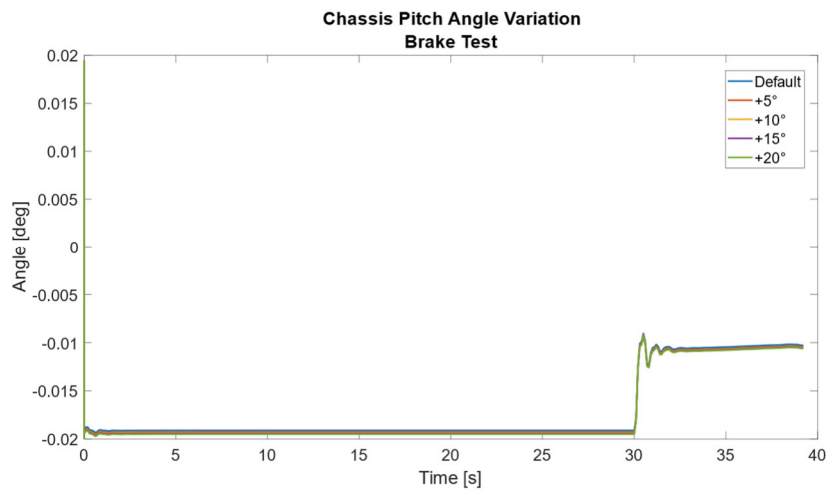


Figure 57 – Chassis Pitch Angle Variation – Brake Test

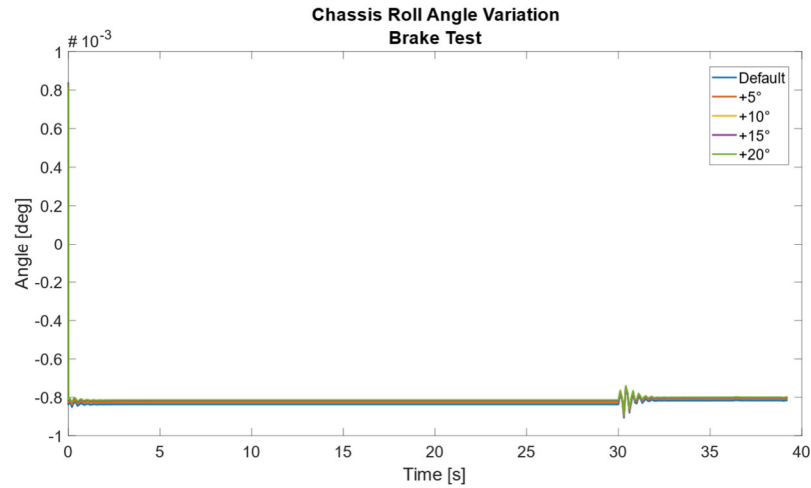


Figure 58 – Chassis Roll Angle Variation – Brake Test

Similarly, in the case of the Speed Bump Test, we have obtained the same results, that is, a considerable variation in the lateral components of the force and displacements but nothing or extremely low in the other categories. An evident peculiarity that we can notice is that the duration of the oscillatory phase of the examined variables decreases with increasing inclination.

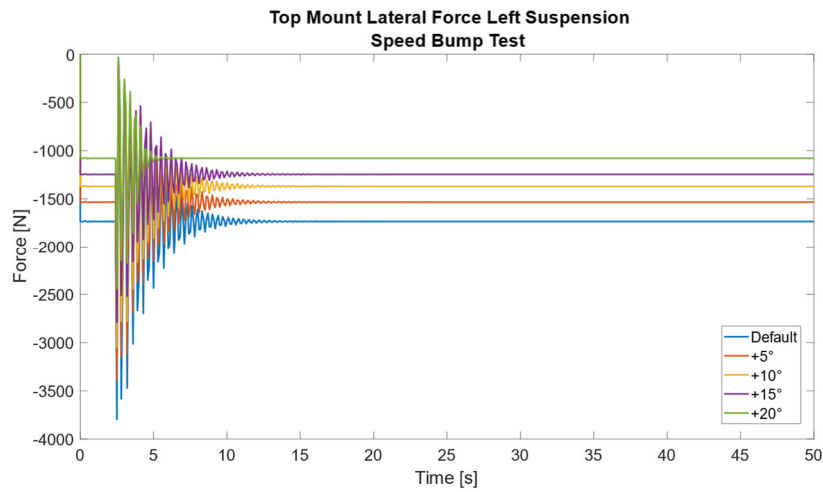


Figure 59 – Top Mount Lateral Force Left Suspension – Speed Bump Test

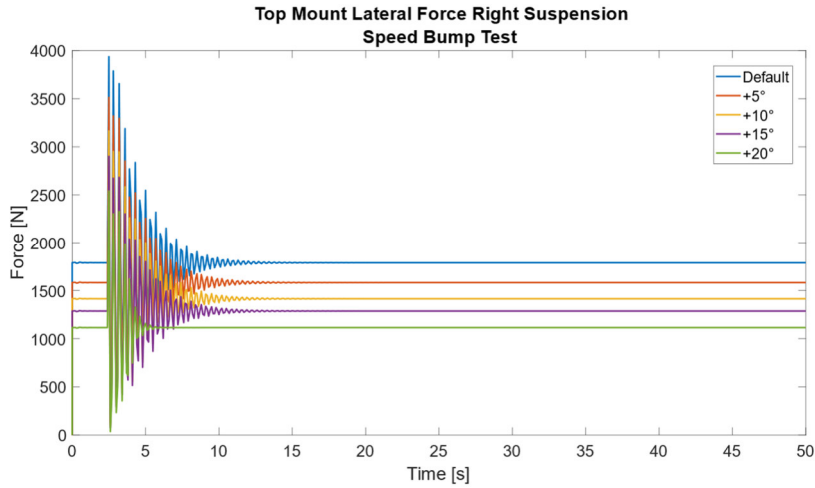


Figure 60 – Top Mount Lateral Force Right Suspension – Speed Bump Test

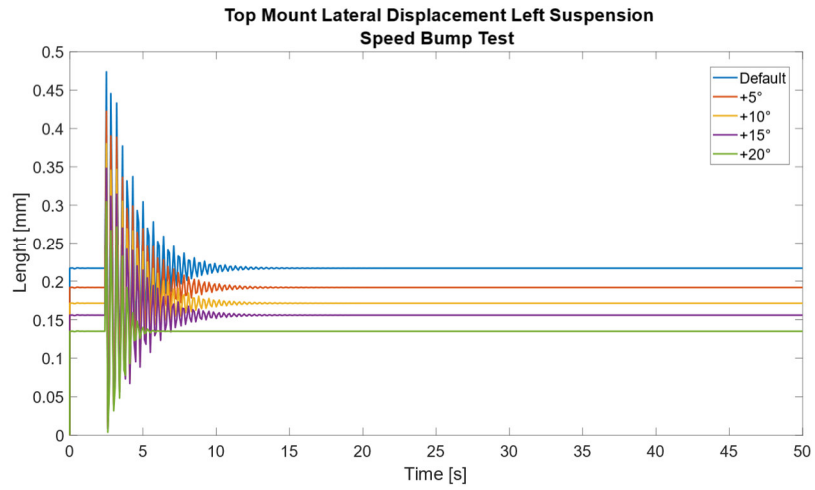


Figure 61 – Top Mount Lateral Displacement Left Suspension – Speed Bump Test

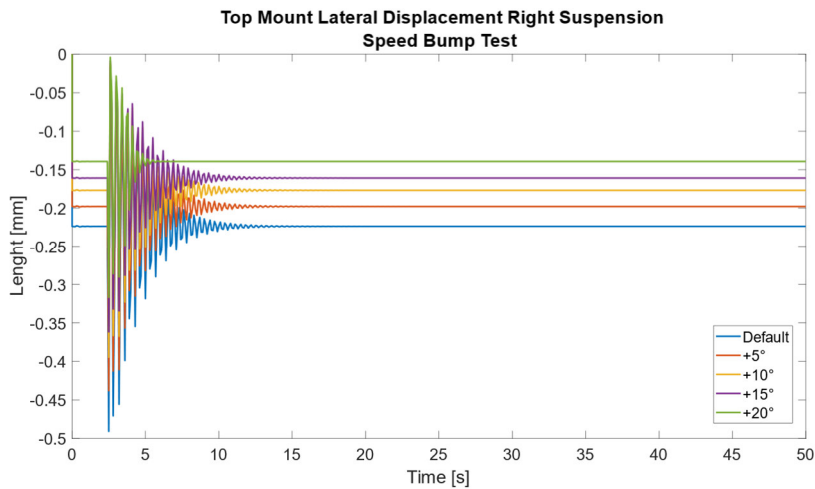


Figure 62 – Top Mount Lateral Displacement Right Suspension – Speed Bump Test

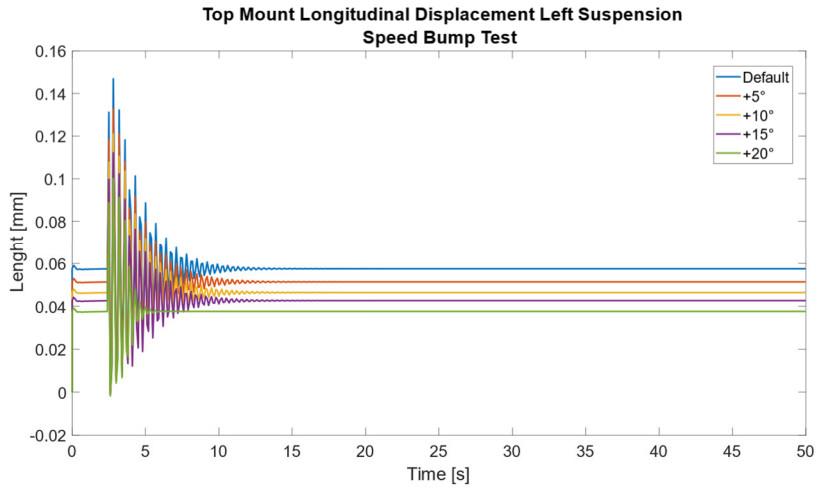


Figure 63 – Top Mount Longitudinal Displacement Left Suspension – Speed Bum Test

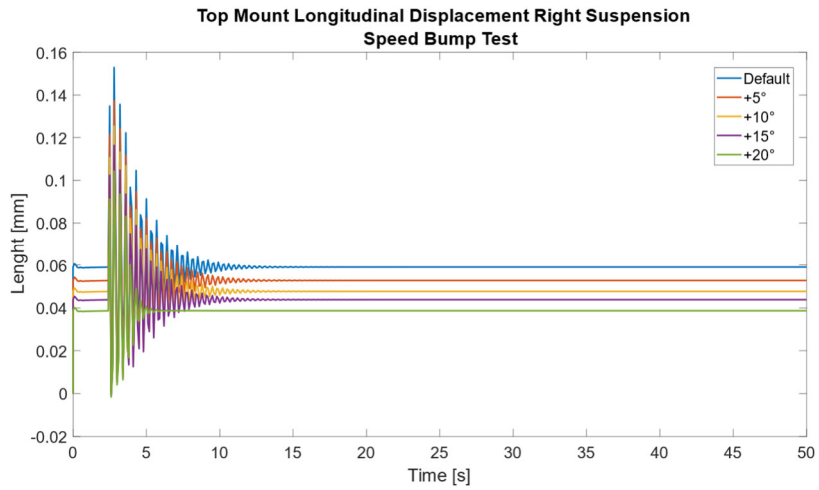


Figure 64 – Top Mount Longitudinal Displacement Right Suspension – Speed Bump Test

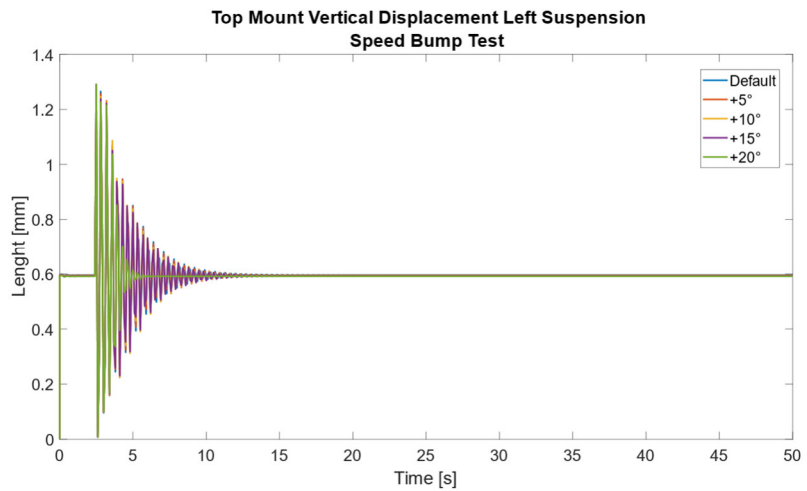


Figure 65 – Top Mount Vertical Displacement Left Suspension – Speed Bump Test

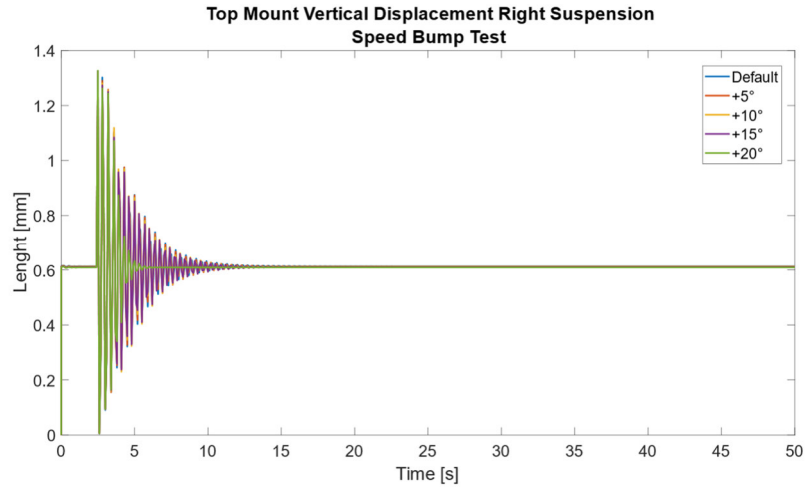


Figure 66 – Top Mount Vertical Displacement Right Suspension – Speed Bump Test

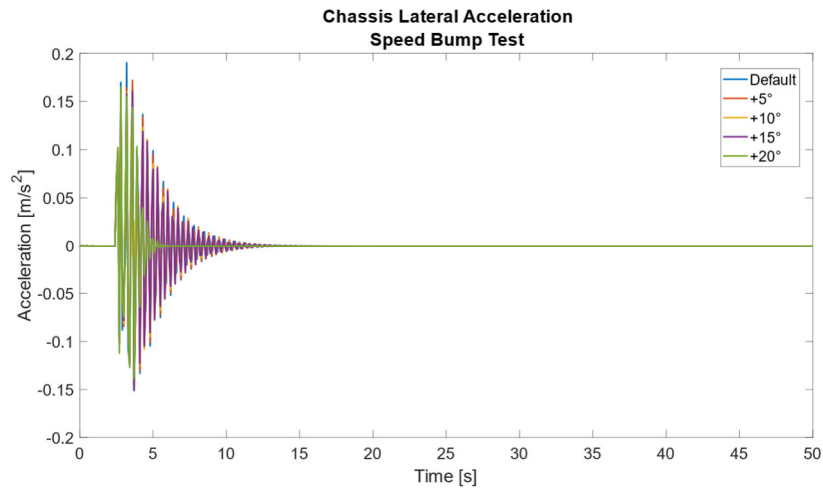


Figure 67 – Chassis Lateral Acceleration – Speed Bump Test

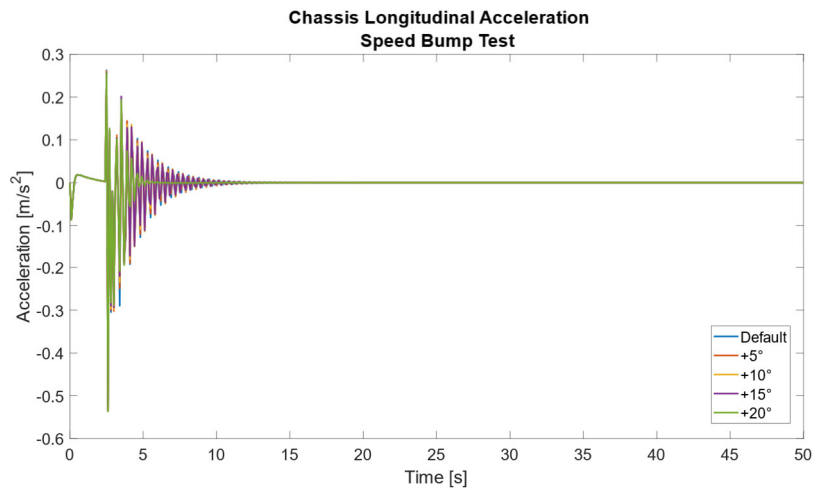


Figure 68 – Chassis Longitudinal Acceleration – Speed Bump Test

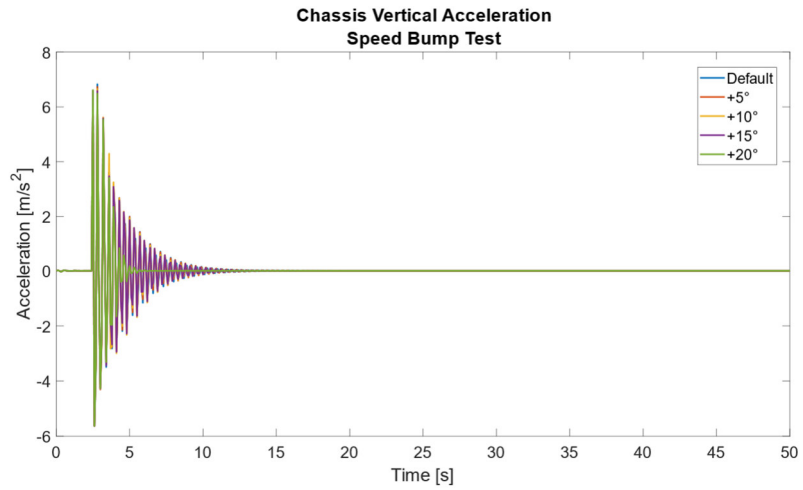


Figure 69 – Chassis Vertical Acceleration – Speed Bump Test

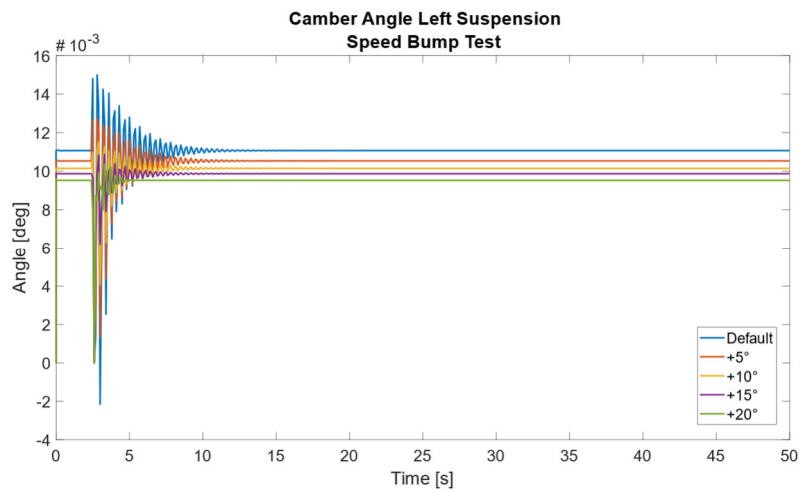


Figure 70 – Camber Angle Left Suspension – Speed Bump Test

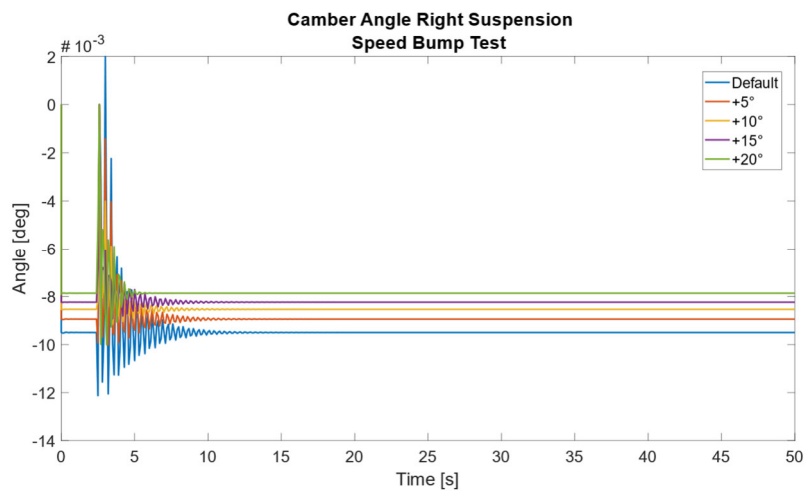


Figure 71 – Camber Angle Right Suspension – Speed Bump Test

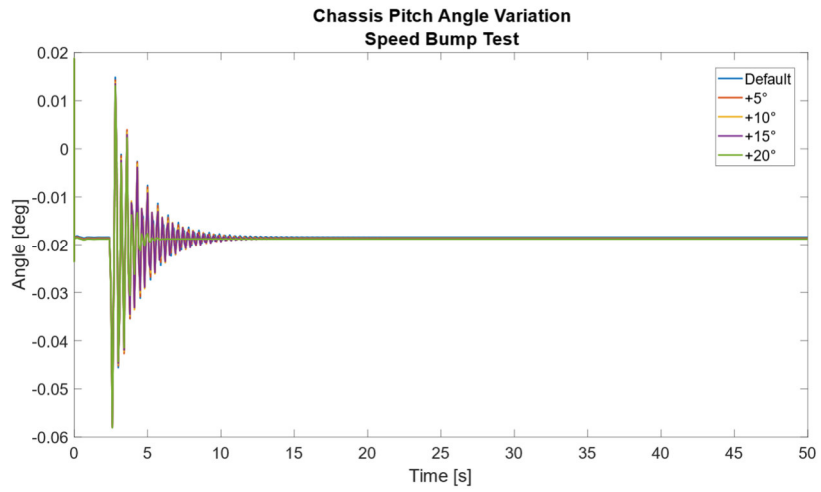


Figure 72 – Chassis Pitch Angle Variation – Speed Bump Test

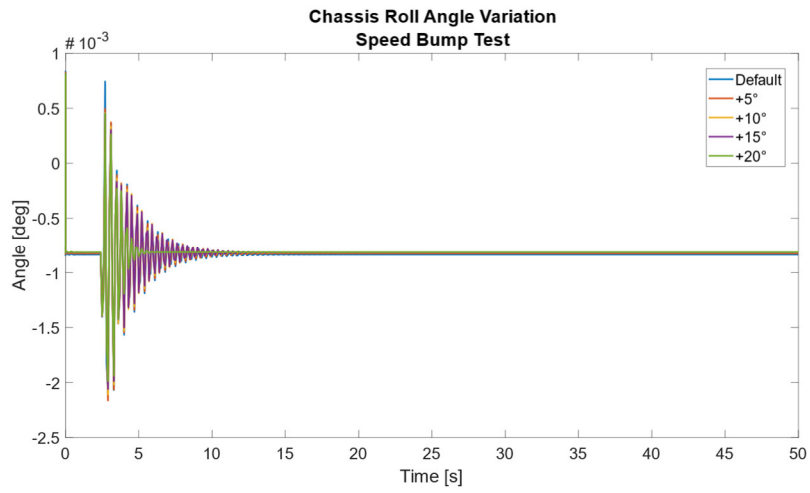


Figure 73 – Chassis Roll Angle Variation – Speed Bump Test

d. Introduction of the Spherical Joint in the Top Mount

A first definition has been reached; the position of the spring greatly influences the lateral component but not by contributions in terms of vehicle dynamics.

So, we hypothesized to change the type of joint that is on the top mount by inserting a spherical joint, to try to obtain a variation of the dynamic characteristics of the vehicle.

Also in this case Adams, in his library, has a spherical joint model that we have been able to replace and replicate the tests previously carried out.

Figs. 74 and 75 show the rotational stiffness and translational stiffness for the default joints and the spherical joint chosen for the test.

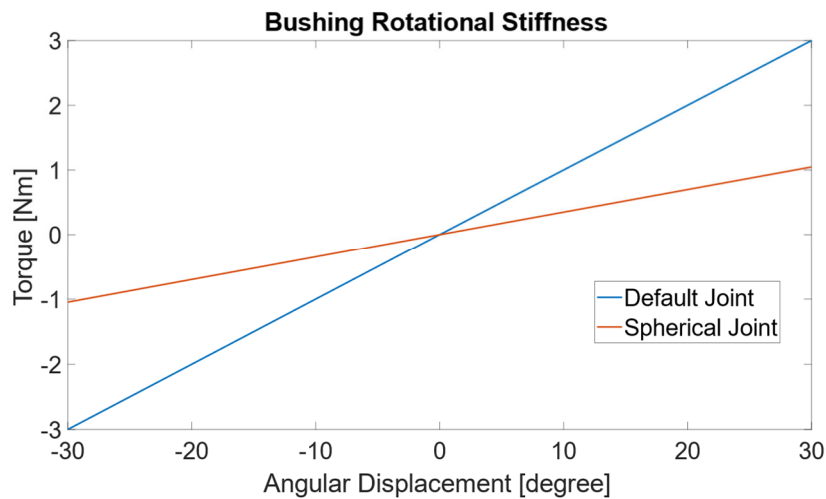


Figure 74 – Bushing Rotational Stiffnesses

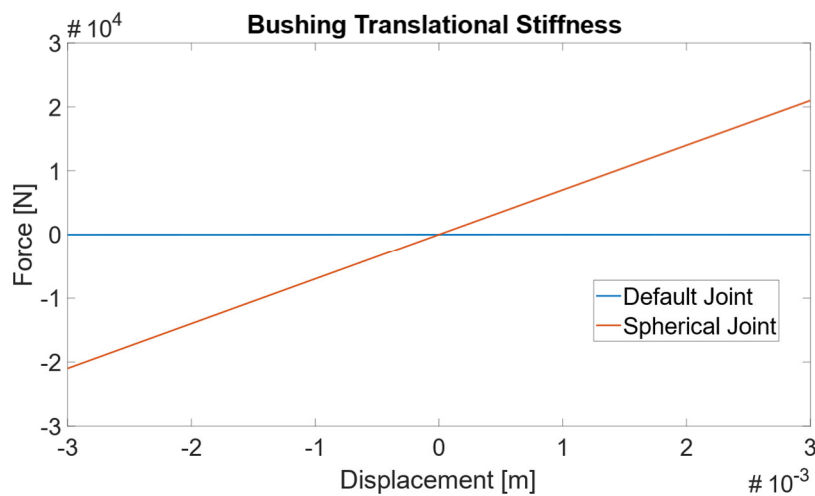


Figure 75 – Bushing Translational Stiffness

The graphs of the tests carried out using the procedures previously defined with the modification of the joint are shown below.

For simplicity we have considered the case with no inclination of the spring axis.

With reference to the moose test we can see how the introduction of the spherical joint further lowers the lateral force acting on the top mount (figs. 76 and 77), and also has a positive influence on the lateral and longitudinal displacement (figs. 78, 79, 80, and 81).

As far as vertical displacements are concerned (fig. 82), we have a negative influence as for lateral, longitudinal and vertical acceleration (figs. 83, 84 and 85).

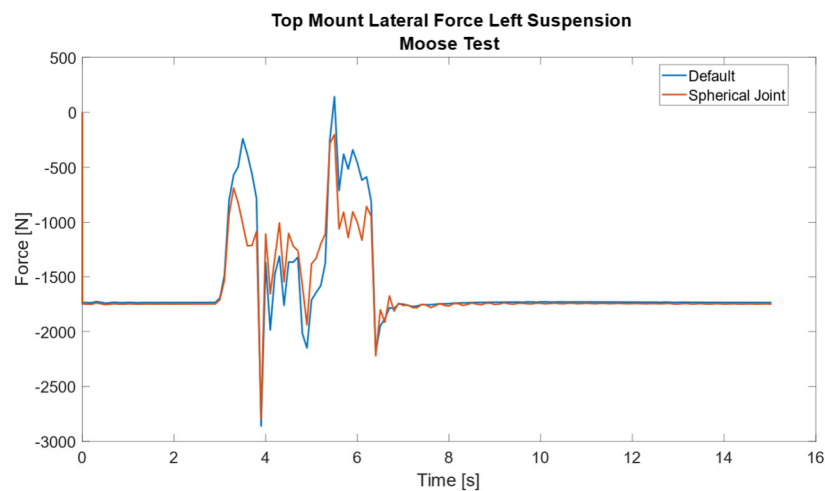


Figure 76 – Top Mount Lateral Force Left Suspension – Moose Test – Spherical Joint

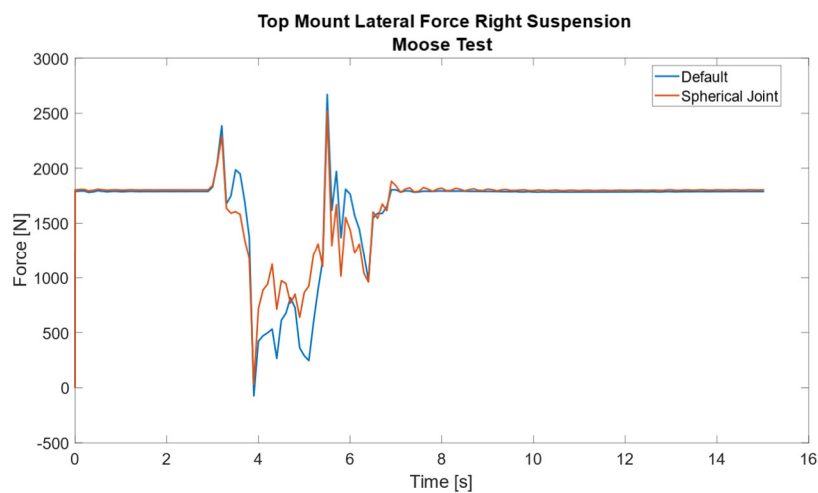


Figure 77 – Top Mount Lateral Force Right Suspension – Moose Test – Spherical Joint

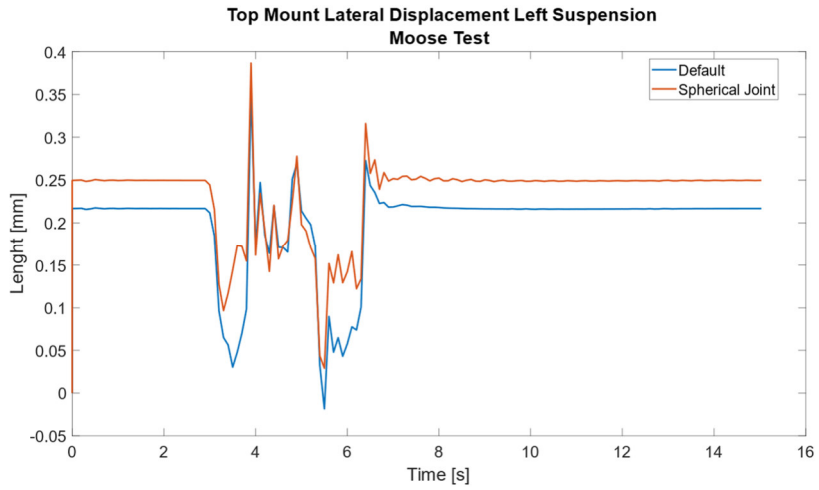


Figure 78 – Top Mount Lateral Displacement Left Suspension – Moose Test – Spherical Joint

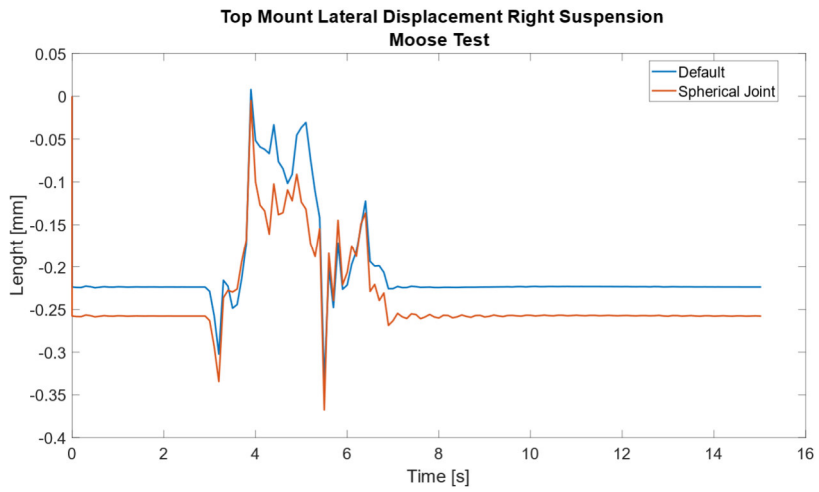


Figure 79 – Top Mount Lateral Displacement Right Suspension – Moose Test – Spherical Joint

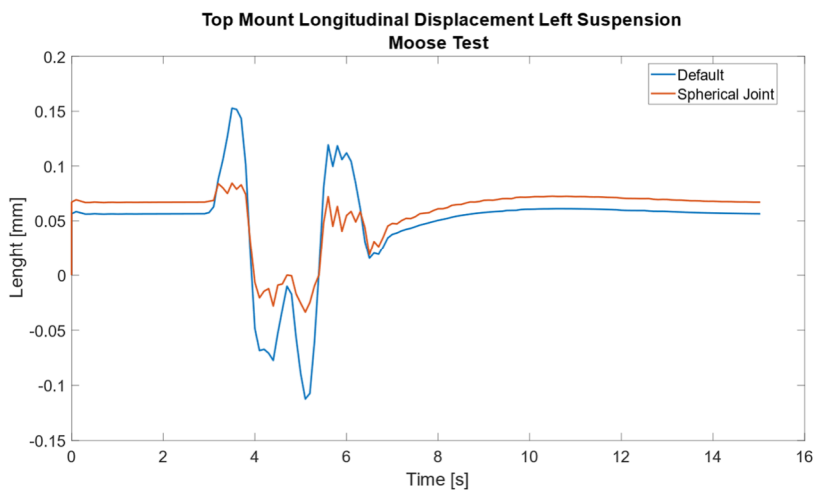


Figure 80 – Top Mount Longitudinal Displacement Left Suspension – Moose Test Spherical Joint

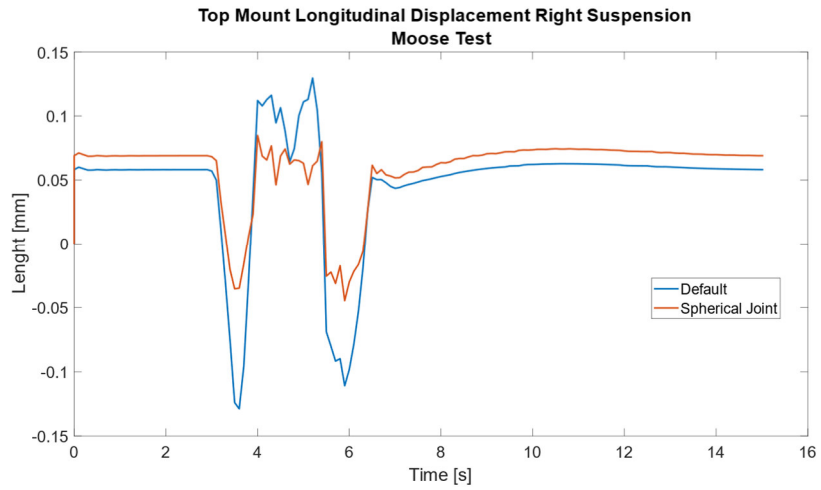


Figure 81 – Top Mount Longitudinal Displacement Right Suspension – Moose Test
Spherical Joint

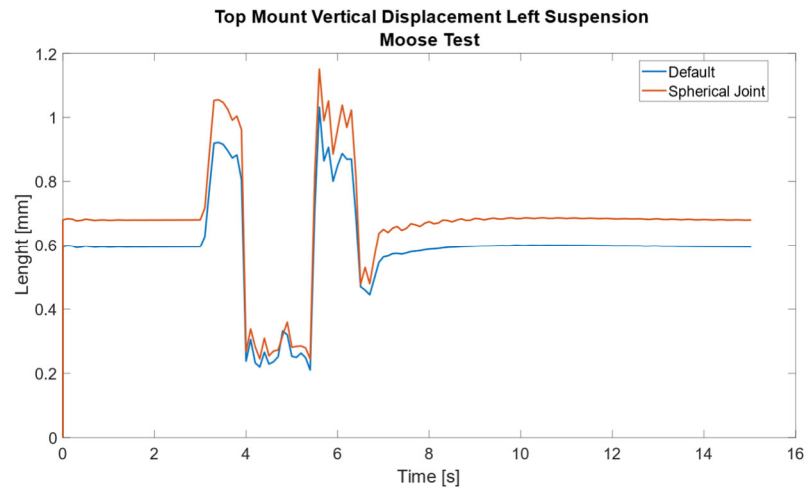


Figure 82 – Top Mount Vertical Displacement Left Suspension – Moose Test – Spherical Joint

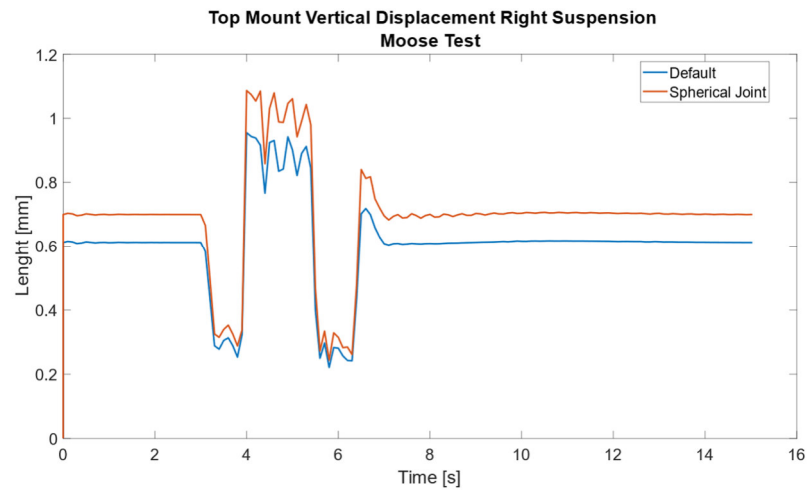


Figure 83 – Top Mount Vertical Displacement Right Suspension – Moose Test – Spherical Joint

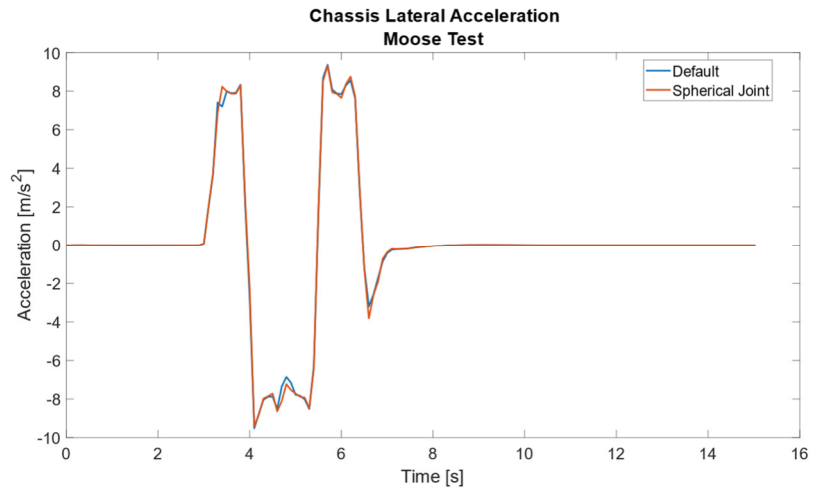


Figure 84 – Chassis Lateral Acceleration – Moose Test – Spherical Joint

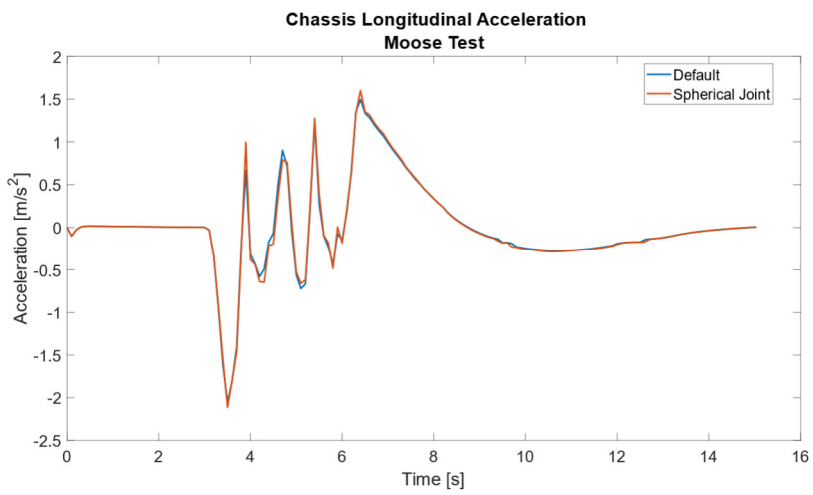


Figure 85 – Chassis Longitudinal Acceleration – Moose Test – Spherical Joint

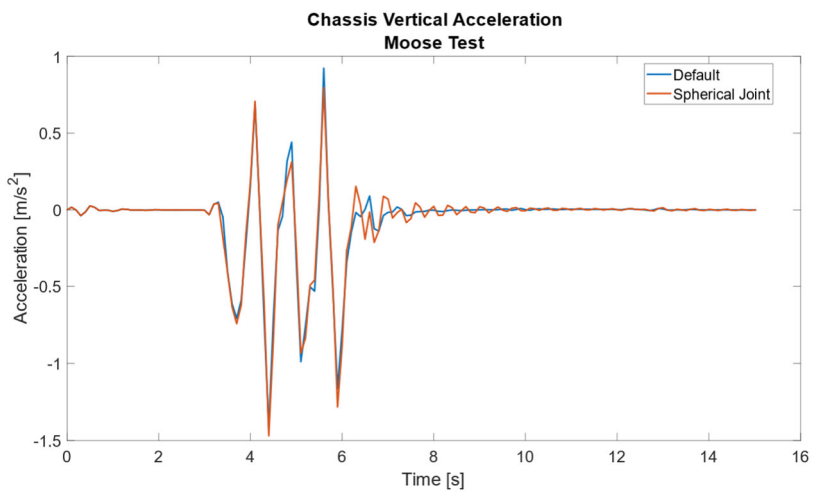


Figure 86 – Chassis Vertical Acceleration – Moose Test – Spherical Joint

Same goes for the camber angle (figs. 87 and 88), pitch angle (fig 89) and roll angle (fig. 90), the influence of the spherical joint is not significant.

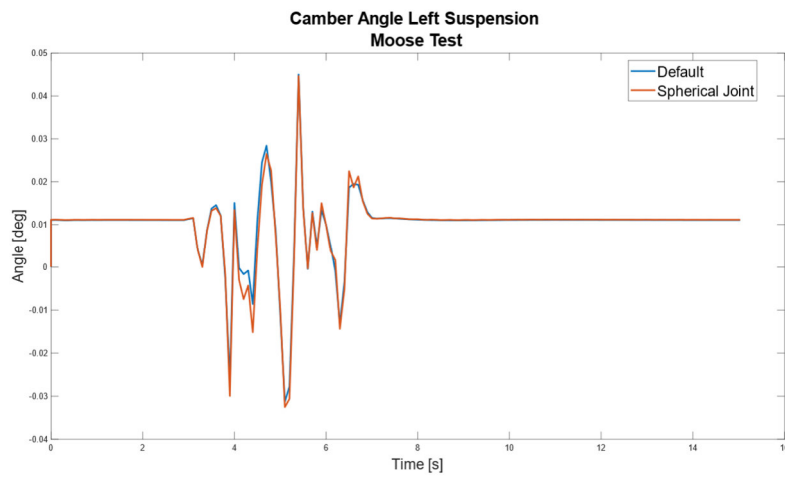


Figure 87 – Camber Angle Left Suspension – Moose Test – Spherical Joint

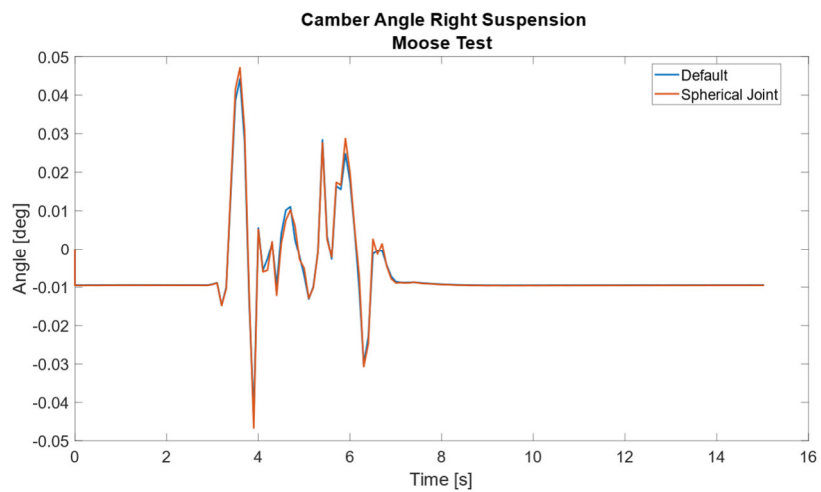


Figure 88 – Camber Angle Right Suspension – Moose Test – Spherical Joint

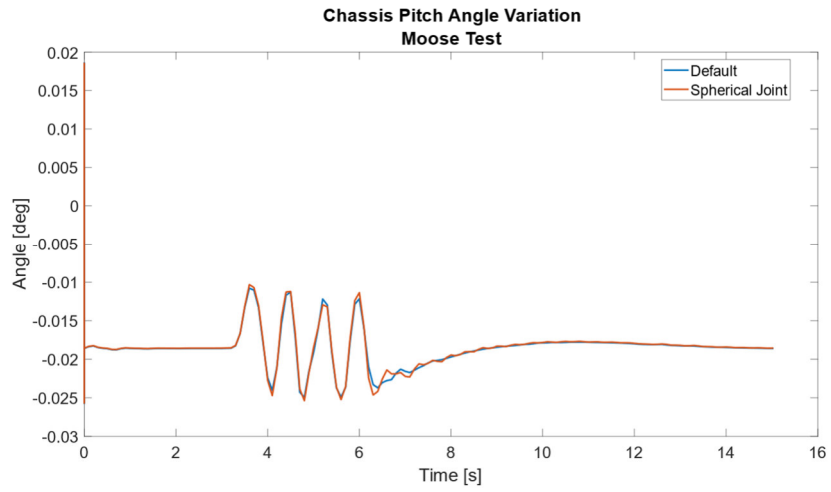


Figure 89 – Chassis Pitch Angle Variation – Moose Test – Spherical Joint

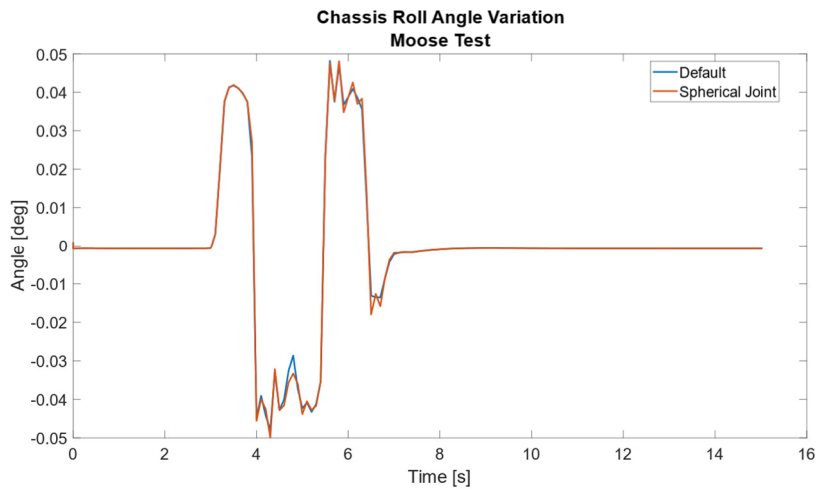


Figure 90 – Chassis Roll Angle Variation – Moose Test – Spherical Joint

Considering the brake test, we have a slight increase in lateral force (figs. 91 and 92), lateral and longitudinal displacement (figs 93, 94, 95 and 96), and a more significant increase in vertical displacement (figs. 97 and 99).

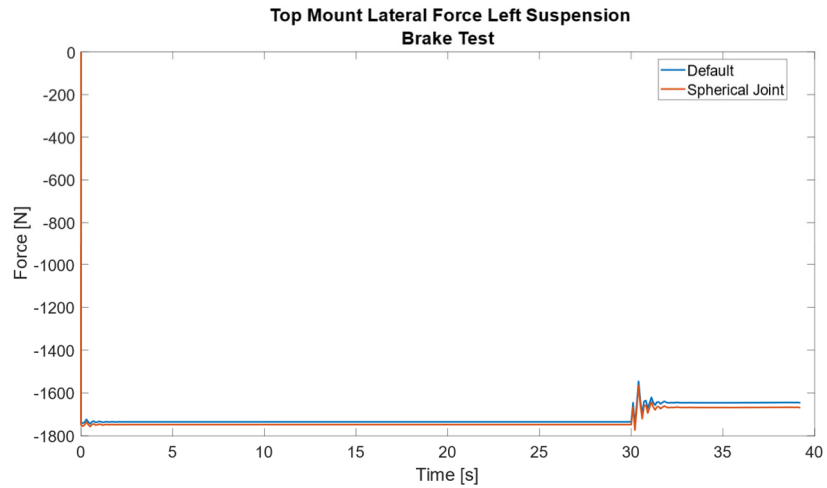


Figure 91 – Top Mount Lateral Force Left Suspension – Brake Test – Spherical Joint

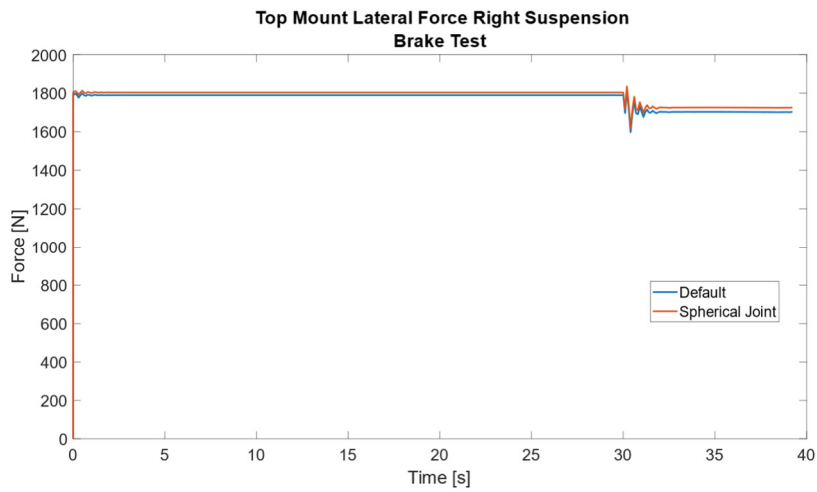


Figure 92 – Top Mount Lateral Force Right Suspension – Brake Test – Spherical Joint

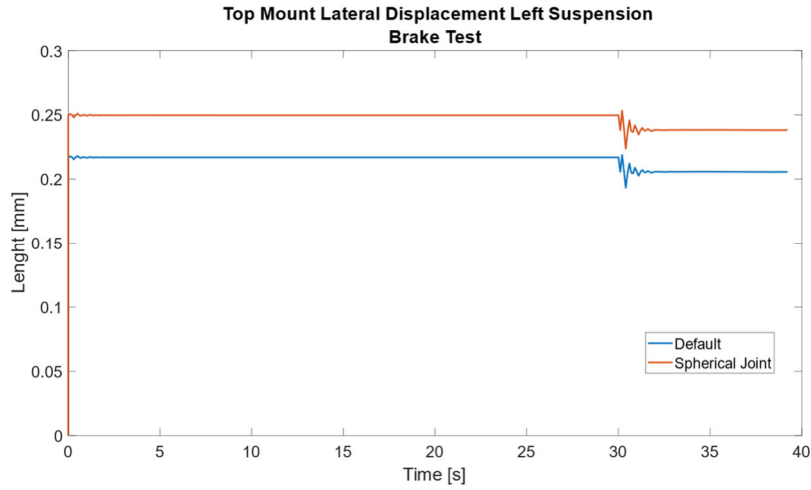


Figure 93 – Top Mount Lateral Displacement Left Suspension – Brake Test – Spherical Joint

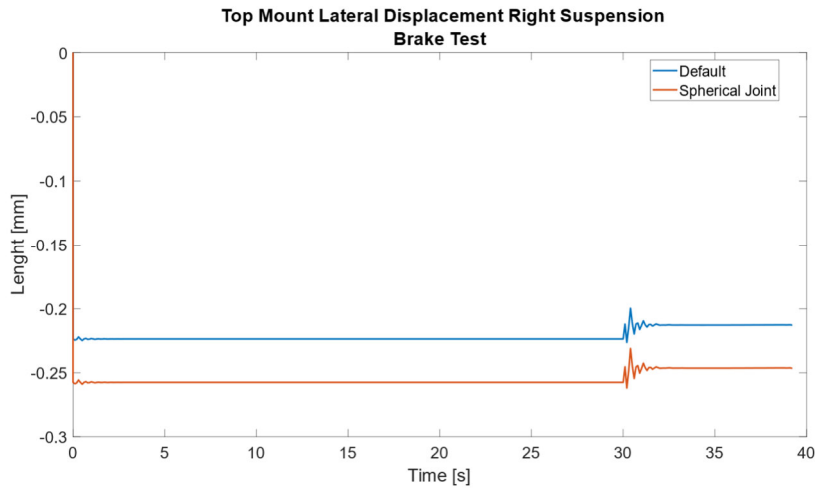


Figure 94 – Top Mount Lateral Displacement Right Suspension – Brake Test – Spherical Joint

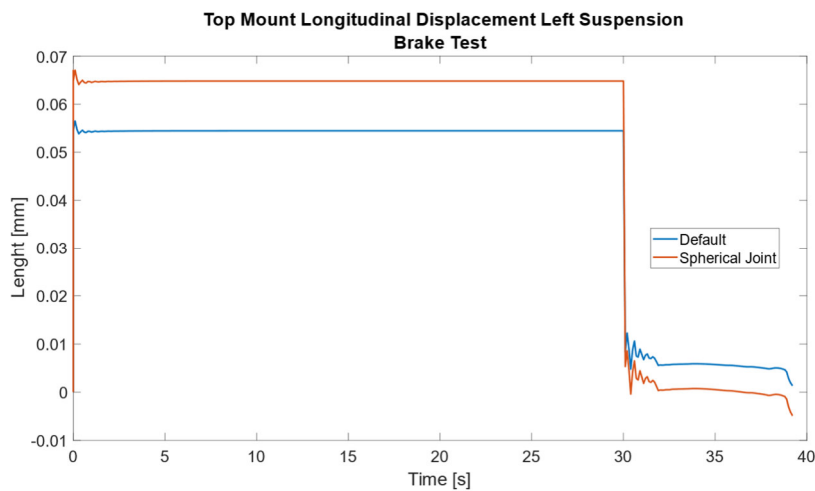


Figure 95 – Top Mount Longitudinal Displacement Left Suspension – Brake Test Spherical Joint

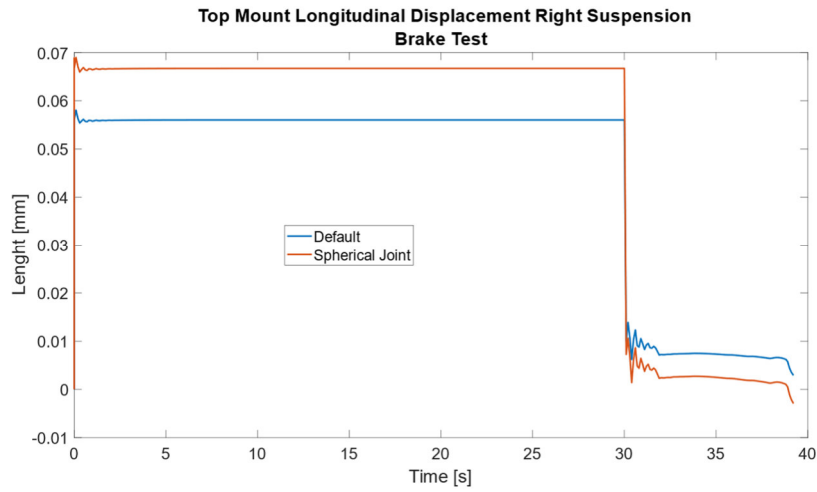


Figure 96 – Top Mount Longitudinal Displacement Right Suspension – Brake Test Spherical Joint

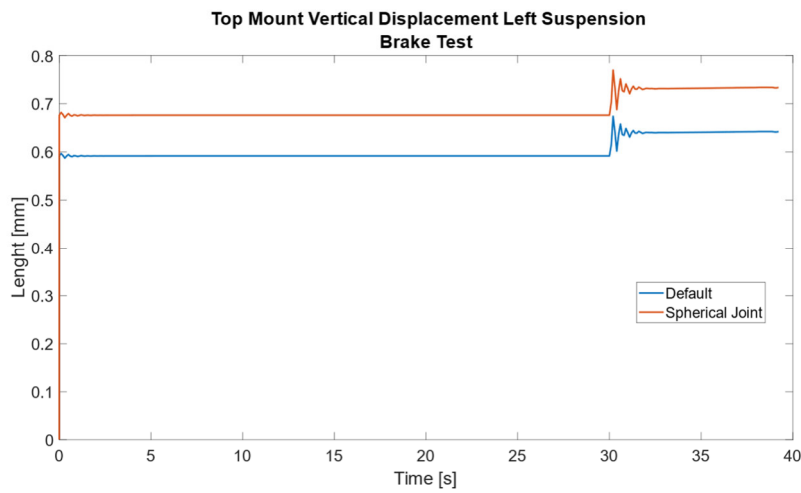


Figure 97 – Top Mount Vertical Displacement Left Suspension – Brake Test – Spherical Joint

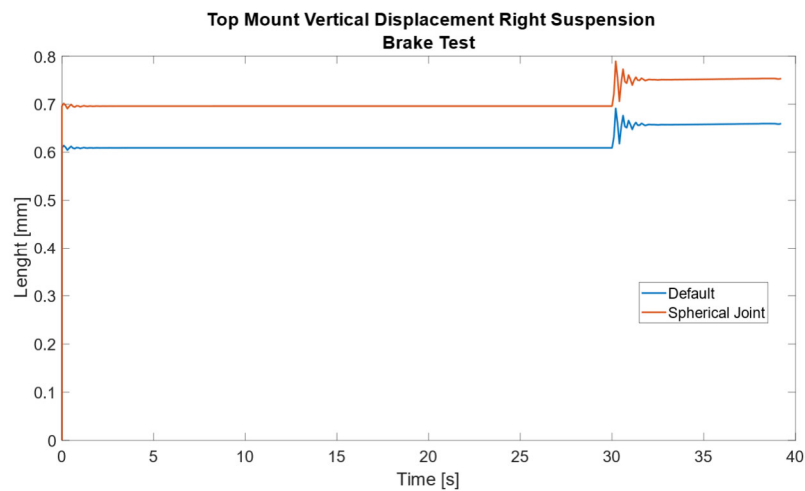


Figure 98 – Top Mount Vertical Displacement Right Suspension – Brake Test – Spherical Joint

The lateral, longitudinal and vertical accelerations (fig. 99, 100 and 101), the camber angle (fig 102 and 103), the pitch angle (fig. 104) and the roll angle (fig. 105), as can be seen from their respective graphs, do not undergo any significant change with the adoption of the spherical joint in the brake test.

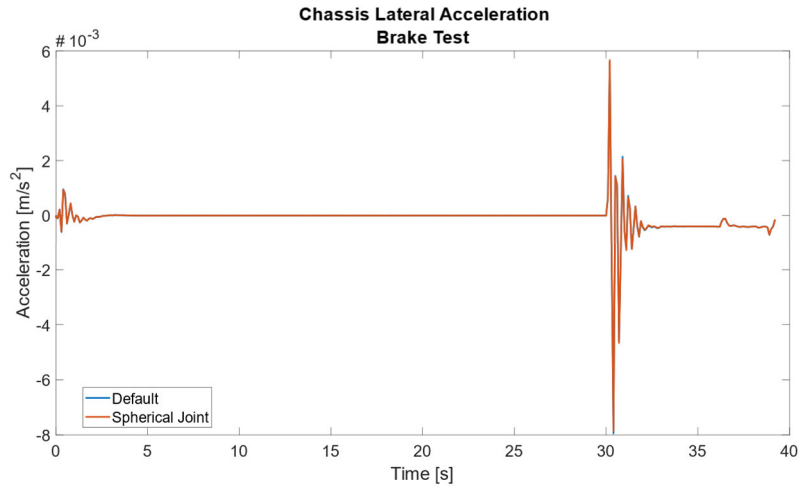


Figure 99 – Chassis Lateral Acceleration – Brake Test – Spherical Joint

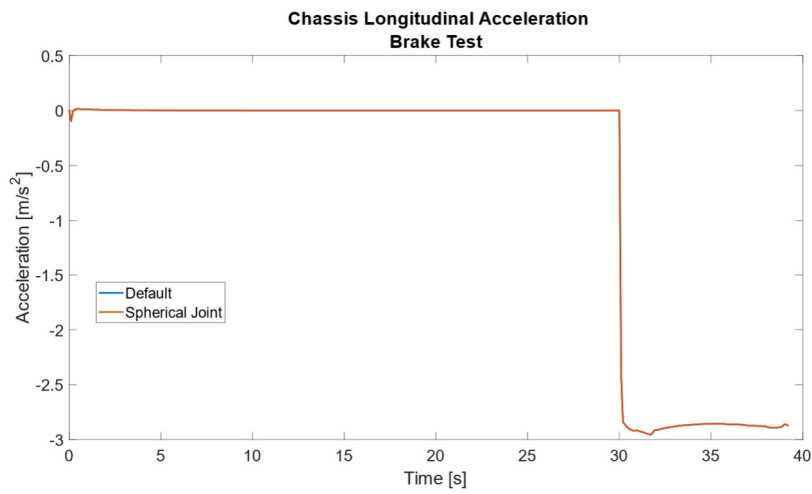


Figure 100 – Chassis Longitudinal Acceleration – Brake Test – Spherical Joint

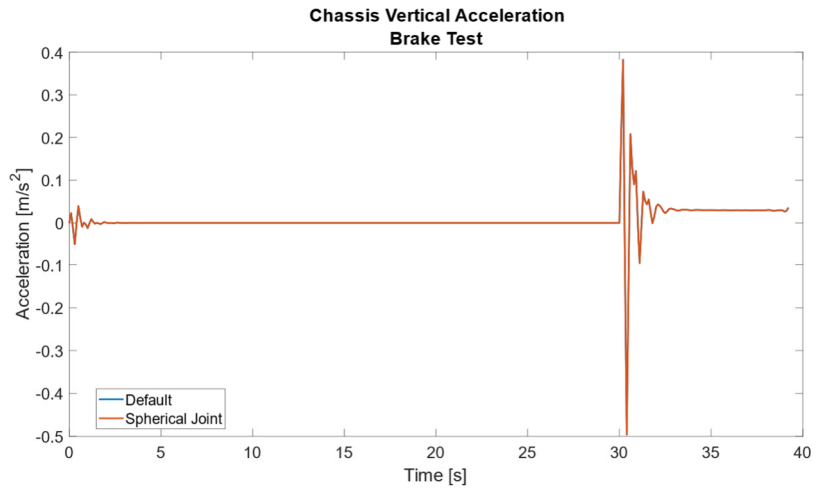


Figure 101 – Chassis Vertical Acceleration – Brake Test – Spherical Joint

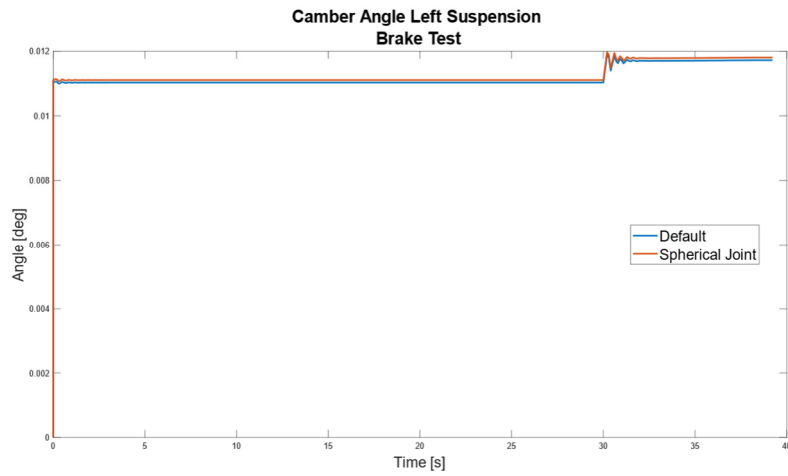


Figure 102 – Camber Angle Left Suspension – Brake Test – Spherical Joint

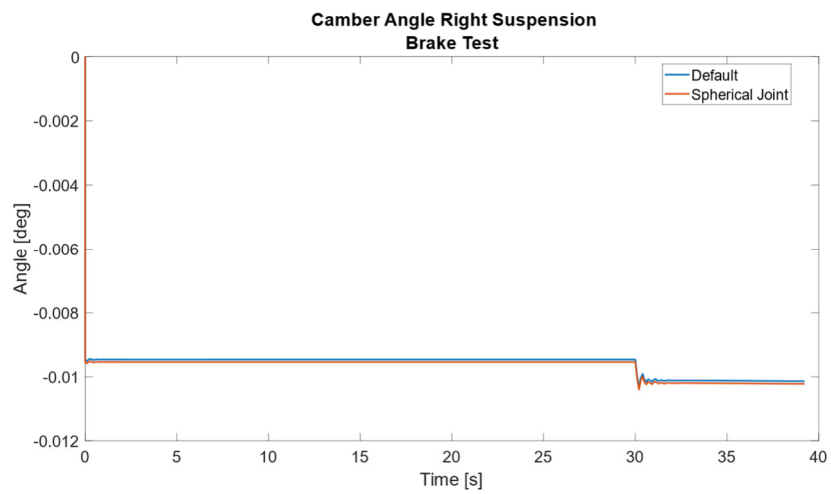


Figure 103 – Camber Angle Right Suspension – Brake Test – Spherical Joint

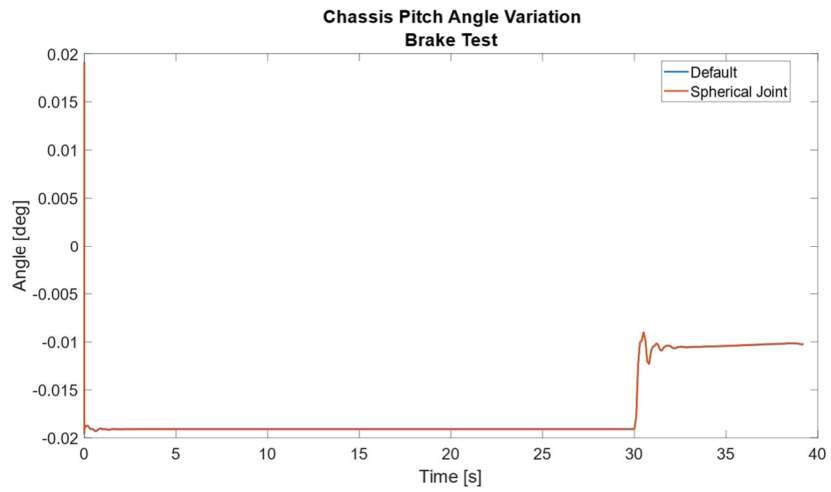


Figure 104 – Chassis Pitch Angle Variation – Brake Test – Spherical Joint

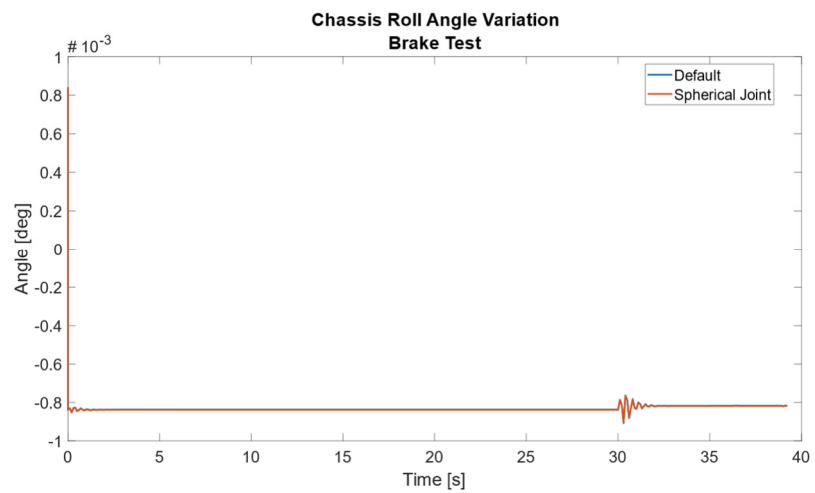


Figure 105 – Chassis Roll Angle Variation – Brake Test – Spherical Joint

Finally, by analyzing the contribution of the spherical joint in the speed bump test (figures from 106 to 120), we can note that the adoption of the spherical joint does not bring any benefit, on the contrary, it increases the amplitude of the oscillatory phase, causing instability.

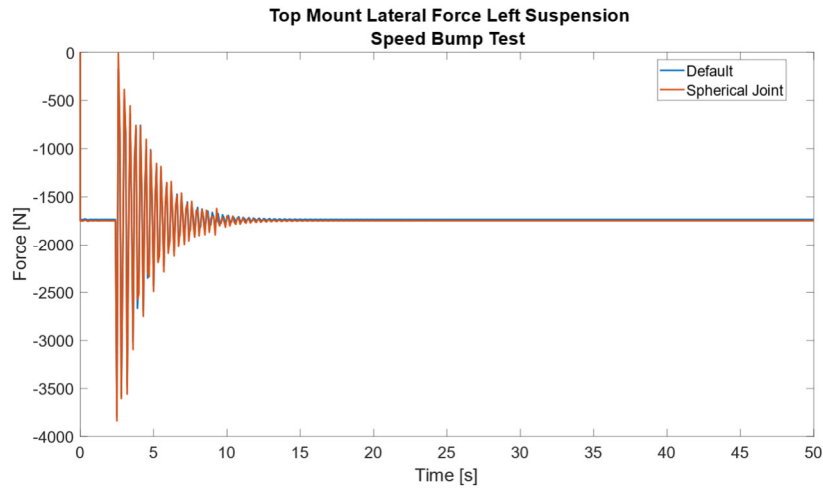


Figure 106 Top Mount Lateral Force Left Suspension – Speed Bump Test – Spherical Joint

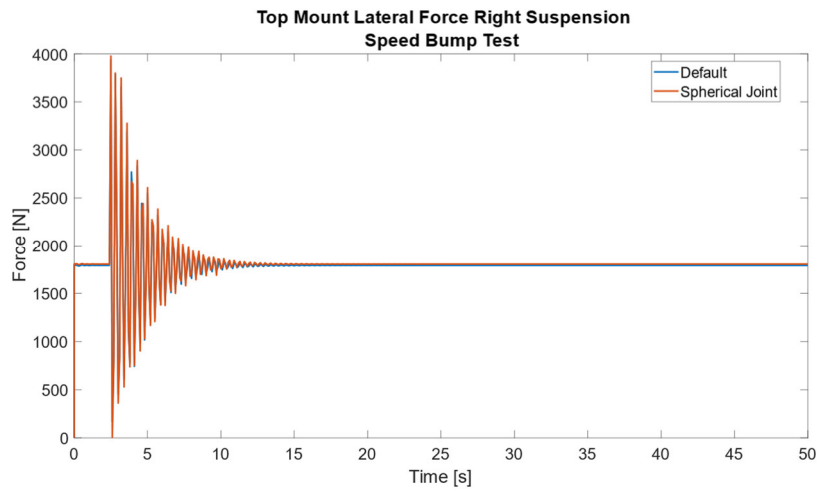


Figure 107 – Top Mount Lateral Force Right Suspension – Speed Bump – Spherical Joint

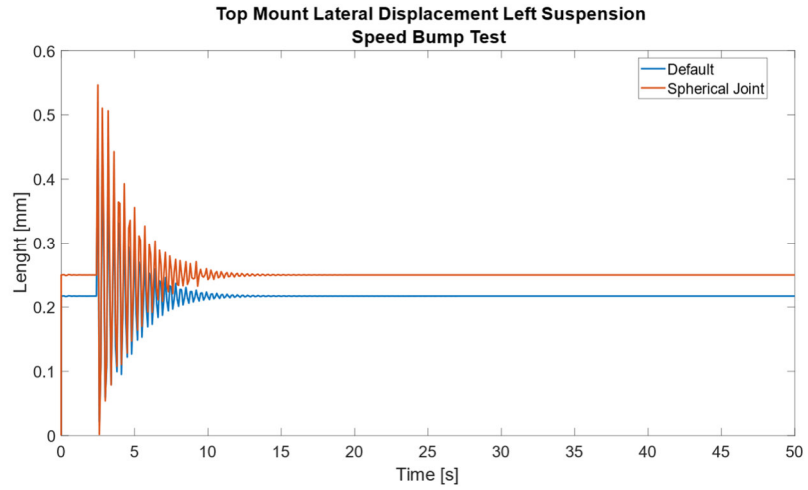


Figure 108 – Top Mount Lateral Displacement Left Suspension – Speed Bump Test
Spherical Joint

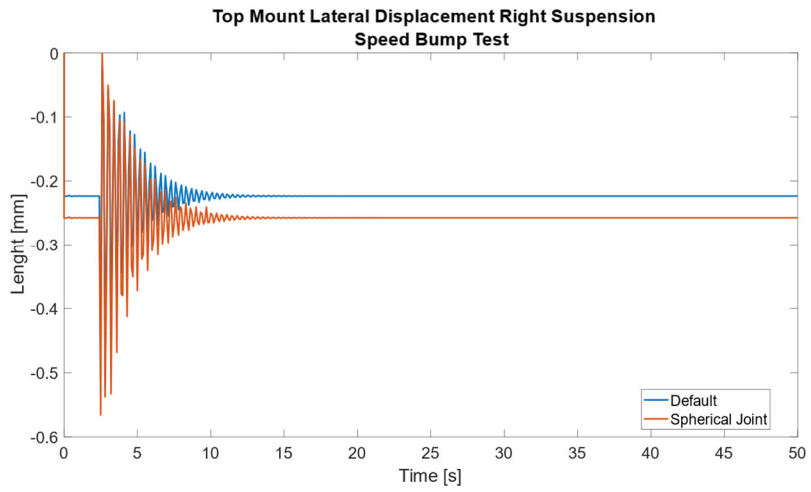


Figure 109 – Top Mount Lateral Displacement Right Suspension – Speed Bump Test
Spherical Joint

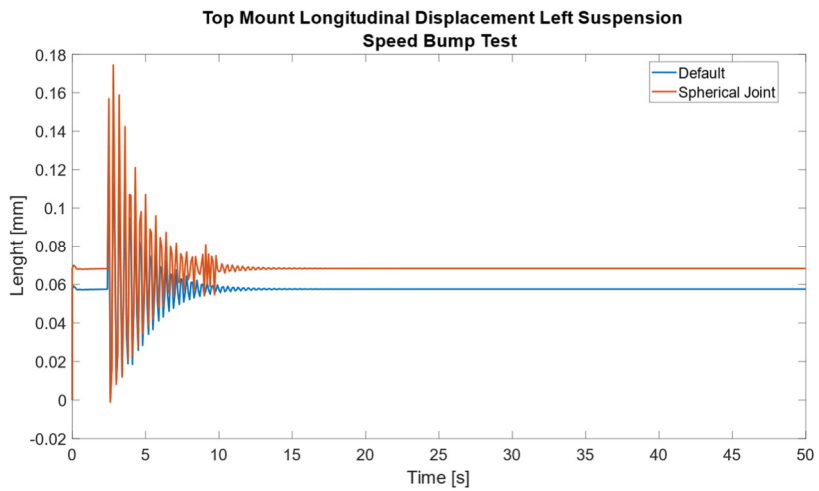


Figure 110 – Top Mount Longitudinal Displacement Left Suspension – Speed Bump Test
Spherical Joint

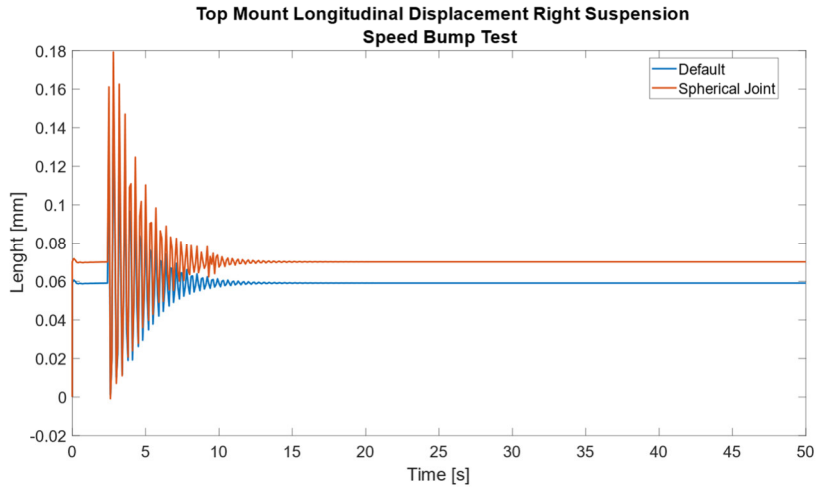


Figure 111 – Top Mount Longitudinal Displacement – Right Suspension – Speed Bump Test Spherical Joint

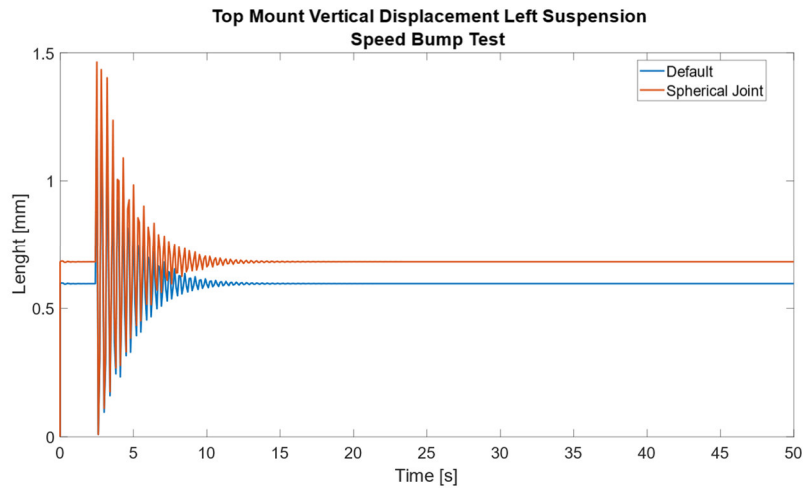


Figure 112 – Top Mount Vertical Displacement Left Suspension – Speed Bump – Spherical Joint

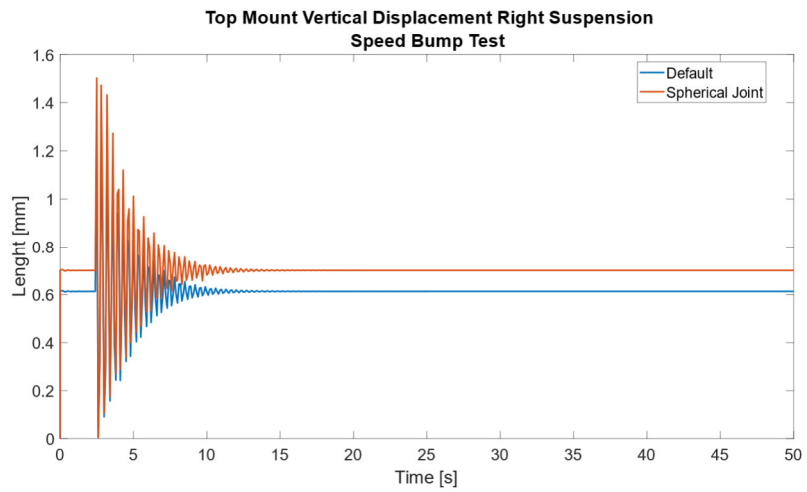


Figure 113 – Top Mount Vertical Displacement Right Suspension – Speed Bump – Spherical Joint

Particularly for lateral (fig. 114) and longitudinal acceleration (fig. 115) we have the appearance of another oscillatory phase after the passage of the car on the bump, which does not improve the dynamic behavior of the vehicle by increasing the instability perceived by the driver.

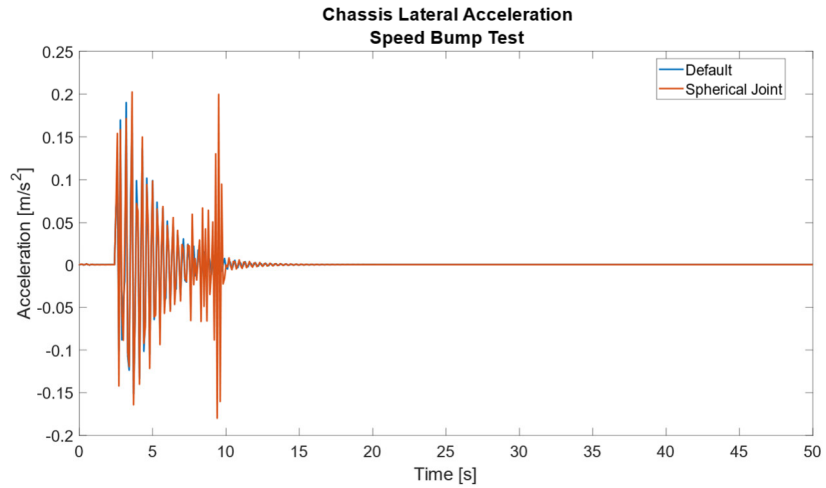


Figure 114 – Chassis Lateral Acceleration – Speed Bump Test – Spherical Joint

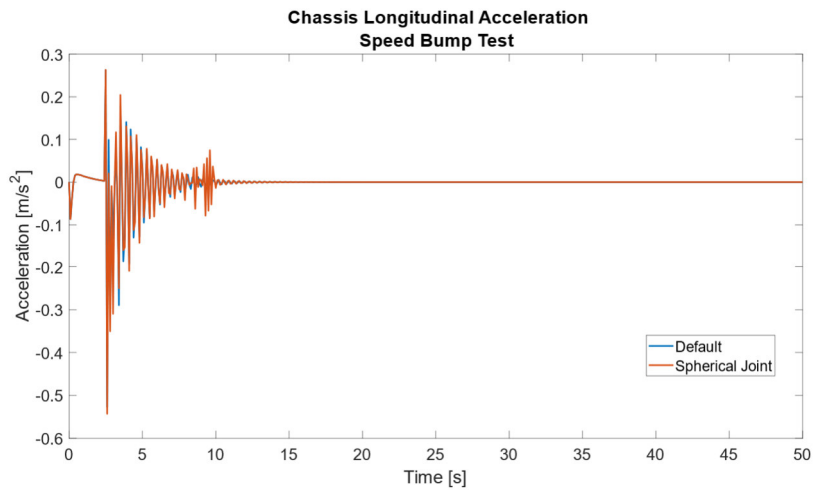


Figure 115 – Chassis Longitudinal Acceleration – Speed Bump Test – Spherical Joint

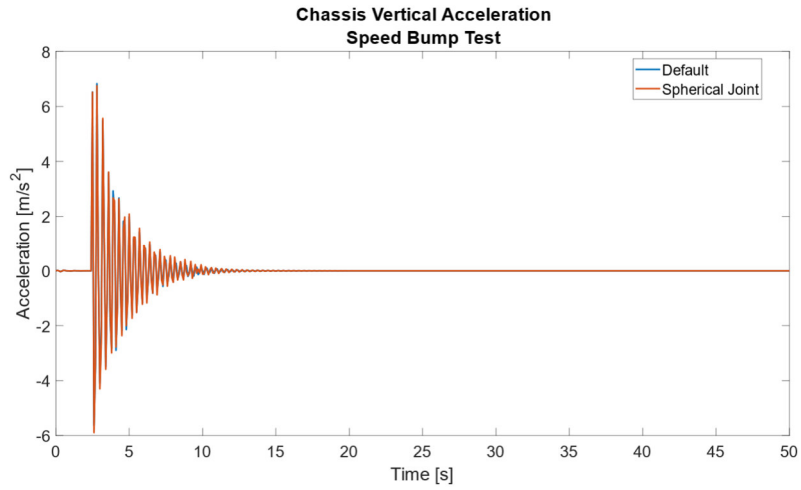


Figure 116 – Chassis Vertical Acceleration – Speed Bump Test – Spherical Joint

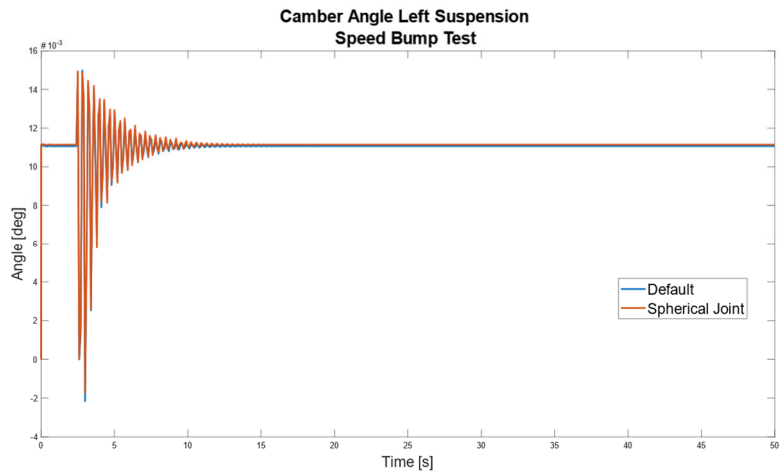


Figure 117 – Camber Angle Left Suspension – Speed Bump Test – Spherical Joint

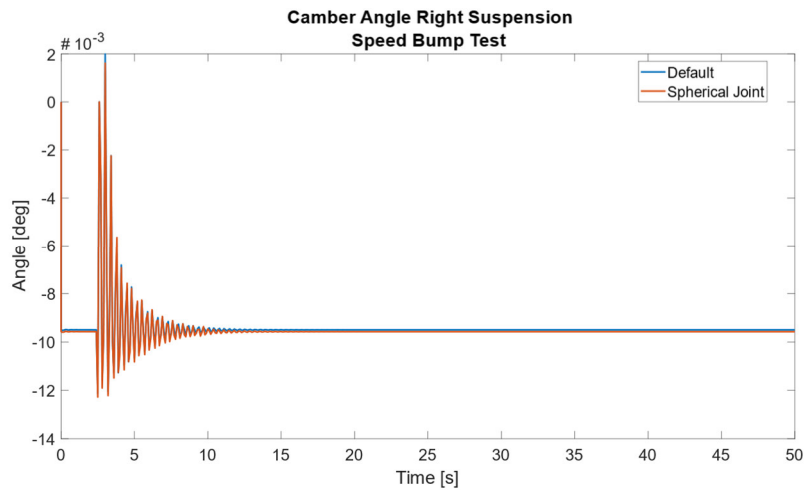


Figure 118 – Camber Angle Right Suspension – Speed Bump Test – Spherical Joint

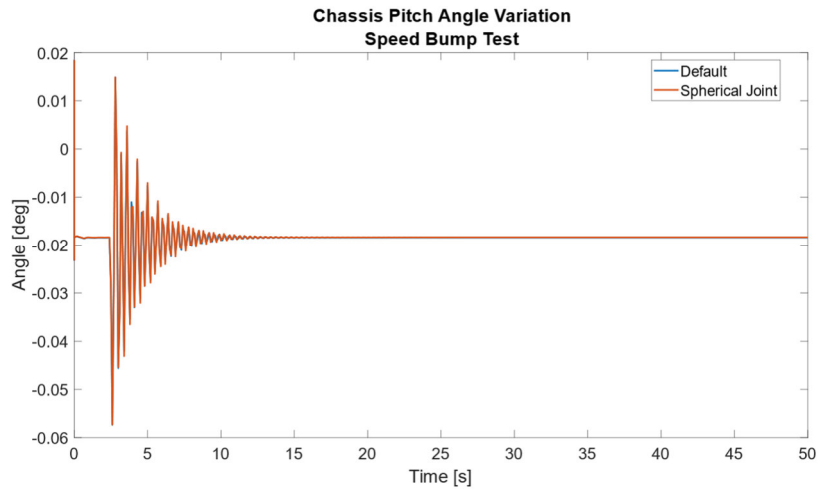


Figure 119 – Chassis Pitch Angle Variation – Speed Bump Test – Spherical Joint

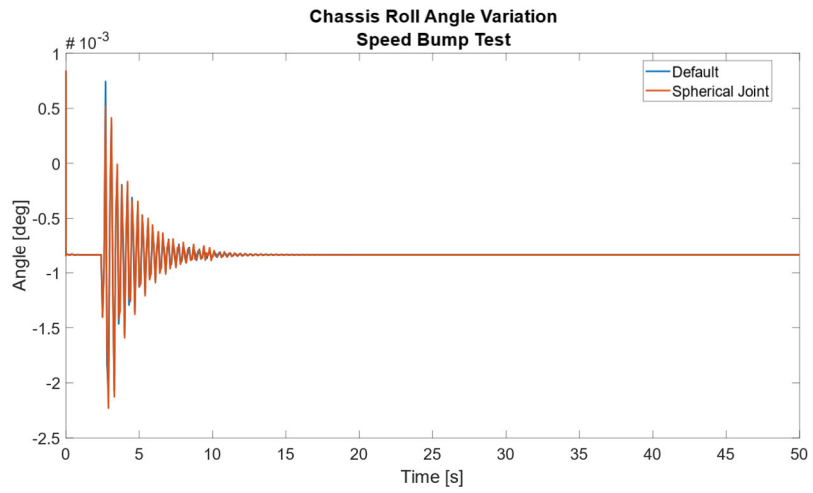


Figure 120 – Chassis Roll Angle Variation – Speed Bump Test – Spherical Joint

4. Conclusion

After all the tests performed on the vehicle under the conditions defined in chapter 4, we can draw conclusions on the results obtained.

The adoption of an angle between the axis of the spring and the axis of the shock absorber involves a significant variation of the lateral load which acts on the top mount, and therefore, consequently, on the damper rod. And this variation is more marked as the angle increases.

As described in the previous chapter, the behaviour of the suspension was described assuming the inclination of the spring with pin on the top mount so that it goes towards the inside of the car with a maximum inclination of 20° (also considering all the structural constraints of the suspension itself). The tests to be carried out to test the car and its behaviour were also chosen. This is the Moose Test, a landslide test and the passage of the car on a speed bump.

At the end of the tests, it was noted that the inclination of the spring axis decreased the force applied on the shock absorber rod by about 800 N, and a decrease in the relative movements of the top mount in the three directions was noted, with less stress on the joint.

In particular, in the case of the Speed Bump test we have obtained, by increasing the angle of inclination of the spring, a decrease in the amplitude and duration of the oscillatory phase due to the passage of the car on the bump.

On the other hand, there were no improvements in vehicle dynamics, therefore the chassis accelerations, lateral, longitudinal and vertical, and in the roll and pitch angles.

To obtain improvements in the dynamic characteristics and on the reduction of the load, it was hypothesized to replace the bush present in the top mount with a ball joint.

The tests carried out considering the suspension without tilting the spring axis were then repeated, to assess the influence of the new component in the dynamics of the vehicle. The results obtained showed a reduction of the force in the Moose Test near the changes of direction of the car but no improvement in the dynamic field, as also in the case of the Brake Test, where instead we have an increase in lateral force if a ball joint is used. Finally, by analysing the Speed Bump Test we notice a marked worsening both in the chassis accelerations and in the lateral force, with an increase in the amplitude of the oscillatory phase and, in the case of lateral and longitudinal accelerations, by an additional oscillatory phase that increases instability of the car.

5. Picture Index

Figure 1.	Multilink Suspension	8
Figure 2.	Double Wishbone Suspension	10
Figure 3.	MacPherson Suspension	11
Figure 4.	Trailing Arm Suspension	13
Figure 5.	Semi Trailing Arm Suspension	15
Figure 6.	Guided Trailing Arm Suspension	16
Figure 7.	Twist Beam Axle Suspension	17
Figure 8.	Forces acting on the MacPherson strut suspension	19
Figure 9.	Generation of the side load	20
Figure 10.	Vehicle vibration model with 8 degrees of freedom	21
Figure 11.	Model of Macpherson suspension	23
Figure 12.	Sedan AWD	28
Figure 13.	MacPherson Suspension (Adams Version)	29
Figure 14.	Top Mount Lateral Force Left Suspension – Static Test	32
Figure 15.	Top Mount Lateral Force Right Suspension – Static Test	32
Figure 16.	Top Mount Lateral Displacement Left Suspension – Static Test	33
Figure 17.	Top Mount Lateral Displacement Right Suspension – Static Test	33
Figure 18.	Top Mount Longitudinal Displacement Left Suspension – Static Test	34
Figure 19.	Top Mount Longitudinal Displacement Right Suspension – Static Test	34
Figure 20.	Top Mount Vertical Displacement Left Suspension – Static Test	34
Figure 21.	Top Mount Vertical Displacement Right Suspension – Static Test	35
Figure 22.	Camber Angle Left Suspension – Static Test	35
Figure 23.	Camber Angle Right Suspension – Static Test	35
Figure 24.	Chassis Pitch Angle Variation – Static Test	36
Figure 25.	Chassis Roll Angle Variation – Static Test	36
Figure 26.	Moose Test Procedure	37
Figure 27.	Braking Test Speed	38
Figure 28.	Speed Bump Profile	38
Figure 29.	Top Mount Lateral Force Left Suspension – Moose Test	39
Figure 30.	Top Mount Lateral Force Right Suspension – Moose Test	39
Figure 31.	Top Mount Lateral Displacement Left Suspension – Moose Test	40
Figure 32.	Top Mount Lateral Displacement Right Suspension – Moose Test	40
Figure 33.	Top Mount Longitudinal Displacement Left Suspension – Moose Test	40
Figure 34.	Top Mount Longitudinal Displacement Right Suspension – Moose Test	41
Figure 35.	Top Mount Vertical Displacement Left Suspension – Moose Test	41
Figure 36.	Top Mount Vertical Displacement Right Suspension – Moose Test	41
Figure 37.	Chassis Lateral Acceleration – Moose Test	42
Figure 38.	Chassis Longitudinal Acceleration – Moose Test	42
Figure 39.	Chassis Vertical Acceleration – Moose Test	43
Figure 40.	Camber Angle Left Suspension – Moose Test	43
Figure 41.	Camber Angle Right Suspension – Moose Test	43
Figure 42.	Chassis Pitch Angle Variation – Moose Test	44
Figure 43.	Chassis Roll Angle Variation – Moose Test	44
Figure 44.	Top Mount Lateral Force Left Suspension – Brake Test	45
Figure 45.	Top Mount Lateral Force Right Suspension – Brake Test	45
Figure 46.	Top Mount Lateral Displacement Left Suspension – Brake Test	46
Figure 47.	Top Mount Lateral Displacement Right Suspension – Brake Test	46
Figure 48.	Top Mount Longitudinal Displacement Left Suspension – Brake Test	46

Figure 49.	Top Mount Longitudinal Displacement Right Suspension – Brake Test	47
Figure 50.	Top Mount Vertical Displacement Left Suspension – Brake Test	47
Figure 51.	Top Mount Vertical Displacement Right Suspension – Brake Test	47
Figure 52.	Chassis Lateral Acceleration – Brake Test	48
Figure 53.	Chassis Longitudinal Acceleration – Brake Test	48
Figure 54.	Chassis Vertical Acceleration – Brake Test	48
Figure 55.	Camber Angle Left Suspension – Brake Test	49
Figure 56.	Camber Angle Right Suspension – Brake Test	49
Figure 57.	Chassis Pitch Angle Variation – Brake Test	49
Figure 58.	Chassis Roll Angle Variation – Brake Test	50
Figure 59.	Top Mount Lateral Force Left Suspension – Speed Bump Test	50
Figure 60.	Top Mount Lateral Force Right Suspension – Speed Bump Test	51
Figure 61.	Top Mount Lateral Displacement Left Suspension – Speed Bump Test	51
Figure 62.	Top Mount Lateral Displacement Right Suspension – Speed Bump Test	51
Figure 63.	Top Mount Longitudinal Displacement Left Suspension – Speed Bump Test	52
Figure 64.	Top Mount Longitudinal Displacement Right Suspension – Speed Bump Test	52
Figure 65.	Top Mount Vertical Displacement Left Suspension – Speed Bump Test	52
Figure 66.	Top Mount Vertical Displacement Right Suspension – Speed Bump Test	53
Figure 67.	Chassis Lateral Acceleration – Speed Bump Test	53
Figure 68.	Chassis Longitudinal Acceleration – Speed Bump Test	53
Figure 69.	Chassis Vertical Acceleration – Speed Bump Test	54
Figure 70.	Camber Angle Left Suspension – Speed Bump Test	54
Figure 71.	Camber Angle Right Suspension – Speed Bump Test	54
Figure 72.	Chassis Pitch Angle Variation – Speed Bump Test	55
Figure 73.	Chassis Roll Angle Variation – Speed Bump Test	55
Figure 74.	Bushing Rotational Stiffnesses	56
Figure 75.	Bushing Translational Stiffness	56
Figure 76.	Top Mount Lateral Force Left Suspension – Moose Test – Spherical Joint	57
Figure 77.	Top Mount Lateral Force Right Suspension – Moose Test – Spherical Joint	57
Figure 78.	Top Mount Lateral Displacement Left Suspension – Moose Test – Spherical Joint	58
Figure 79.	Top Mount Lateral Displacement Right Suspension – Moose Test – Spherical Joint	58
Figure 80.	Top Mount Longitudinal Displacement Left Suspension – Moose Test – Spherical Joint	58
Figure 81.	Top Mount Longitudinal Displacement Right Suspension – Moose Test – Spherical Joint	59
Figure 82.	Top Mount Vertical Displacement Left Suspension – Moose Test – Spherical Joint	59
Figure 83.	Top Mount Vertical Displacement Right Suspension – Moose Test – Spherical Joint	59
Figure 84.	Chassis Lateral Acceleration – Moose Test – Spherical Joint	60
Figure 85.	Chassis Longitudinal Acceleration – Moose Test – Spherical Joint	60
Figure 86.	Chassis Vertical Acceleration – Moose Test – Spherical Joint	60
Figure 87.	Camber Angle Left Suspension – Moose Test – Spherical Joint	61
Figure 88.	Camber Angle Right Suspension – Moose Test – Spherical Joint	61
Figure 89.	Chassis Pitch Angle Variation – Moose Test – Spherical Joint	62
Figure 90.	Chassis Roll Angle Variation – Moose Test – Spherical Joint	62
Figure 91.	Top Mount Lateral Force Left Suspension – Brake Test – Spherical Joint	63
Figure 92.	Top Mount Lateral Force Right Suspension – Brake Test – Spherical Joint	63
Figure 93.	Top Mount Lateral Displacement Left Suspension – Brake Test – Spherical Joint	64
Figure 94.	Top Mount Lateral Displacement Right Suspension – Brake Test – Spherical Joint	64
Figure 95.	Top Mount Longitudinal Displacement Left Suspension – Brake Test – Spherical Joint	64
Figure 96.	Top Mount Longitudinal Displacement Right Suspension – Brake Test – Spherical Joint	65
Figure 97.	Top Mount Vertical Displacement Left Suspension – Brake Test – Spherical Joint	65
Figure 98.	Top Mount Vertical Displacement Right Suspension – Brake Test – Spherical Joint	65
Figure 99.	Chassis Lateral Acceleration – Brake Test – Spherical Joint	66

Figure 100.	Chassis Longitudinal Acceleration – Brake Test – Spherical Joint.....	66
Figure 101.	Chassis Vertical Acceleration – Brake Test – Spherical Joint.....	67
Figure 102.	Camber Angle Left Suspension – Brake Test – Spherical Joint.....	67
Figure 103.	Camber Angle Right Suspension – Brake Test – Spherical Joint.....	67
Figure 104.	Chassis Pitch Angle Variation – Brake Test – Spherical Joint.....	68
Figure 105.	Chassis Roll Angle Variation – Brake Test – Spherical Joint.....	68
Figure 106.	Top Mount Lateral Force Left Suspension – Speed Bump Test – Spherical Joint.....	69
Figure 107.	Top Mount Lateral Force Right Suspension – Speed Bump – Spherical Joint.....	69
Figure 108.	Top Mount Lateral Displacement Left Suspension – Speed Bump Test – Spherical Joint.....	70
Figure 109.	Top Mount Lateral Displacement Right Suspension – Speed Bump Test – Spherical Joint.....	70
Figure 110.	Top Mount Longitudinal Displacement Left Suspension – Speed Bump Test – Spherical Joint.....	70
Figure 111.	Top Mount Longitudinal Displacement – Right Suspension – Speed Bump Test – Spherical Joint.....	71
Figure 112.	Top Mount Vertical Displacement Left Suspension – Speed Bump – Spherical Joint.....	71
Figure 113.	Top Mount Vertical Displacement Right Suspension – Speed Bump – Spherical Joint.....	71
Figure 114.	Chassis Lateral Acceleration – Speed Bump Test – Spherical Joint.....	72
Figure 115.	Chassis Longitudinal Acceleration – Speed Bump Test – Spherical Joint.....	72
Figure 116.	Chassis Vertical Acceleration – Speed Bump Test – Spherical Joint.....	72
Figure 117.	Camber Angle Left Suspension – Speed Bump Test – Spherical Joint.....	73
Figure 118.	Camber Angle Right Suspension – Speed Bump Test – Spherical Joint.....	73
Figure 119.	Chassis Pitch Angle Variation – Speed Bump Test – Spherical Joint.....	74
Figure 120.	Chassis Roll Angle Variation – Speed Bump Test – Spherical Joint.....	74

6. Bibliography

- [1] Giancarlo Genta – *Motor Vehicle Dynamics – Modeling and Simulation*, World Scientific, 1997
- [2] Jornsens Reimpell, Helmut Stoll, Jurgen W. Betzler, Society of Automotive Engineers – *The Automotive Chassis – Engineering Principles*, SAE International, 2001
- [3] William F. Milliken – *Race Car Vehicle Dynamics*, SAE International, 1995
- [4] Giancarlo Genta, Lorenzo Morello – *The Automotive Chassis Volume I Components Design*, Springer, 2009
- [5] Don Knowles – *Automotive Suspension & Steering Systems*, Delmar Cengage Learning, 2006
- [6] Herman Van der Auweraer, Tommaso Tamarozzi, Enrico Risaliti, Mathieu Sarrazin, Jan Croes, Bart Forrier, Frank Naets, Wim Desmet – *Virtual Sensing Based on Design Engineering Simulation Models*, International Conference on Structural Engineering Dynamics, At Ericeira, Portugal, 2017
- [7] Byung Chul Choi, Seunghyeon Cho, and Chang-Wan Kim – *Kriging Model Based Optimization of MacPherson Strut Suspension for Minimizing Side Load using Flexible Multi-Body Dynamics*, KSPE and Springer, 2018
- [8] Sadegh Yarmohammadisatri, Mohammad Hasan Shojaeefard, Abolfazl Khalkhali – *A family base optimization of a developed nonlinear vehicle suspension model using gray family design algorithm*, Springer, 2017
- [9] Saber Fallah, Rama B. Bhat, Wen-Fang Xie – *New Nonlinear Model of Macpherson Suspension System for Ride Control Applications*, American Control Conference Westin Seattle Hotel, Seattle, Washington, USA, 2008
- [10] Yat Sheng Kong, M.Z. Omar, Shahrum Abdullah, Sallehuddin Mohamed Haris – *Side force analysis of suspension strut under various load cases*, Jurnal Teknologi, 2016
- [11] J. P. Haste, Jacques Baudelet, Eric Gerard, Colin Jones, Christelle Viel – *Optimization on Mac Pherson Suspensions with a Spring*, SAE, 1997
- [12] Ryu, Y.I., Kang, D.O., Heo, S.J. et al. – *Development of analytical process to reduce side load in strut-type suspension*, J Mech Sci Technol 24, 351–356, 2010

- [13] Songyu Li, Liquan Wang, Shaoming Yao, Peng Jia, Feihong Yun, Wenxue Jin, and Dong Lv – *Modelling, simulation and experiment of the spherical flexible joint stiffness*, Mech. Sci., 9, 81–89, 2018
- [14] S. Para and A. Kuranowski – *Analysis of the rotational capability of the utilization of range of a spherical joint used in a passenger automobile McPherson suspension*, IOP Conference Series Materials Science and Engineering 421(2):022025, 2018
- [15] M.N. Burcham, R Escobar Jr, C.O. Yenusah, et al. – *Characterization and Failure Analysis of an Automotive Ball Joint*, Journal of Failure Analysis and Prevention. 17, 262–274, 2017
- [16] E. A. Ossa, Carlos Palacio, Marco Paniagua – *Failure analysis of a car suspension system ball joint*, Engineering Failure Analysis 18, 2011
- [17] ISO 3888: 2011 Passenger cars — Test track for a severe lane-change manoeuvre — Part 2: Obstacle avoidance
- [18] DPR 495/1992, as modified by DPR 610/96, in Art. 179. (Art. 42 Cod. Str.) Comma 5
- [19] *Adams/Help (Adams 2015.1)*, MSC Software, 2015

7. Acknowledgements

È stato un viaggio lungo, forse più del previsto, con qualche intoppo di troppo. Ma è stato emozionante e sicuramente lo rifarei. Ed essendo lungo la lista di persone che dovrei ringraziare è veramente lunga. I primi non possono essere che i miei genitori, *Carmelo* e *Vera*, che nonostante tutto mi sono stati vicini e mi hanno supportato per tutto il tempo. Mio fratello *Salvatore* e mia sorella *Elena* che hanno creduto in me dandomi la forza di andare avanti. I miei nonni, quelli che ci sono ancora, *Giovanni*, e quelli che non ci sono più, *Elena*, *Carmela* e *Salvatore*, di cui percepisco sempre la loro presenza accanto a me.

Una menzione speciale va alla persona che amo, che mi ha supportato e, *prima di tutto*, sopportato in questi anni, *Giulia*. La sua presenza e il suo buon senso mi hanno aiutato nei momenti più difficili, ma ha gioito con me nei momenti felici. Ora avrò più tempo da dedicarle come promesso. I miei amici *Corrado*, *Livio*, *Stefano*, *Giulio* e tutti gli altri che hanno condiviso con me i momenti più importanti della mia vita universitaria e non, e che continuano a supportarmi. I miei colleghi del lavoro (oriundi e non), la cui lista è veramente lunga, che hanno vissuto il mio ultimo periodo e con la loro presenza e i loro consigli mi hanno aiutato ad andare avanti.

Vi voglio bene.

Un ringraziamento anche a *Nunzia*, che mi ha aiutato a superare i momenti difficili con i suoi ottimi consigli.

Infine, non posso che ringraziare il prof. *Giovanni Maizza* per l'opportunità di fare una tesi con lui, e di un argomento a cui tenevo particolarmente, e *Umid* che con una pazienza olimpica mi ha aiutato a completare il mio ultimo passo.

Ma vorrei dedicare questa tesi anche a *me stesso*, che, nonostante le volte in cui ho creduto di non farcela, ho sempre pensato che in qualche modo ce l'avrei fatta.

Un pensiero a tutte le persone che stanno soffrendo e hanno sofferto per l'emergenza sanitaria che ha colpito il mondo in questo periodo. Questi sono i momenti in cui si vede di che pasta siamo fatti, noi italiani in particolare.

Non ci fermerà nulla.